

NATIONAL HIGHWAY TRAFFIC SAFETY ADMINISTRATION  
WASHINGTON, D.C.

---

## CONTRACTOR FINAL REPORT

TEST #

130

130 AFS

43-50

**DOT HS-800 924**

# **DOOR CRASHWORTHINESS CRITERIA**

**Contract No. DOT-HS-031-2-382**

**September 1973**

**Final Report**

**PREPARED FOR:**

**U.S. DEPARTMENT OF TRANSPORTATION**

**NATIONAL HIGHWAY TRAFFIC SAFETY ADMINISTRATION**

**WASHINGTON, D.C. 20590**

Document is available to the public through  
the National Technical Information Service,  
Springfield, Virginia 22151

This document is disseminated under the sponsorship of the Department of Transportation in the interest of information exchange. The United States Government assumes no liability for its contents or use thereof.

1 Report No DOT HS-800 924		2 Government Accession No		3 Recipient's Catalog No	
4 Title and Subtitle  Door Crashworthiness Criteria				5 Report Date September, 1973	
				6 Performing Organization Code	
7 Author(s) R.L. Stalnaker, V.L. Roberts, J.H. McElhaney				8 Performing Organization Report No UM-HSRI-B1-73-2	
9 Performing Organization Name and Address  Highway Safety Research Institute The University of Michigan Huron Parkway and Baxter Road Ann Arbor, Michigan 48105				10 Work Unit No	
				11 Contract or Grant No DOT-HS-031-2-382	
12 Sponsoring Agency Name and Address U.S. Department of Transportation National Highway Traffic Safety Administration Washington, D.C. 20590				13 Type of Report and Period Covered Final Report 12 June 1972-11 June 1973	
				14 Sponsoring Agency Code	
15 Supplementary Notes					
16 Abstract  <p>The object of this program has been to extend the scope of the report written pursuant to NHTSA Contract FH-11-7288 (21 June 1969-20 June 1971) to include long duration head impacts and to develop scaling relationships to allow extrapolation of impact data for infra-human primates to living humans.</p> <p>A series of primate side impacts, to the head and body was conducted in parallel with a series of impacts to human cadavers. Dimensional analysis techniques were employed to estimate <u>in vivo</u> human tolerance to side impacts.</p> <p>The threshold of closed brain injury to humans was found to be 76G's for a pulse duration of 20 msec and an impact velocity of 29.5 mph. The maximum tolerable penetration to the chest was found to be 2.65 inches for both the left and right sides.</p> <p>Scaling of abdominal injuries to humans was accomplished by employing a factor which relates impact contact area, animal mass, impact force, and pulse duration, to injury severity. The maximum tolerable contact pressure to the upper abdomen of a human was found to be 32 psi.</p>					
17 Key Words Human Tolerance, Chest, Head, Abdominal Monkey Impact, Animal Scaling			18 Distribution Statement Unlimited available through the National Technical Information Service, Springfield, Virginia 22151		
19 Security Classif (of this report) Unclassified		20. Security Classif.(of this page) Unclassified		21 No of Pages 97	
				22 Price	

## TABLE OF CONTENTS

	Page
Table of Contents	i
Figures	iii
Tables	v
Acknowledgements	vi
1.0 Introduction	1
1.1 Side Impacts in Highway Safety	1
1.2 Current Research Knowledge	2
2.0 Experimental Studies	5
2.1 Introduction	5
2.2 Experimental Methods	6
2.2.1 Padded Head Impacts	10
2.2.1.1 Sub-human Primate Head Impact Study	10
2.2.1.2 Human Cadaver Head Impact Study	14
2.2.2 Torso Impacts	16
2.2.2.1 Sub-human Primate Impacts	20
2.2.2.2 Human Cadaver Impacts	20
2.2.3 Direct Organ Impacts	23
2.2.4 Thoracic Mechanical Impedance	25
2.3 Biomedical Data Collection	27
3.0 Test Results	33
3.1 Results of Padded Head Impacts	33
3.2 Results of Thoracic Impacts	37
3.3 Results of Abdominal Impacts	44
3.4 Results of Whole Body Impact	55

TABLE OF CONTENTS  
(Continued)

	Page
3.5 Results of Direct Organ Impacts	55
3.6 Results of Chest Mechanical Impedance	62
4.0 Primate Scaling	67
4.1 Head Injury Scaling	67
4.2 Thoracic Injury Scaling	70
4.3 Abdominal Injury Scaling	76
5.0 Discussion and Conclusions	80
6.0 References	83

## FIGURES

	Page
Figure 1. Skulls of Primates	7
Figure 2. Block Diagram of Head Impact Facility	9
Figure 3. Accelerometer Mounting for Head Impacts	11
Figure 4. Maximum Strain Criterion for Primates, Side Head Impacts (Triangular Pulse)	12
Figure 5. Primate Side Head Impact Set-Up (Rhesus Shown)	13
Figure 6. Targeting and Instrumentation for Side Head Impacts	15
Figure 7. Human Cadaver Side Head Impact (Padded) Set-Up	17
Figure 8. Body Impact Regions for Left Side	18
Figure 9. Body Impact Regions for Right Side	19
Figure 10. Primate Side Torso Impact Set-Up (Baboon Shown)	21
Figure 11. Human Cadaver Side Thoracic Impact Set-Up.	22
Figure 12. Set-Up for Direct Organ Impacts	24
Figure 13. Loading Fixture	26
Figure 14. Side Thoracic Mechanical Impedance Test Set-Up.	28
Figure 15. Sections Through Brain Showing Internal Injury	34
Figure 16. Section of Cerebrum, Showing Hemorrhaging in the Putamen	35
Figure 17. Hemorrhaging of the Superior Sagittal Sinus	36
Figure 18. Human Cadaver Side Head Impacts (Padded) Force-Time Curves	41
Figure 19. Human Cadaver Side Head Impact (Padded) Acceleration Time Curves	42
Figure 20. Human Cadaver Side Head Impact (Padded) Acceleration Time Curves	43
Figure 21. Lung Tissue, Showing the Three Most Common Kinds of Injury	45
Figure 22. Blowout Failure at the Junction of the Superior Vena Cava and the Right Atrium	46

# FIGURES (continued)

	Page
Figure 23. Dynamic Load-Penetration Curves for Side Chest Impacts with a 6" DIA Flat Impactor	51
Figure 24. Dynamic Load-Penetration Curves for Side Chest Impacts with Simulated Arm Rest Impactor	52
Figure 25. Dynamic Load-Penetration Curves for Human Cadaver Side Chest Impacts	53
Figure 26. Typical Liver Injuries	54
Figure 27. Load -Deflection Trace for Direct-Liver Impact	61
Figure 28. Stress-Strain Curves for Direct Impacts on Perfused Livers (Rhesus)	63
Figure 29. Driving point Mechanical Impedance Curves for Side Thorax	65
Figure 30. Transfer Point Acceleration Curves for Side Thorax	66
Figure 31. Velocity Scaling Parameter for Side Head Impacts	69
Figure 32. Acceleration Scaling Parameter for Side Head Impacts	71
Figure 33. Maximum Strain Criterion for Human	73
Figure 34. Scaling Factor for Thoracic Impact Injury Sensitivity	75
Figure 35. Average Pressure vs Injury Index for Primate Side Abdominal Impacts with Scaled Arm Rest	77
Figure 36. Experimental Scaling Factor for Abdominal Impact Injury Sensitivity	79



## TABLES

	Page
Table 1. Summary of Long Duration Sub-Human Primate Head Impacts	38
Table 2. Summary of Long Duration Human Head Impacts	40
Table 3. Summary of Primate Side Thoracic Impacts	47
Table 4. Cadaver Side Thoracic Impact Data	49
Table 5. Summary of Primate Side Abdominal Impacts	56
Table 6. Summary of Torso Side Impacts for Primates	59
Table 7. Summary of Direct Organ Impacts	64
Table 8. Summary of Scaling Parameters for Long Duration Head Impacts	72
Table 9. Summary of Abdominal Tolerance Values	82

## ACKNOWLEDGEMENTS

This research program was carried out by the staff of the Biosciences Division of The Highway Safety Research Institute, the University of Michigan. The authors would like to thank Mr. Arnold Johnson for his special guidance, suggestions, cooperation and support. We are also indebted to Glenn Myers and Dinesh Mohan for their assistance in animal and cadaver preparations as well as collection and reduction of data. Special thanks go to Dr. Michael Trollope of The University Hospital, Surgical Section.

## 1.0 INTRODUCTION

This report describes the work performed for the National Highway Traffic Safety Administration under Contract No. DOT-HS-031-2-382, entitled, "Door Crashworthiness Criteria."

In the performance of this study, the Contractor was required to perform the following tasks within the limits of time and funds available:

1. The Contractor shall perform with yielding and padded surfaces side impacts to the heads of sub-human primates and to human cadavers so that the data generated will validate a human tolerance curve for those impacts whose duration exceeds ten milliseconds.

2. The Contractor shall perform side impacts to the torsos of sub-human primates and to human cadavers so that the data generated will permit the development and validation of a suitable mechanical model that will significantly improve the accuracy of extrapolating this data to humans. The end products will be appropriate and validated human tolerance curves for various types of side impacts to the torso that would be expected to occur in side impacts to motor vehicles.

### 1.1 SIDE IMPACTS IN HIGHWAY SAFETY

The National Safety Council and the Bureau of Public Roads' statistics on auto accidents indicate that in the United States 6,000 people die every year from injuries sustained in side collisions (Green, 1973). According to the Automotive Crash Injury Research (ACIR) project at Calspan (1967), side collisions accounted for 13.3% of all injury producing accidents, but were responsible for 18.5% of the dangerous or fatal injuries (Green, 1973). These facts clearly demonstrate the need for thorough research into all aspects of side collisions.

## 1.2 CURRENT RESEARCH KNOWLEDGE

There is a considerable lack of factual knowledge involving human response to lateral ( $\pm G_y$ ) acceleration forces. A large number of studies have been made on impact tolerance involving vertical, forward or rearward accelerations but relatively few have been conducted for lateral accelerations. Most of these studies used restraint systems which were considerably different from those provided in today's automobiles.

Tests utilizing baboons as subjects (Snyder, et. al., 1967) resulted in findings which indicate that at every level of impact studied (15 to 44 G) there were significantly greater injuries in lateral impacts than in forward impacts. These tests, unlike the earlier ones conducted with bears (Clarke, 1962), chimpanzees (Stapp, 1952, 1955), and Rhesus monkeys (Robinson, 1963), were conducted with the minimal restraint of a lap belt and their results may have greater significance to the lap belted human automobile occupant. Five animals received ruptured bladders, contusions, tears, lacerations or completely severed uterus. The ruptured bladders were reported in the lateral impact cases only. In addition, three of the lateral impacts caused cervical fractures and a complete atlanto-occipital separation and transection of the spinal chord occurred in one 30 G impact. A very significant, though quite unexpected, finding was that of pancreatic hemorrhage in all lateral cases autopsied. Subsequent investigations were conducted on baboon subjects exposed to lateral impact wearing 3 point, Y-yoke, or a European type upper torso single diagonal belt (Snyder, et. al., 1968b, 1967a).

Human volunteer lateral impact tests have been conducted by Clarke (1963), Weiss (1963), Chandler (1966), Reader (1967), and Payne (1961). They used various sophisticated restraint systems and report no injuries for sled accelerations up to 18.7 G's.

There apparently has been only one published study involving impact tolerances of the human while restrained by lap belt only. In 1963, Zaborowski, Rothstein, and Brown published the first medical investigation of humans (restrained by lap belt only) in lateral impacts. These impacts had to be discontinued at 9 G (with impact durations of 0.1 sec) due "to subject discomfort with prolonged stiffness and soreness in the neck musculature." Fifty percent of the subjects complained of physical discomfort at 6 G.

A more recent study of more than 100 lateral impacts at 9.2 to 10.0 sled G (12 to 14 chest G) is still unpublished (Sonntag, 1966). One subject fainted and another subject received severe neck muscle strain. In other tests of human volunteer tolerance in side impact, from 18 to 92° body orientation (from the forward facing position), Beeding (1958) has reported effects of chest pains, headaches up to 18 hours, brief disorientation, or difficult breathing, a single case of mild ischemia, hyoid dislocation, shock, and albuminuria. In another test, zero blood pressure was recorded immediately post run in one subject.

The physiological effects of lateral impact as found from both human and animal impact tolerance research studies have been summarized by Eiband (1965), Snyder (1966, 1969b) and by Stapp (1968, 1969). Results to date indicate that the human body is less tolerant to  $\pm G_y$  accelerative forces than to either  $\pm G_x$  or  $\pm G_z$  accelerations.

In 1971, a coordinated effort to determine human tolerance to lateral impact was undertaken at the Highway Safety Research Institute of The University of Michigan. That study, entitled "Door Crashworthiness Criteria," (Stalnaker and McElhaney, 1971) was the immediate predecessor of the present study.

This earlier study consisted of 45 short duration side head impacts, 13 impacts to the upper abdomen, 7 to the thorax and 15 whole body impacts. All subjects were living infra-human primates. One human cadaver side head impact was also conducted. All impacts were conducted under conditions specifically designed to simulate those of an automobile side collision.

In conjunction with the above mentioned impact studies, a quantitative model for side head impacts was developed. Parameters were determined so that side head impacts to infra-human primates could be scaled to analogous impacts to living humans.

The present study incorporates most of the data of the earlier study. In addition, side head impacts were conducted on human cadavers and on living infra-human primates. The cadaver impacts were coordinated with the animal impacts so that the combined data could be used to construct a matrix which would represent the behavior of a living human in a side head impact. This was accomplished by combining the mechanical response information from the cadaver impacts with the physiological response information from the animal impacts.

The response of the infra-human primates to head impacts is very similar to that of a living human. The important differences are evident in the mechanical behavior of the system studied and arise from differences in size and proportion of the subjects. The human cadaver side impacts are used to provide accurate information about the mechanical behavior of the living human.

The first door crashworthiness study did not provide sufficient data for analysis of problems in the following areas: long duration head impacts, impacts to the thorax, and impacts to the lower abdomen. This study complements the previous one by providing data in the above mentioned areas.

## 2.0 EXPERIMENTAL STUDIES

### 2.1 INTRODUCTION

During the contract FH-11-7288, 1971, "Door Crashworthiness Criteria," a substantial amount of experimental injury data was generated. Accident data for motor vehicles involved in side impacts indicate that most occupant deaths were due at least in part, to head injuries suffered when the head struck windows, door pillars, and other rigid objects. Therefore, most of this data was generated by impacts to the head of short duration against unyielding surfaces. This data was extrapolated to man by use of dimensional analysis and the theory of modeling. These results were then presented as tolerance curves generated by the Maximum Strain Criterion (MSC) for head injury.

The torso side impact injuries were produced by a blunt wedge shaped impactor simulating an arm rest, and a large flat impactor that contacted the animal over the whole torso. The results of the blunt wedge impacts were presented as curves of the average peak contact pressure (computed by dividing the peak impactor force by the maximum projected impactor contact area at maximum penetration) and impactor velocity versus the injury levels. It should be noted that the slopes of these curves were small, indicating that only small changes in either contact pressure or impactor velocity greatly changed the injury level. The depth of penetration of the impactor was also found to be an important variable in determining tolerance levels.

Dimensional analysis of this data did not produce an identifiable pattern for torso injury criteria owing to the lack of a suitable torso injury model. In the present experimental study, the data base was expanded for the head injury criterion and the torso.

## 2.2 EXPERIMENTAL METHODS

Five primates (Figure 1) were considered for these tests:

1. Saimiri sciurius squirrel monkey [SM]
2. Macaca mulatta Rhesus monkey [RH]
3. Papio cynocephalus baboon [BA]
4. Pan satyrus chimpanzee [CH]
5. Homo sapiens man (cadaver [MA])

Baboons were not used in the side head impact experiments in either this study or the 1971 "Door Crashworthiness Criteria" (DCC) report because of large differences in the shape and the dynamic response of human and baboon heads. All the other species used in the head impact study fit the human Maximum Strain Criterion head model developed by Stalnaker and McElhaney (1970, 1971). Chimpanzees were not used in the torso impact tests because of their unavailability in large numbers.

All test animals were housed in the Biomedical Laboratory Vivarium in the Highway Safety Research Institute for a minimum of two days. During this time the animals were examined and their physical condition recorded. This pre-impact physical condition was used as the basis for comparison with the post-impact condition to evaluate the extent of injury.

The animal to be tested was anesthetized with 30 mg/kg of Vetalar [dl 2-(0-chlorophenyl)-2-(methyldamino) cyclohexanone Hydrochloride)]. This drug is a rapid-acting general anesthetic which produces a state characterized by profound analgesia, normal pharyngeal-laryngeal reflexes and normal or slightly enhanced skeletal muscle tone. With this drug the post impact state of consciousness can be determined. The good muscle tone provided by this drug made the test conditions more realistic and representative of the responses of the alert animal.



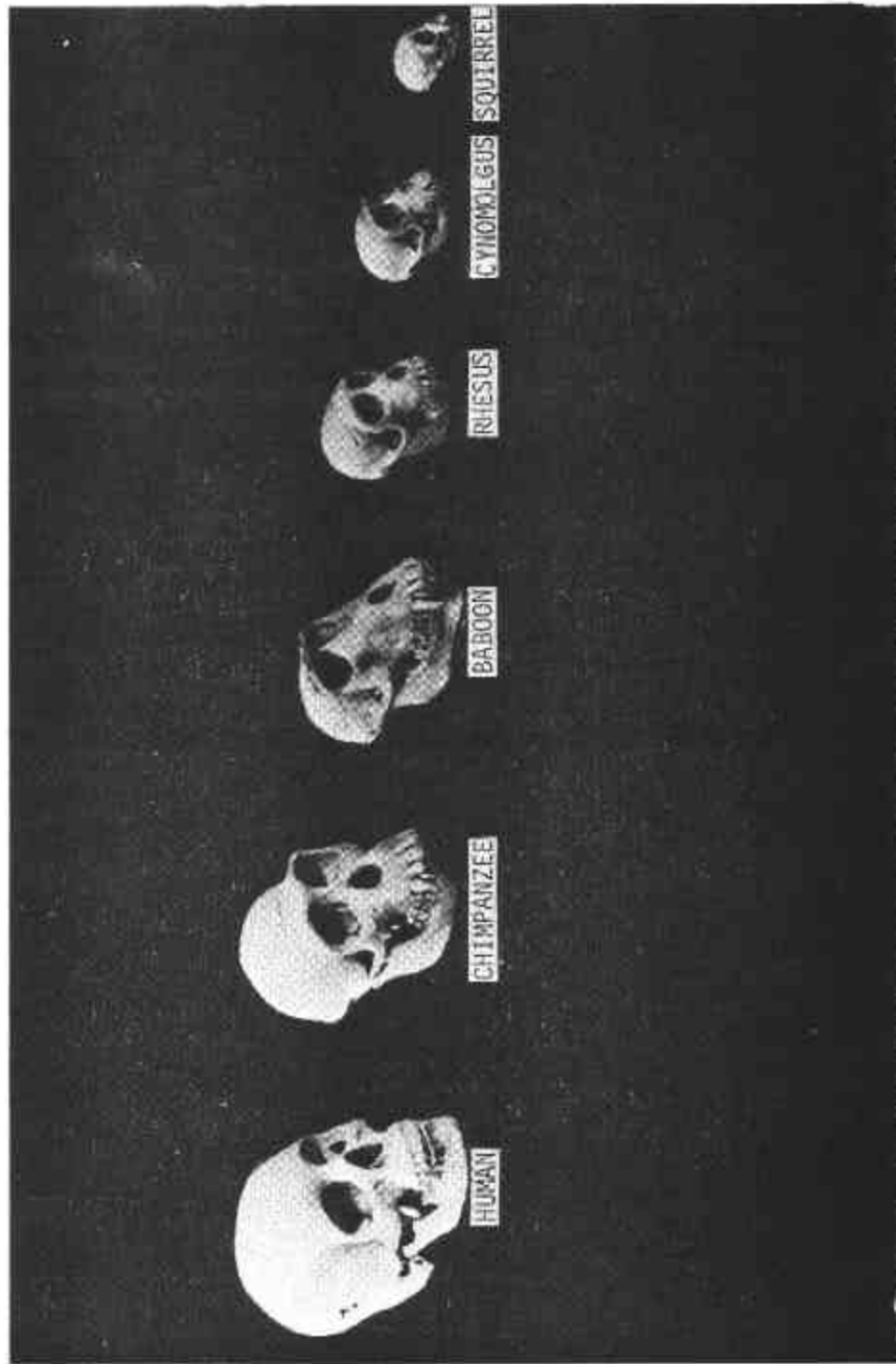


FIGURE 1. SKULLS OF PRIMATES

The radiographic laboratory, vivarium, impact facility, operating room and the autopsy room are all in close proximity in the biomedical laboratory. This arrangement made it very convenient to move the animal from one area to another throughout the test sequence. A hospital type Picker radiographic unit with a capacity of 300 MA and 140 KvP was available for radiographic uses.

The animal was fully anesthetized, shaved and targeted for high speed photographic analysis. The animal was then taken to the impact room where respiratory rate and reflex state were recorded. Complete anthropometric measurements were taken for each test animal. The test animal was seated for the impact tests on a bench type seat and supported by surgical thread through the ears. This method of support makes the animal essentially a free body. It was found to provide reproducible results and eliminated the complicated boundary conditions of a restraint seat or sling.

All impacts were carried out by a pneumatically operated testing machine specially constructed for impact studies. The machine consists of an air reservoir and a ground and honed cylinder with two carefully fitted pistons. The transfer piston is propelled by compressed air through the cylinder and transfers its momentum to the impact piston. A striker plate attached to the impact piston travels a distance of three to six inches and an inversion tube absorbs the energy of the impact piston and halts its movement after impact.

The stroke of the impactor was precisely controlled by its initial position, and its velocity was controlled by the reservoir pressure. The impactor was instrumented with an accelerometer and an inertia-compensated force transducer. High speed motion pictures (3000 fps) were taken for photometric analysis (Figure 2).

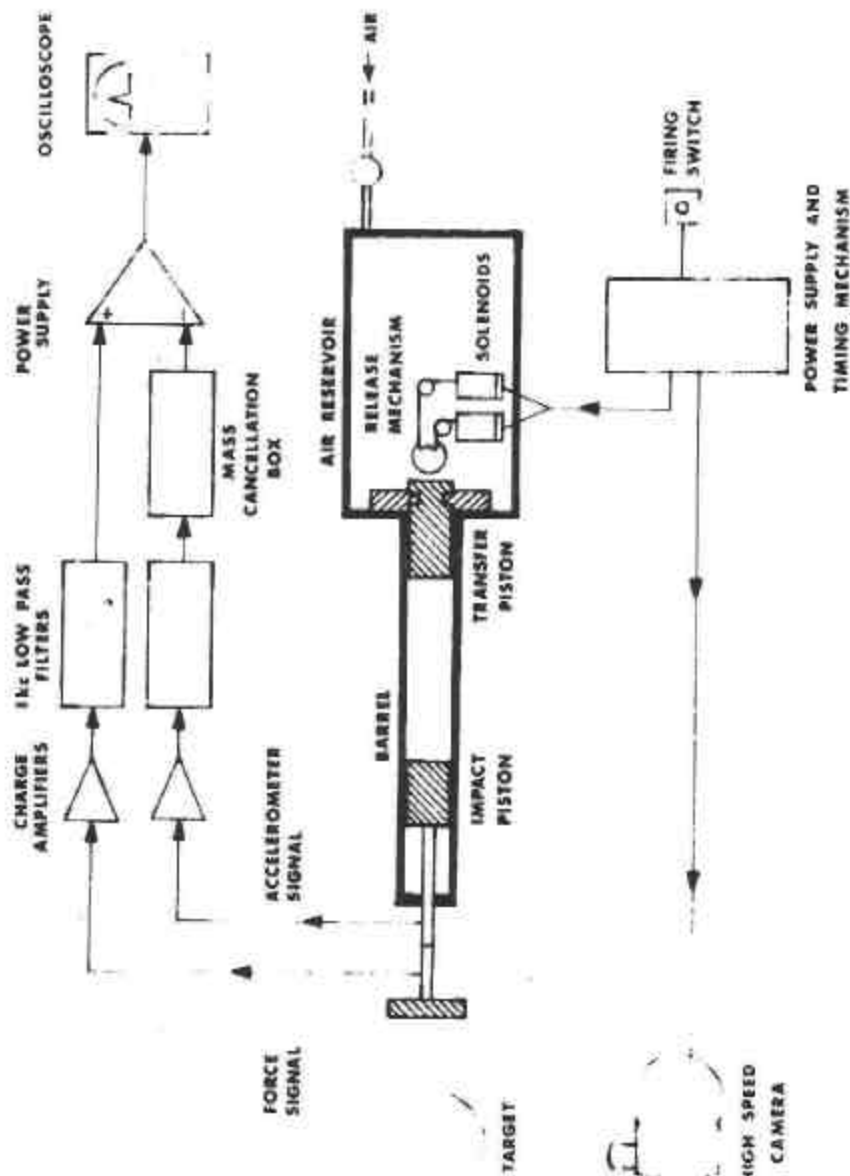


**FIGURE 2. BLOCK DIAGRAM of HEAD IMPACT FACILITY**

Fresh, unembalmed cadavers obtained from the Anatomy Department of The University of Michigan Medical School were used in this study. Each cadaver was stored at 37° F for one to seven days between time of death and impact. The specimens were then transported to HSRI and allowed to reach room temperature before testing. These procedures insured that the effects of rigor mortis had disappeared and that the blood was again fluid.

#### 2.2.1 Padded Head Impacts

##### 2.2.1.1 Sub-human Primate Head Impact Study

A Wilcoxon biaxial accelerometer was used to record head accelerations for the sub-human primate study. The accelerometers were glued to the skull with Eastman-910 at a point directly opposite the point of impact (Figure 3).

Based on the MSC tolerance curves obtained in the 1971 DCC report, a series of long duration head impacts was conducted. The shortest pulse durations in the constant acceleration portion of the MSC curve were selected as the desired pulse duration for this set of head impacts. These are indicated by a triangle at the appropriate point on each curve in Figure 4.

The pulse duration was controlled by using different kinds of padding on the impactor. Polystyrene cellular plastics of three material densities (1.0, 3.4 and 1.2 pounds per cubic foot) were used as padding. Different levels of injury were obtained by varying the impact velocity for a particular pulse duration.

The test animal was placed with its head a predetermined distance from the impactor so as to allow for the proper crush distance of the padding material without overextending the neck during impact (Figure 5). The weight of the impactor used in this study was 22 pounds, approximately five times the head weight of the largest monkey used. This was designed to insure

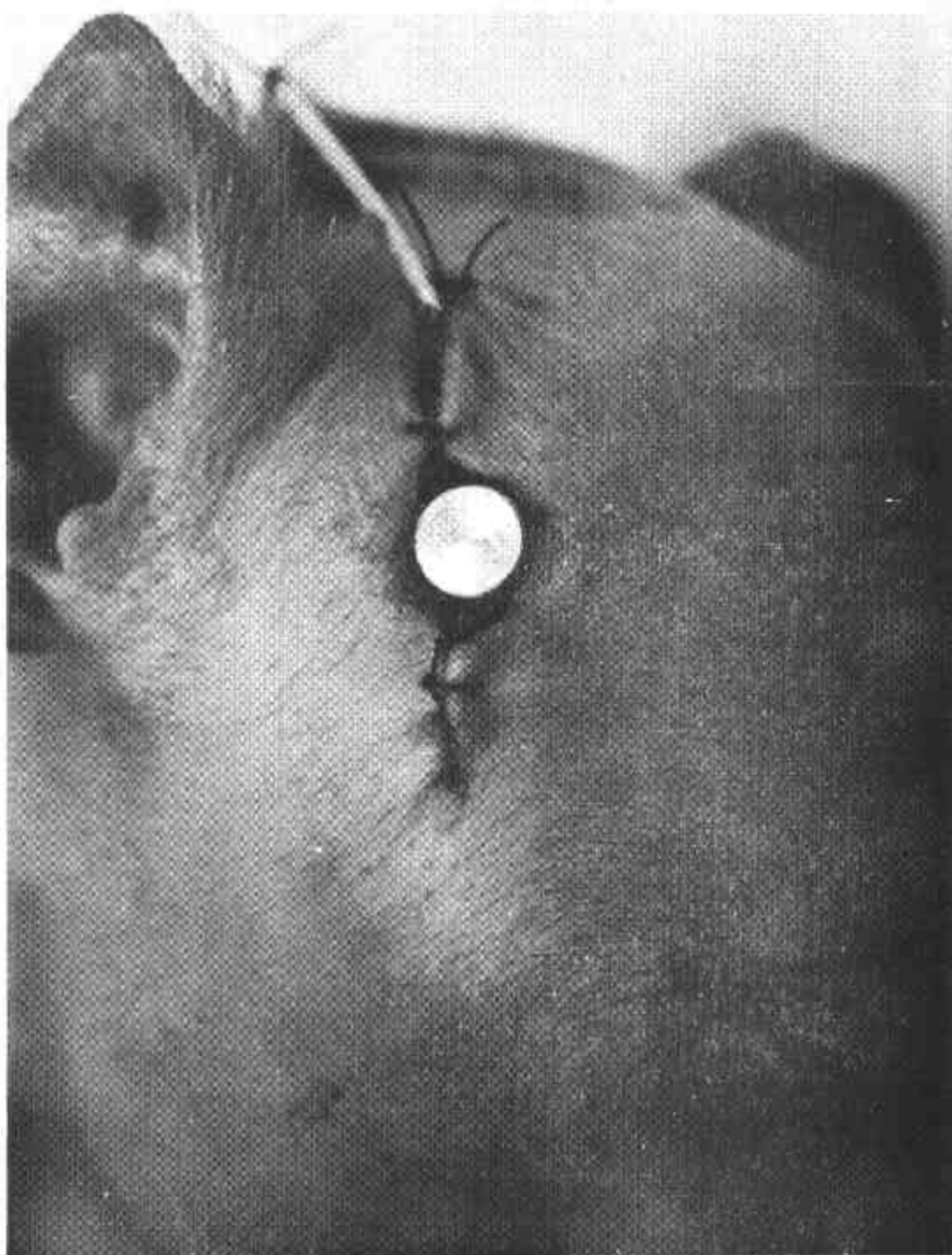


FIGURE 3. ACCELEROMETER MOUNTING FOR HEAD IMPACTS

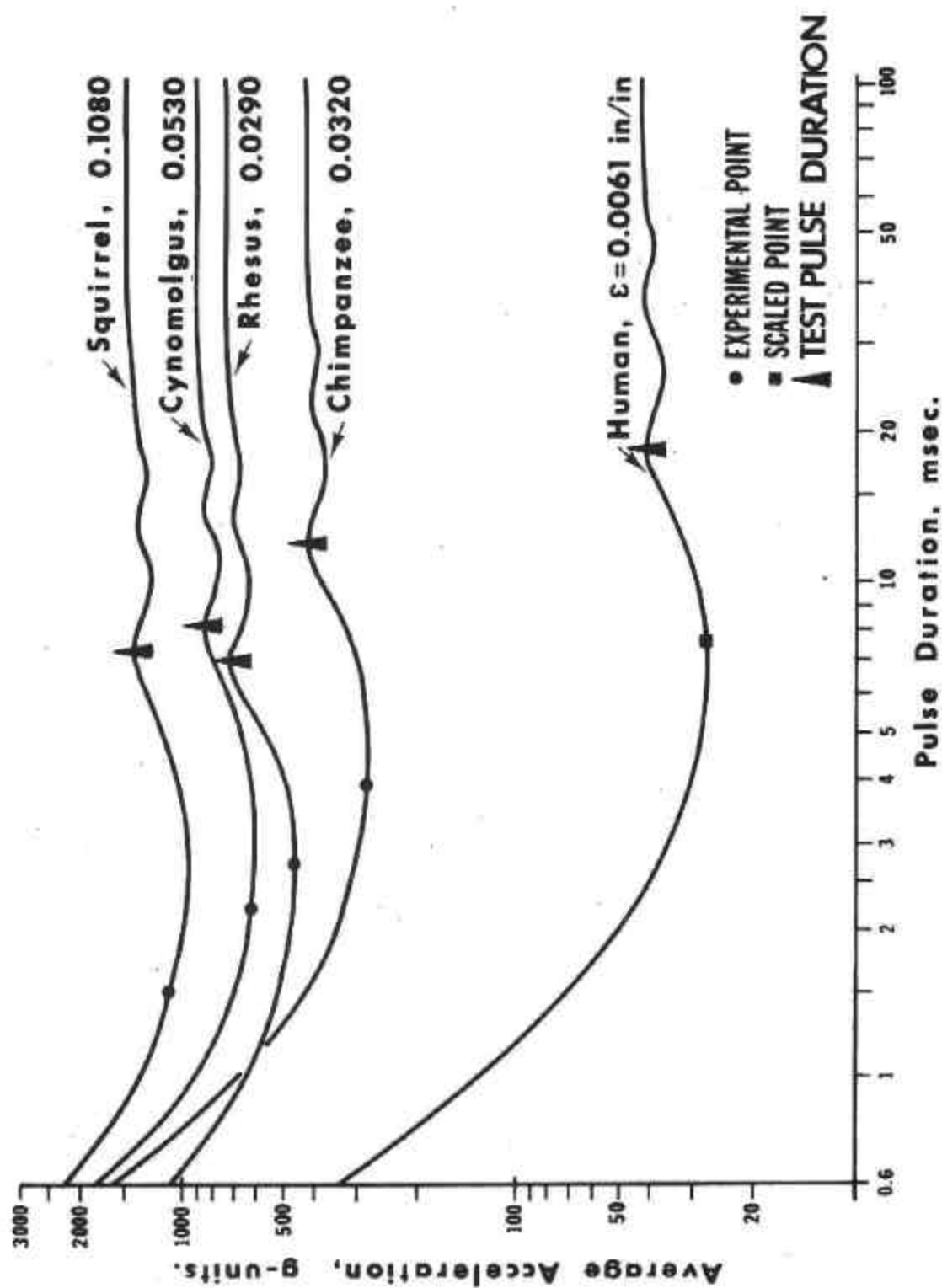


FIGURE 4. MAXIMUM STRAIN CRITERION FOR PRIMATES,  
SIDE HEAD IMPACTS (TRIANGULAR PULSE)

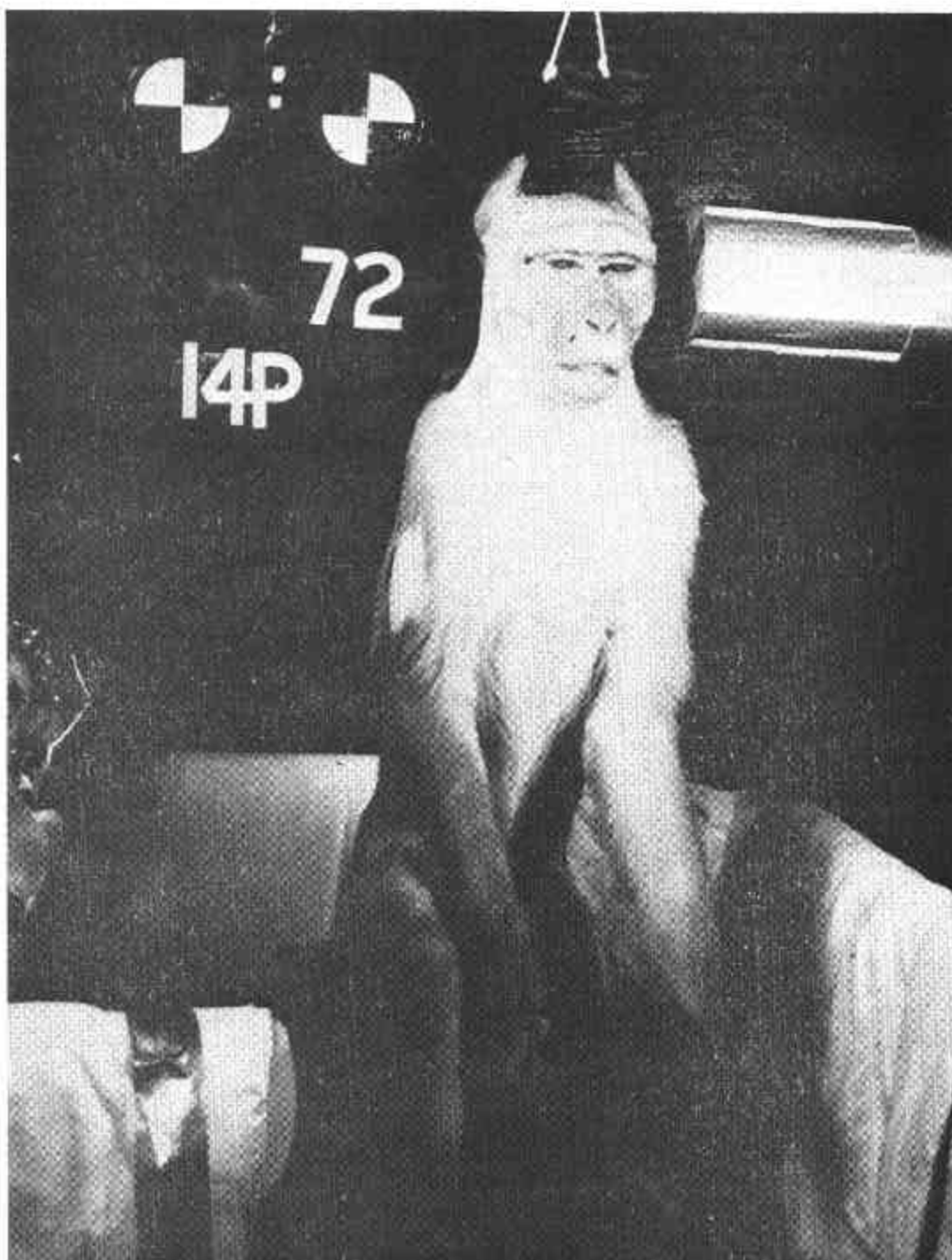


FIGURE 5. PRIMATE SIDE HEAD IMPACT SET-UP (RHESUS SHOWN).



that the impactor did not slow down significantly when it struck the primate's head. The force-time plots and acceleration-time plots were recorded on a light beam oscillograph. The high speed movies of each test were analyzed and processed on a Vanguard film analyzer. Computer assisted differentiation and smoothing techniques were used to determine the angular velocity and acceleration of each head impact.

#### 2.2.1.2 Human Cadaver Head Impact Study

The point of impact was the left temporal region, two inches superior to the external acoustic meatus. Photographic targets for L-R head impacts were secured to the supra-orbital ridge, two inches on either side of the glabella (i.e., two inches either side of the mid-sagittal plane).

A biaxial accelerometer was mounted on a screw, which was driven into the skull at a point directly opposite the point of impact. Care was taken so that the accelerometer axes were normal and parallel to the impacting surface, not to the skull (Figure 6). The class 1000 frequency response value was used for all head accelerations as recommended by J211.

After being targeted and equipped with accelerometers, the cadaver was placed in a chair, which was modified for this impact study. All surfaces the cadaver could come in contact with in its post-impact movements were thickly padded with styrofoam to prevent damage to the cadaver. A special foam apparatus was employed to absorb the energy of the head and to protect the accelerometers from damage.

The cadaver was carefully positioned so that its head was in the correct position relative to the impactor and at the same time the whole cadaver was allowed to act as a free body. The head was suspended and held in place by



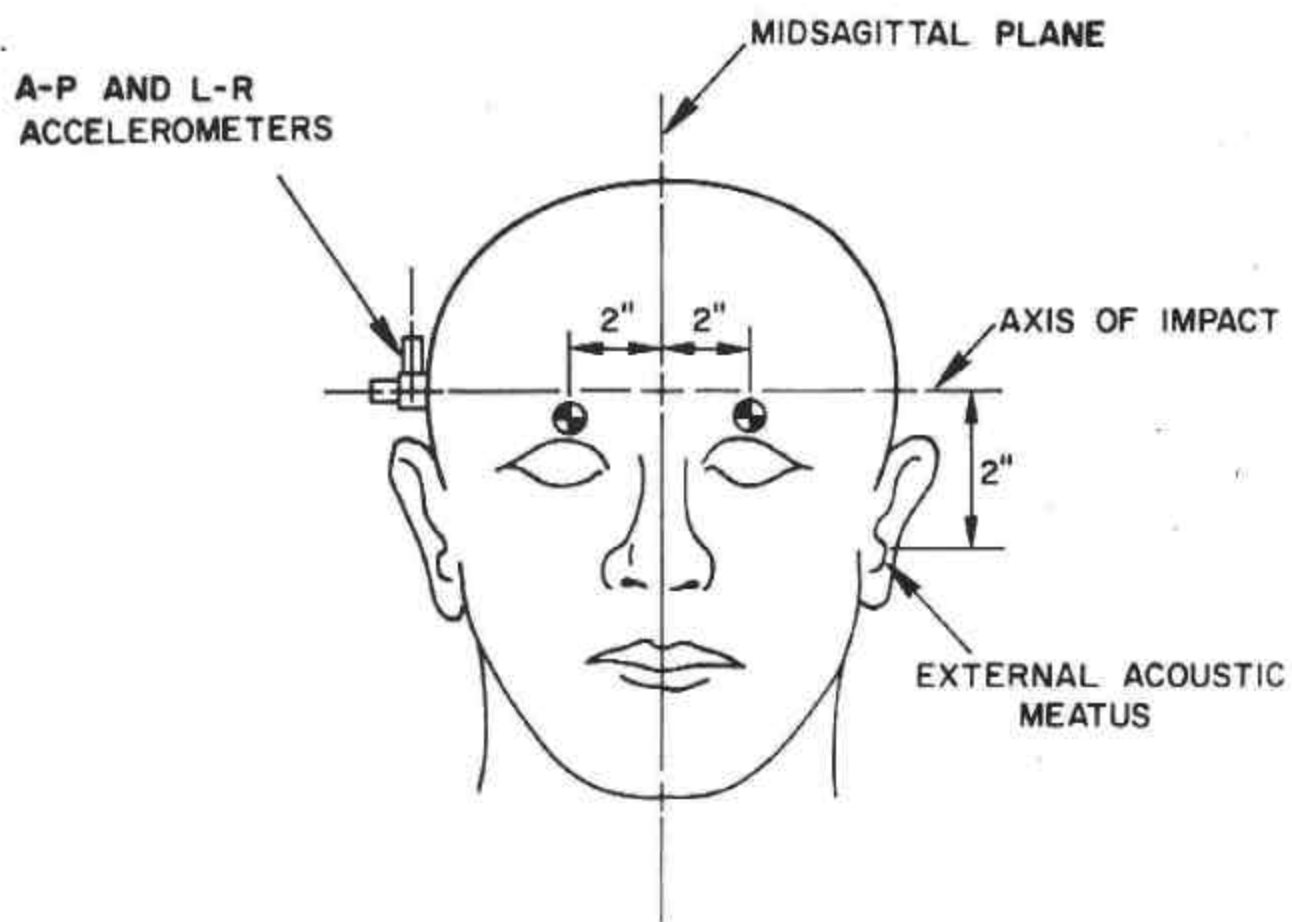


**FIGURE 6. TARGETING AND INSTRUMENTATION FOR SIDE HEAD IMPACTS.**

surgical thread. This thread supported only the weight of the head and broke easily on impact (Figure 7). The impacts were carried out in the HSRI Impact Facility described in the animal test set-up section of this report.

The same polystyrene plastic materials used in the animal study were used in the cadaver study to obtain a wide range of pulse durations. The impact velocity as well as the polystyrene materials were varied to give a wide range and combination of accelerations and pulse duration impacts. Pulse durations of up to 20 msec were needed to make these human head impacts comparable to those of the monkeys.

### 2.2.2 Torso Impacts

The thorax and abdominal body areas were divided into three major impact regions. Region I consisted of the thorax as located between the jugular notch of the sternum and the diaphragm. Region II was defined as including the area between the diaphragm (9th rib) and a horizontal plane transisting the abdomen along the inferior margin of the liver and stomach, and located approximately 1-3 cm superior to the umbilicus on the surface. Region III included the entire thorax and abdominal area, from the jugular notch to the iliac crest. All body impacts to Region I were carried out midway between the superior mediastinum and the diaphragm. All impacts were carried out with the axis of the impactor in the transverse plane. Impacts to Region III included all of Region III. All of these points were located as accurately as possible on sub-human primates before each test. The body regions are illustrated for the left and right side views in Figures 8 and 9.

All impacts made to Regions I and II used a 22-pound impactor with a scaled arm rest for contacting surface. This contacting surface was made from a 9 lb/ft<sup>3</sup> high density polyethylene foam to distribute the contact load. The

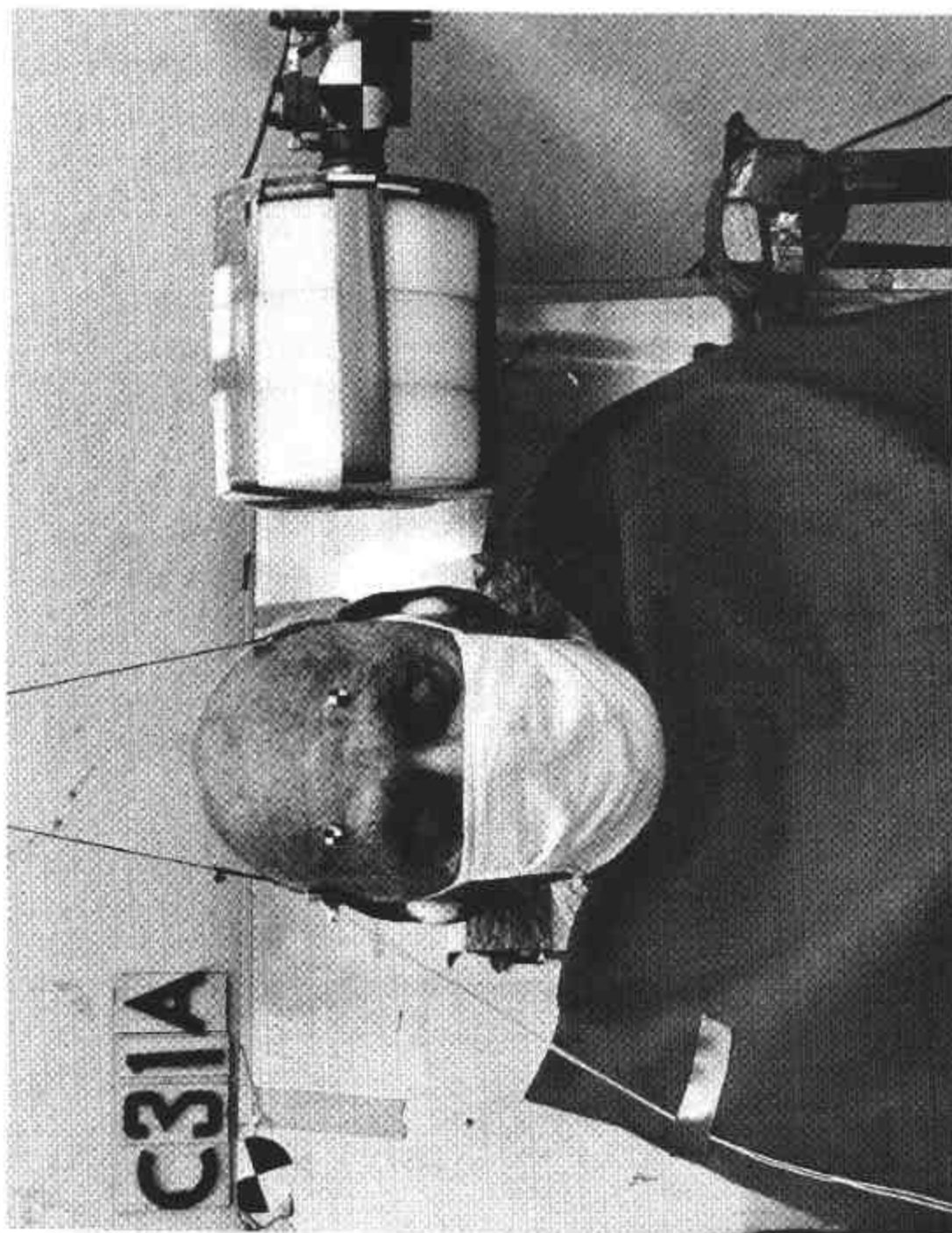
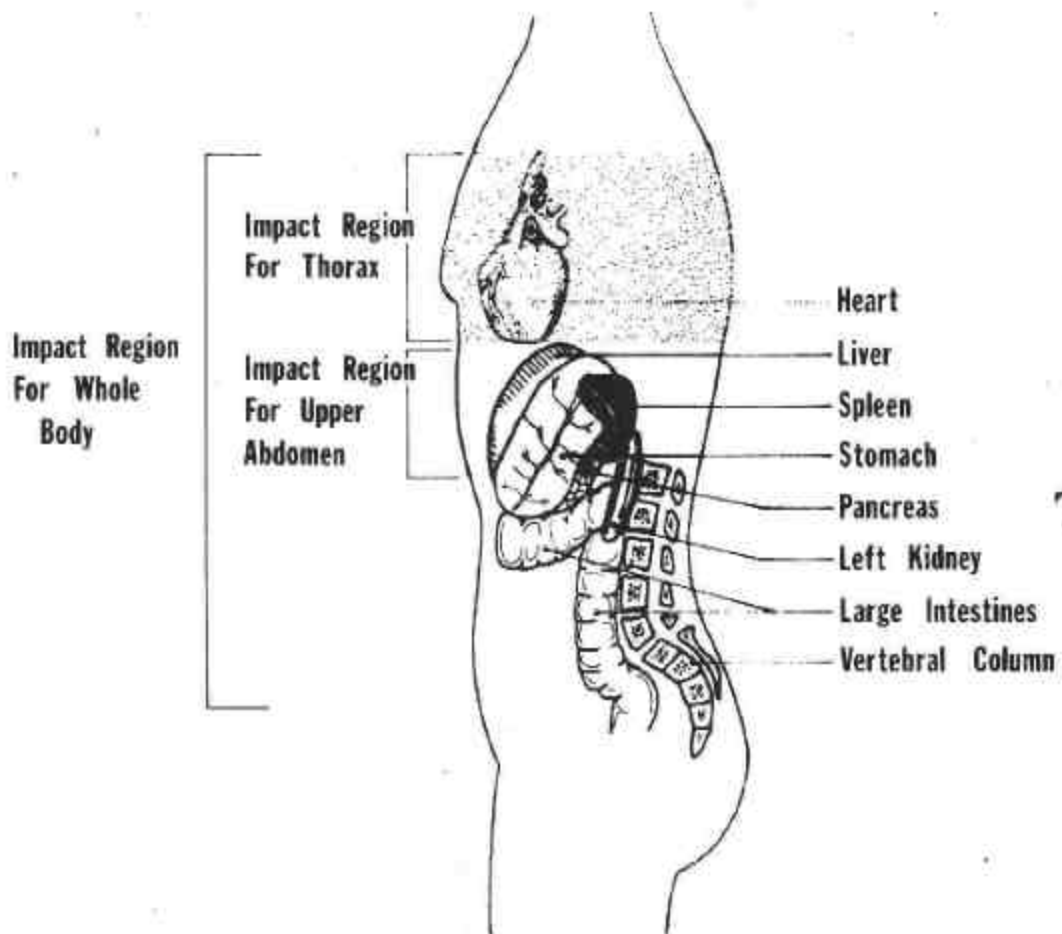


FIGURE 7. HUMAN CADAVER SIDE HEAD IMPACT (PADDED) SET-UP.



**FIGURE 8. BODY IMPACT REGIONS FOR LEFT SIDE**

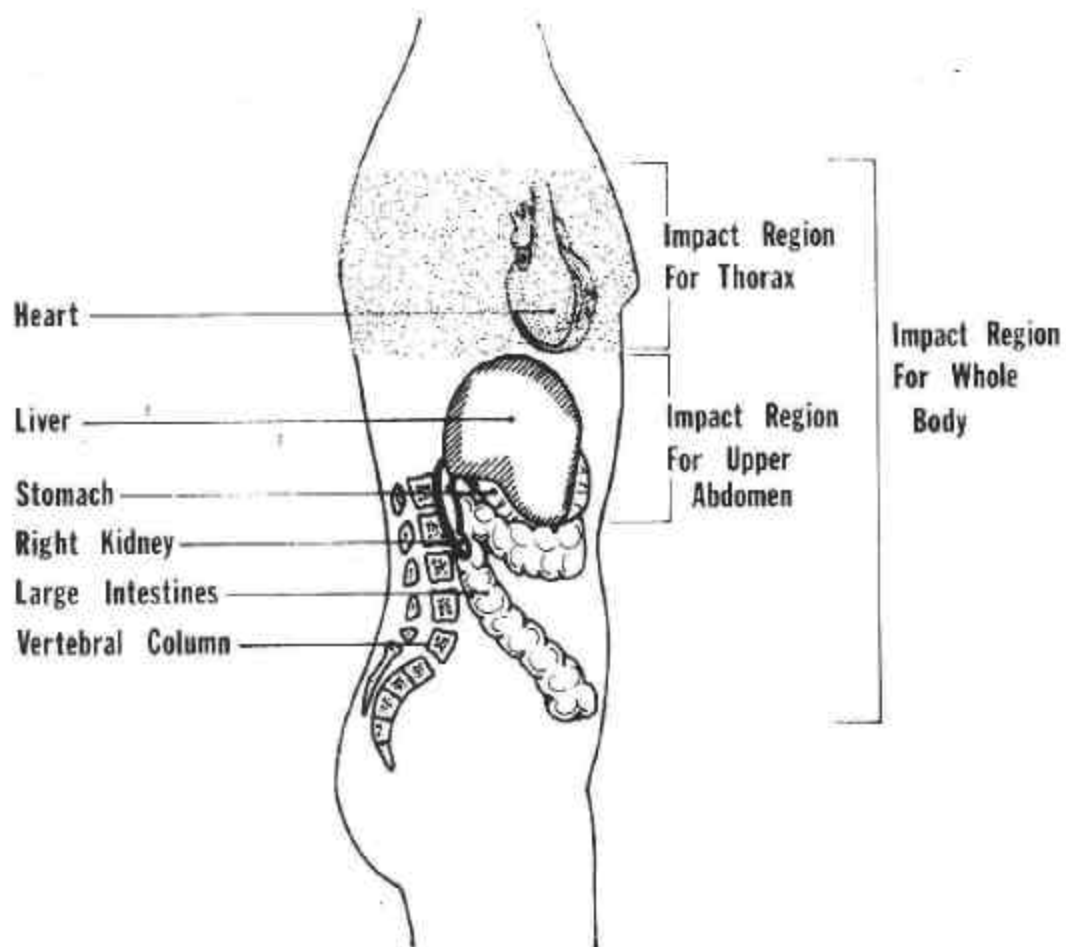


FIGURE 9. BODY IMPACT REGIONS FOR RIGHT SIDE

scaled arm rest was replaced by a scaled flat rigid plate for all impacts to Region III.

#### 2.2.2.1 Sub-Human Primate Impacts

The animals were positioned to limit the depth of penetration between 35% and 60% of body width, and a one-foot thick soft foam pad was arranged to prevent injury after impact.

The same testing procedure was used for each test sequence. The animal was impacted on the right side, and the injury evaluated. If the injury was not serious, then the next animal was impacted at a higher velocity. This procedure was continued until a serious injury was obtained. The next sequence of impacts was on the left side of the region completed (Figure 10).

The engineering parameters recorded for each test were force-time histories from an oscilloscope trace, depth of penetration from the photographic record, and velocity from an electronic chromometer.

#### 2.2.2.2 Human Cadaver Impacts

The cadavers were positioned in a heavily padded chair with no side supports. The test subject was held in an upright position by a harness under the arms, which was in turn fastened to a sliding mechanism over the chair. This support system was found to allow the cadaver to behave as a free body on impact, and still produce repeatable results (Figure 11). A 2" x 2" target for determining depth of penetration was fixed to the cadaver's side at a point directly opposite the point of impact. All cadaver thoracic impacts were made with the impactor centered over the 6th rib.

Two types of impactor heads were used in this study. One was a six-inch diameter rigid flat plate with 0.5 inch radius edges. The other head was a simulated arm rest made from the polyethylene material used in the animal study.

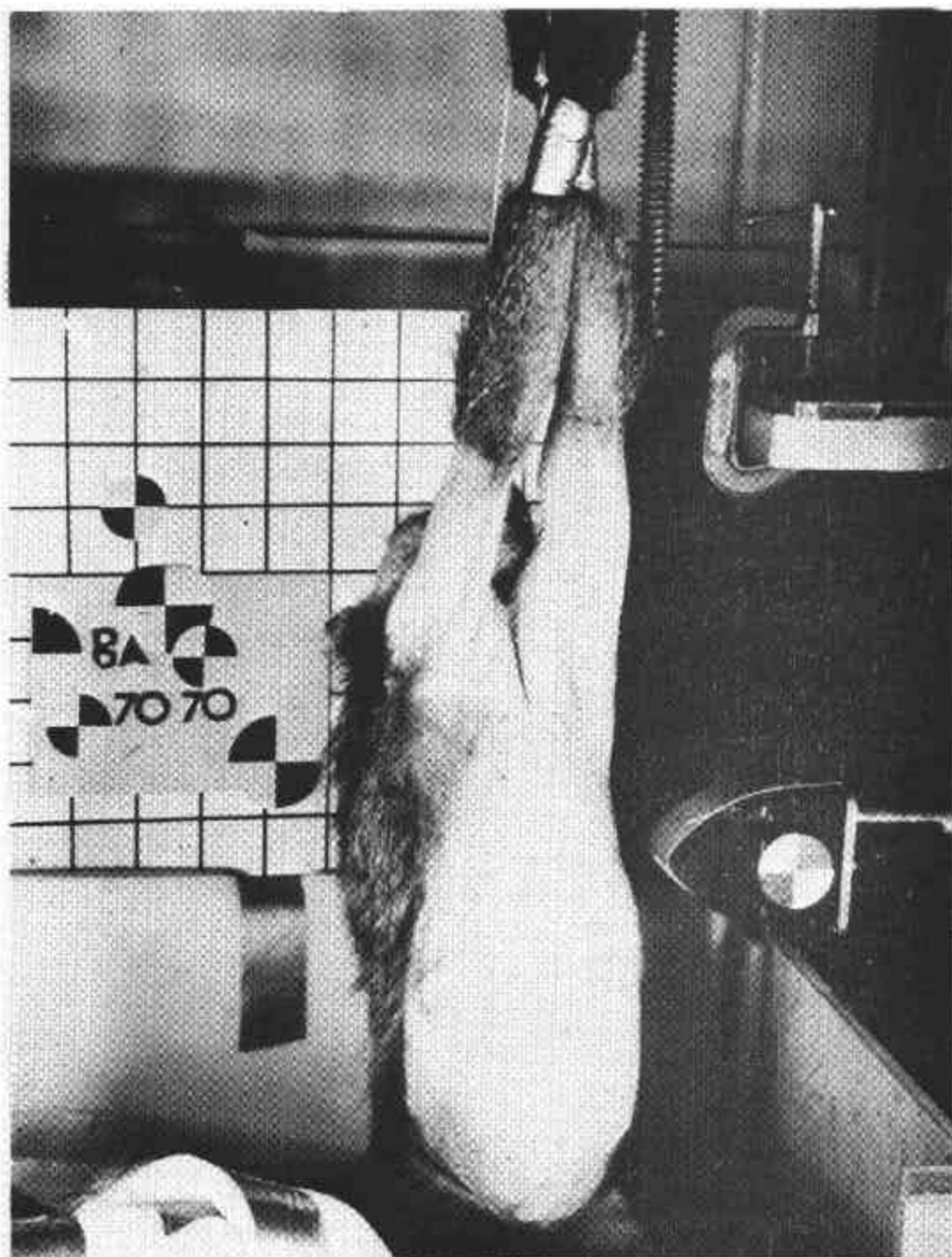


**FIGURE 10. PRIMATE SIDE TORSO IMPACT SET-UP  
(BABOON SHOWN)**

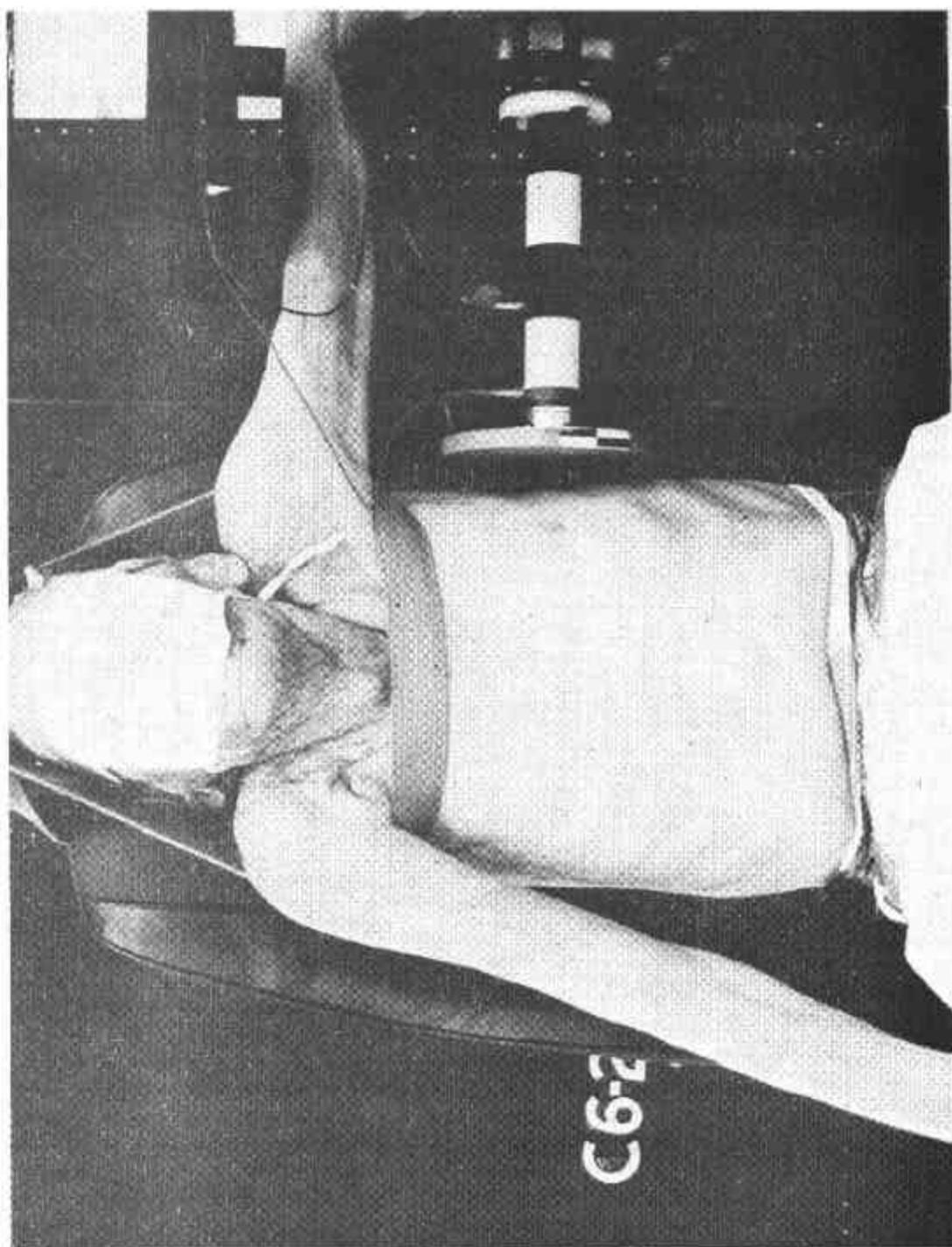


FIGURE 11. HUMAN CADAVER SIDE THORACIC IMPACT SET-UP



The weight of the impactor used in all tests was 22 pounds. This impactor weight was found to give a constant velocity impact up to three inches of penetration. Six side thoracic impacts were made with each head at two velocities. The depth of penetration was preset for any desired value between 1.8 inches and 3.8 inches.

### 2.2.3 Direct Organ Impacts

The purpose of this experiment was to quantitatively describe the relationship between impact parameters (energy, organ penetration, pressure, and impact velocity) and injury to exposed organs. The two organs studied were the liver and kidney because clinical experience indicates that these organs are most frequently injured in side impacts.

The organ to be tested was surgically mobilized in an anesthetized Rhesus monkey. The organ was laid onto a small load cell while still being perfused by the living animal (Figure 12). Load deflection curves were obtained for each impact. Impact velocity and depth of penetration were varied in turn to yield injuries of various severity levels.

The testing machine used in this study to provide both static and dynamic test data was the Plastechon High-Speed testing machine. This machine is an electrohydraulic servo-controlled unit with static load capacities of 3,000 and 12,000 lbs and a stroke of 11 inches. The ram velocity can be varied from a static rate of about 10 inches per minute, to a maximum servo-controlled rate of 12,000 inches per minute at the low load and 3000 inches per minute at the higher load rating. The maximum open loop rates are 30,000 and 12,000 inches per minute respectively.

The load cell used in the tests was a Kistler 933A Piezoelectric force link. This cell has a resonant frequency of 40KHz and compression load capacity of 6000 pounds. The ram displacement was measured by a Physitech Gage-It Optical Extensometer. The resulting data was recorded on storage

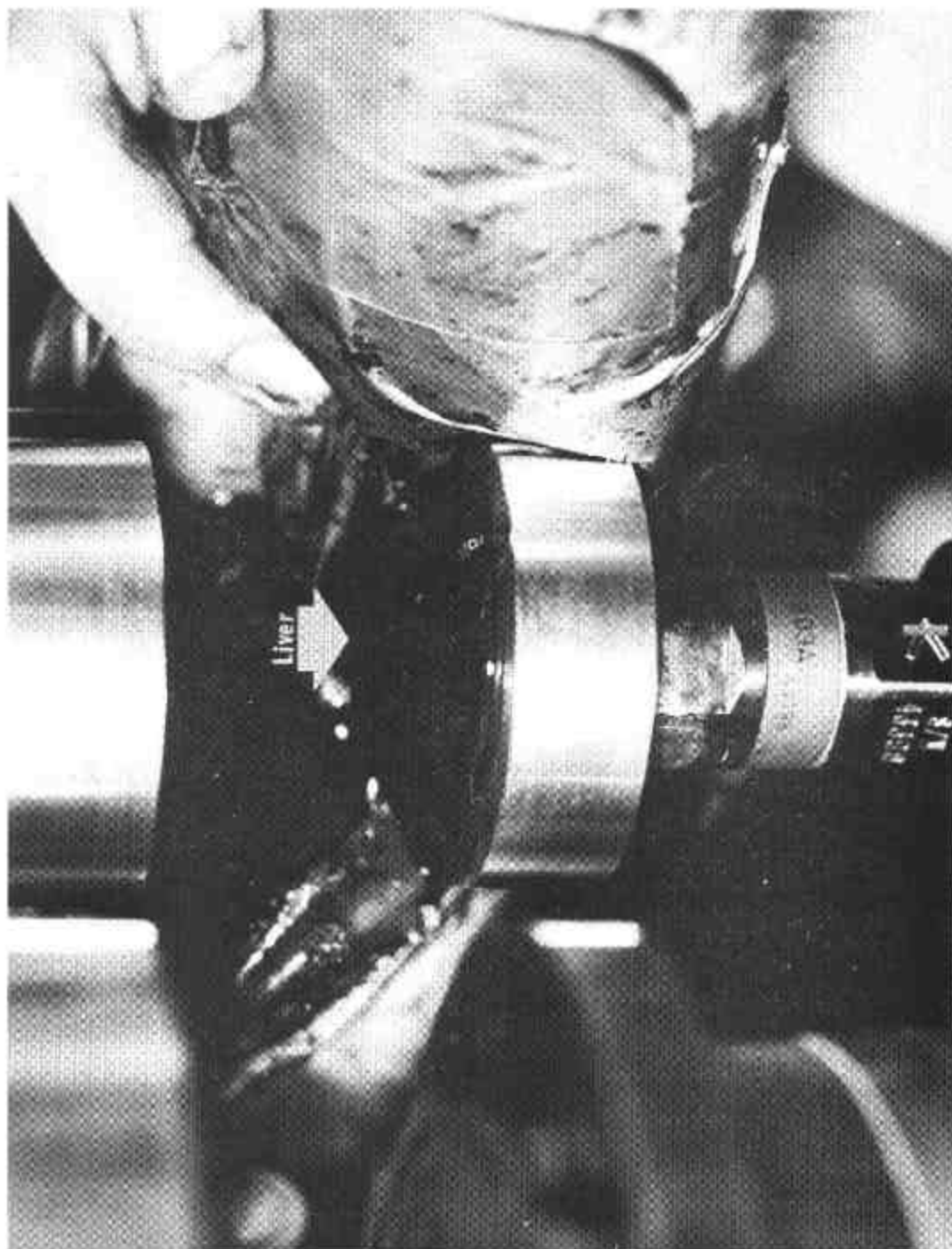


FIGURE 12. SET-UP FOR DIRECT ORGAN IMPACTS

oscilloscopes in two forms: organ load and ram displacement versus time and organ load versus ram displacement. Photographs of the oscilloscope traces were taken as a permanent record.

#### 2.2.4 Thoracic Mechanical Impedance

The design of protective devices for humans subjected to an impact or a vibrational environment requires a knowledge of their mechanical behavior in such environments. Consequently, much effort has been devoted to the concept of treating the human body as a mechanical system and cataloging the system response to mechanical energy transfer from the surrounding environment and its distribution throughout the system.

The overall mechanical response of man, or of a sub-system of man, is perhaps best characterized by its driving point mechanical impedance, defined as the ratio of driving force to velocity, which can be used to determine the energy transfer between environment and man for a known excitation. Impedance techniques thus have a two-fold purpose in biomechanical response: to model the body or sub-system of the body as a mechanical system and to minimize energy transfer in the design of isolation systems.

Each monkey used in this study was anesthetized with 25 mg/kgm I.V. of Sodium Pentobarbital. A six-millimeter circular hole for squirrel monkeys, a ten-millimeter circular hole for Rhesus, and a 15-millimeter circular hole for the baboon was cut in the test subject's thorax between the 4th and 5th rib on the side to be tested. An adapter was then attached to the rib cage as shown in Figure 13. The space between the rib cage and the adapter was then sealed to prevent any more air from entering the interpleural space. A hypodermic needle was then inserted into the interpleural space and the trapped air withdrawn by a syringe. The living monkey's thorax was then attached to the platen of a 300-pound electromagnetic shaker, and the rest of the body

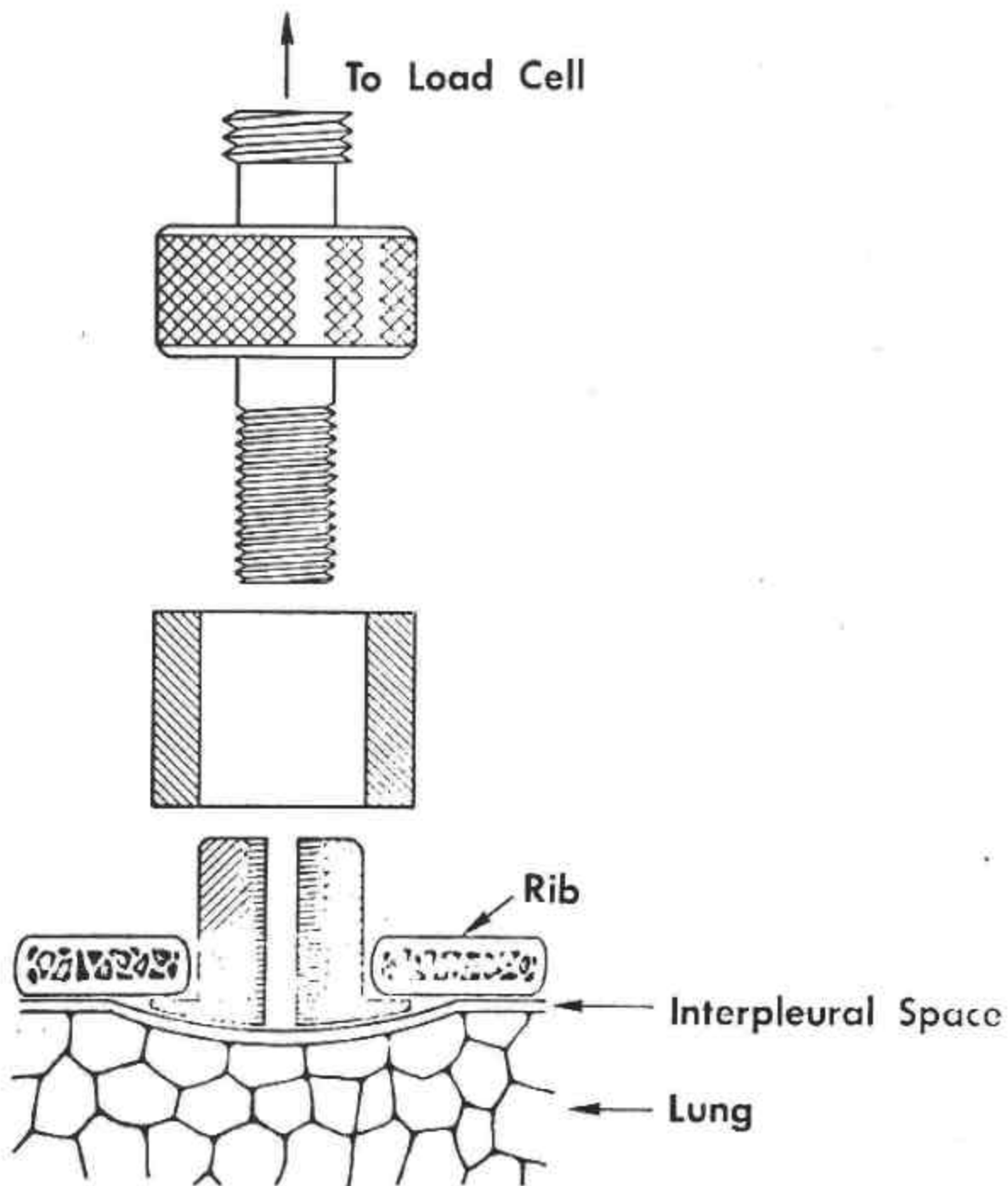


**FIGURE 13. LOADING FIXTURE**

was supported in a sling (Figure 14). The shaker servo-controller was set to apply a sinusoidal force to the thorax over the frequency range 5 to 100 Hz. A sweep oscillator was used to drive the shaker system while a mass cancelling automatic on-line impedance computer converted the force-time and acceleration-time information into plots of phase and impedance versus frequency. A one gram piezoelectric accelerometer with a low frequency response of one Hertz and a high frequency response to 1800 Hertz was attached to the fourth rib on the opposite side of the thorax from the shaker attachment. The acceleration was then recorded for the same frequency range used for the driving-point test. Runs were made at force levels of 50 and 100 pounds for the baboon, at 25 and 50 pounds for the Rhesus, and 5 to 10 pounds for the squirrel monkey. Driving-point and transfer point accelerations were recorded for each run. All monkeys survived the test and showed no injuries other than those caused by the surgery for attachment to the shaker.

The cadaver mechanical impedance tests were conducted in a manner similar to those of the monkey study. The load adapter used in the human cadaver study was 22 millimeters and the applied loads of 50 and 100 pounds. The accelerations on the opposite side of the chest were also recorded.

### 2.3 BIOMEDICAL DATA COLLECTION

Gross autopsy was conducted in the Autopsy Laboratory, specially equipped for dissection. Autopsies were conducted as a blind, according to accepted research procedure, with the investigator conducting the gross autopsy having no knowledge of physical data on the intensity, location of impact, or circumstances of each test. Careful anatomical dissection of the head, face and neck tissues, where head impacts occurred allowed discrete identification of many sites of vascular failure. When gross trauma was found

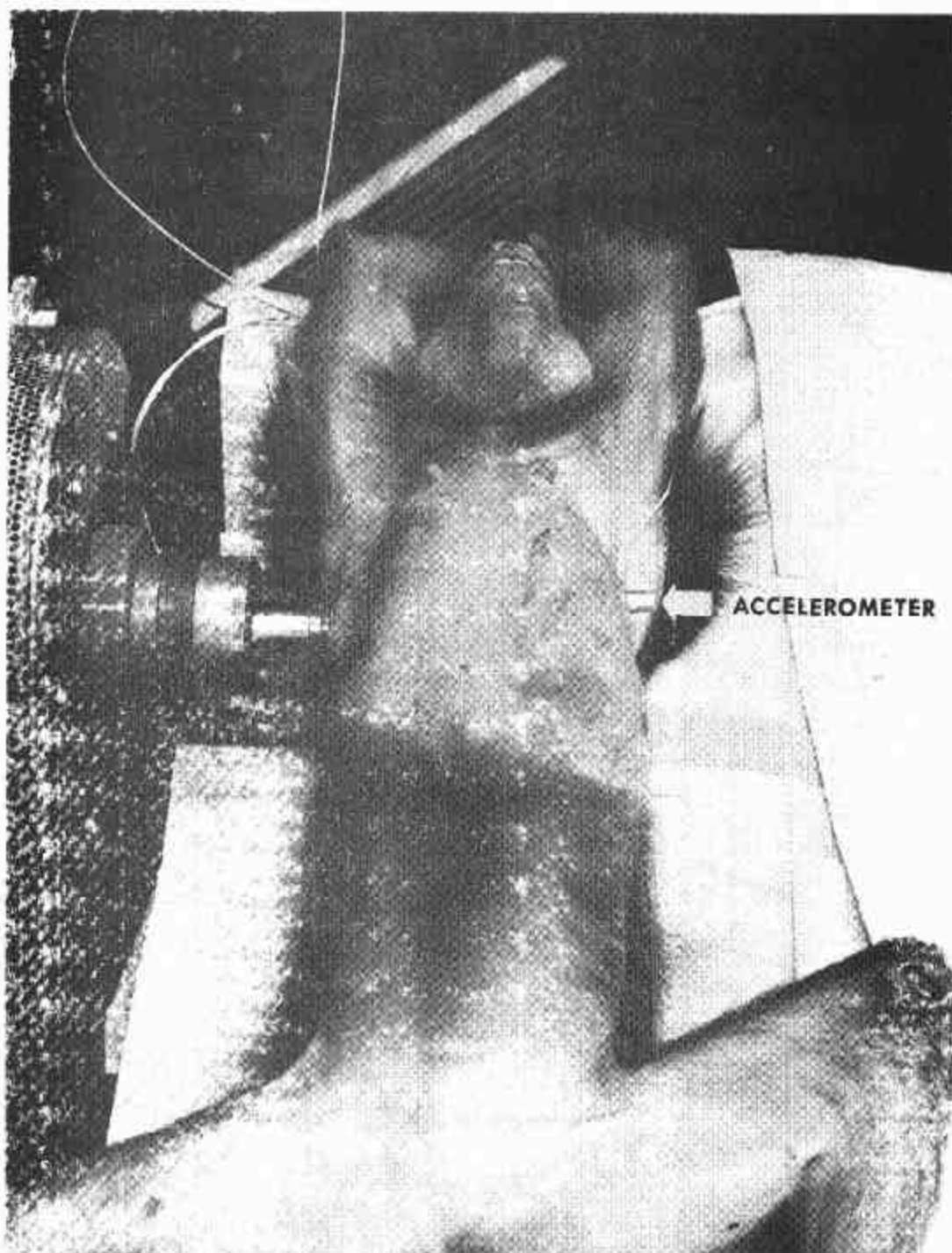


FIGURE 14. SIDE THORACIC MECHANICAL IMPED-  
ANCE TEST SET-UP.

The radiographic laboratory, vivarium, impact facility, operating room and the autopsy room are all in close proximity in the biomedical laboratory. This arrangement made it very convenient to move the animal from one area to another throughout the test sequence. A hospital type Picker radiographic unit with a capacity of 300 MA and 140 KvP was available for radiographic uses.

The animal was fully anesthetized, shaved and targeted for high speed photographic analysis. The animal was then taken to the impact room where respiratory rate and reflex state were recorded. Complete anthropometric measurements were taken for each test animal. The test animal was seated for the impact tests on a bench type seat and supported by surgical thread through the ears. This method of support makes the animal essentially a free body. It was found to provide reproducible results and eliminated the complicated boundary conditions of a restraint seat or sling.

All impacts were carried out by a pneumatically operated testing machine specially constructed for impact studies. The machine consists of an air reservoir and a ground and honed cylinder with two carefully fitted pistons. The transfer piston is propelled by compressed air through the cylinder and transfers its momentum to the impact piston. A striker plate attached to the impact piston travels a distance of three to six inches and an inversion tube absorbs the energy of the impact piston and halts its movement after impact.

The stroke of the impactor was precisely controlled by its initial position, and its velocity was controlled by the reservoir pressure. The impactor was instrumented with an accelerometer and an inertia-compensated force transducer. High speed motion pictures (3000 fps) were taken for photometric analysis (Figure 2).

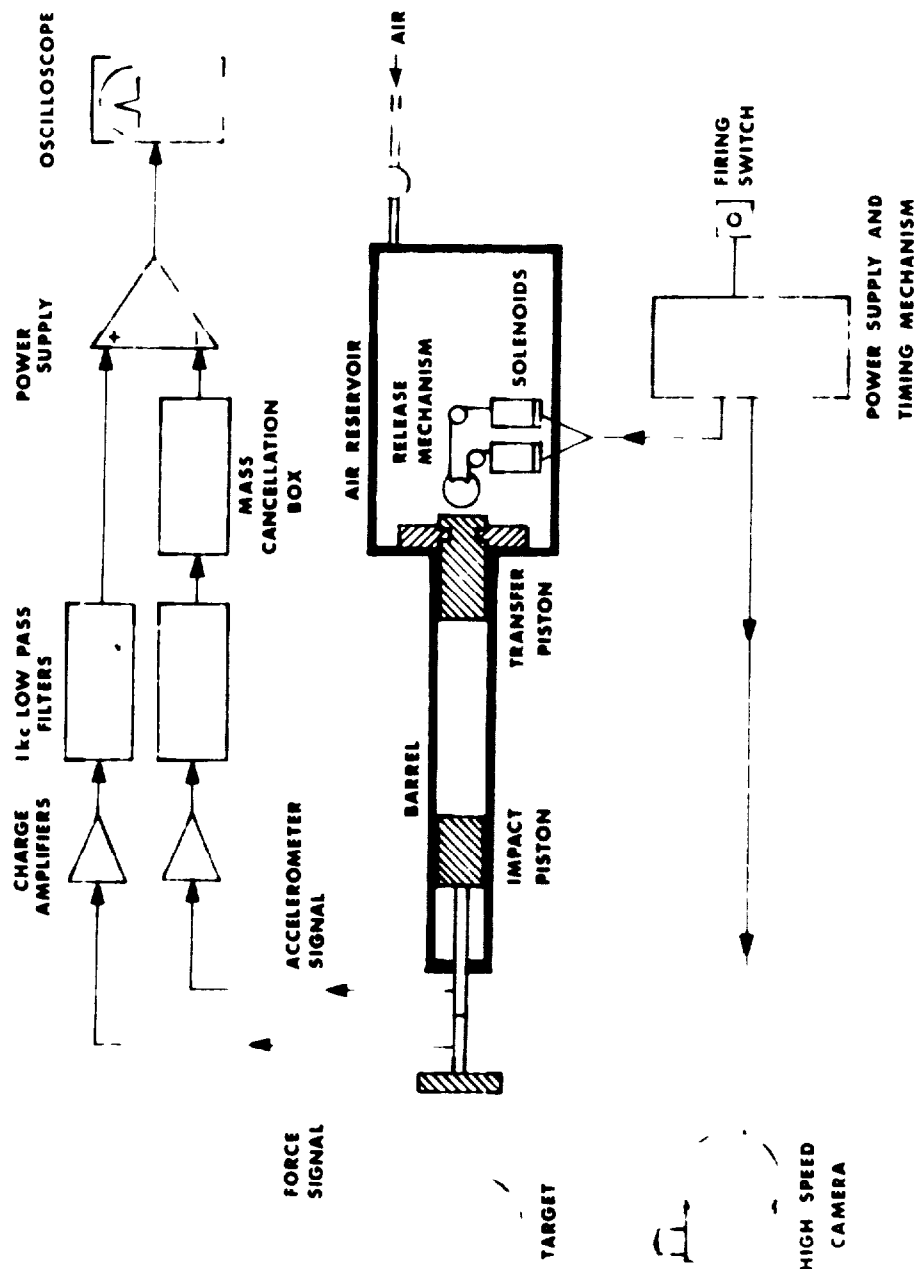


**FIGURE 2.BLOCK DIAGRAM of HEAD IMPACT FACILITY**



Fresh, unembalmed cadavers obtained from the Anatomy Department of The University of Michigan Medical School were used in this study. Each cadaver was stored at 37° F for one to seven days between time of death and impact. The specimens were then transported to HSRI and allowed to reach room temperature before testing. These procedures insured that the effects of rigor mortis had disappeared and that the blood was again fluid.

### 2.2.1 Padded Head Impacts

#### 2.2.1.1 Sub-human Primate Head Impact Study

A Wilcoxon biaxial accelerometer was used to record head accelerations for the sub-human primate study. The accelerometers were glued to the skull with Eastman-910 at a point directly opposite the point of impact (Figure 3).

Based on the MSC tolerance curves obtained in the 1971 DCC report, a series of long duration head impacts was conducted. The shortest pulse durations in the constant acceleration portion of the MSC curve were selected as the desired pulse duration for this set of head impacts. These are indicated by a triangle at the appropriate point on each curve in Figure 4.

The pulse duration was controlled by using different kinds of padding on the impactor. Polystyrene cellular plastics of three material densities (1.0, 3.4 and 1.2 pounds per cubic foot) were used as padding. Different levels of injury were obtained by varying the impact velocity for a particular pulse duration.

The test animal was placed with its head a predetermined distance from the impactor so as to allow for the proper crush distance of the padding material without overextending the neck during impact (Figure 5). The weight of the impactor used in this study was 22 pounds, approximately five times the head weight of the largest monkey used. This was designed to insure

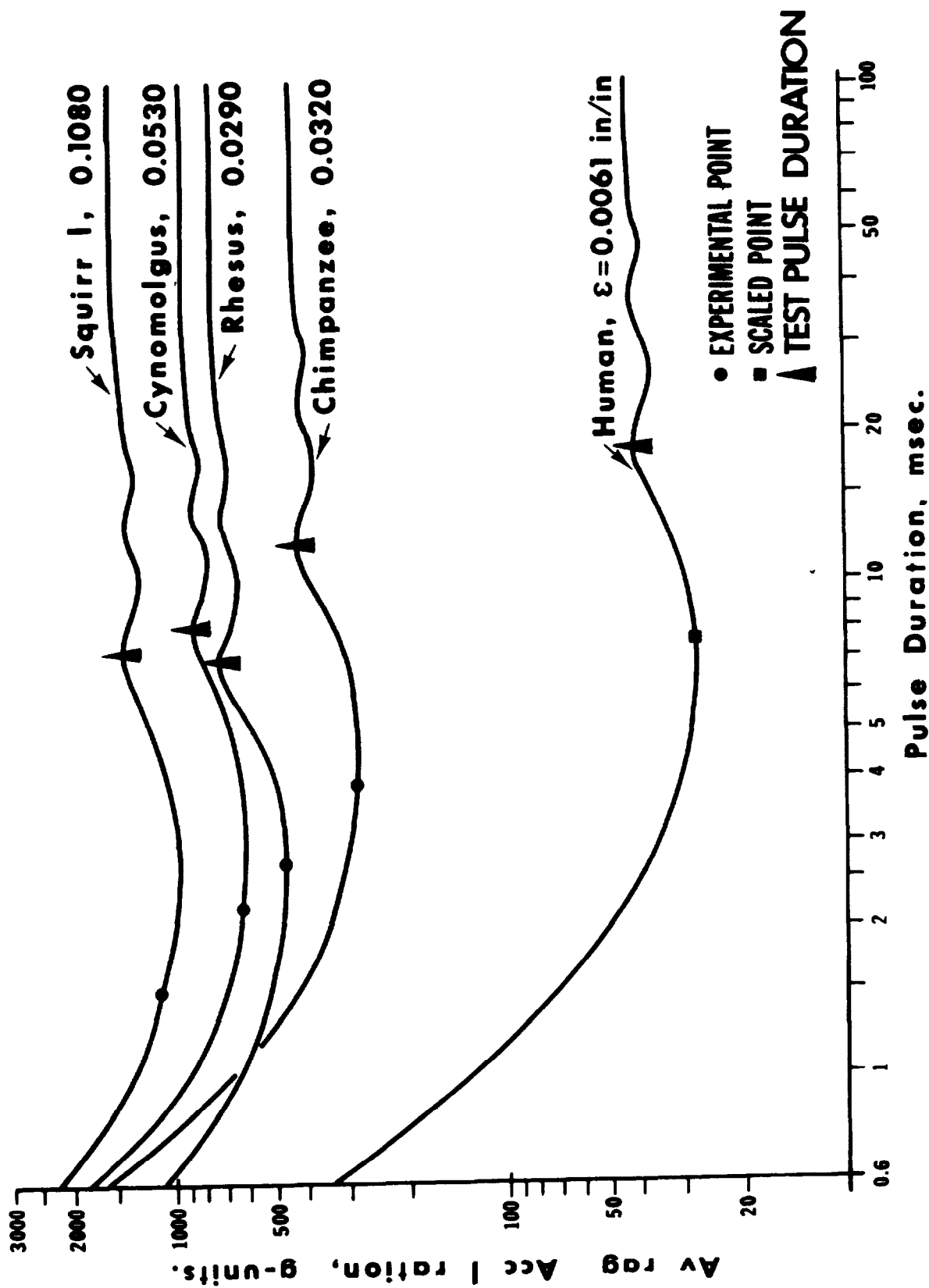


**FIGURE 4. MAXIMUM STRAIN CRITERION FOR PRIMATES,  
SIDE HEAD IMPACTS (TRIANGULAR PULSE)**

that the impactor did not slow down significantly when it struck the primate's head. The force-time plots and acceleration-time plots were recorded on a light beam oscillograph. The high speed movies of each test were analyzed and processed on a Vanguard film analyzer. Computer assisted differentiation and smoothing techniques were used to determine the angular velocity and acceleration of each head impact.

#### 2.2.1.2 Human Cadaver Head Impact Study

The point of impact was the left temporal region, two inches superior to the external acoustic meatus. Photographic targets for L-R head impacts were secured to the supra-orbital ridge, two inches on either side of the glabella (i.e., two inches either side of the mid-sagittal plane).

A biaxial accelerometer was mounted on a screw, which was driven into the skull at a point directly opposite the point of impact. Care was taken so that the accelerometer axes were normal and parallel to the impacting surface, not to the skull (Figure 6). The class 1000 frequency response value was used for all head accelerations as recommended by J211.

After being targeted and equipped with accelerometers, the cadaver was placed in a chair, which was modified for this impact study. All surfaces the cadaver could come in contact with in its post-impact movements were thickly padded with styrofoam to prevent damage to the cadaver. A special foam apparatus was employed to absorb the energy of the head and to protect the accelerometers from damage.

The cadaver was carefully positioned so that its head was in the correct position relative to the impactor and at the same time the whole cadaver was allowed to act as a free body. The head was suspended and held in place by

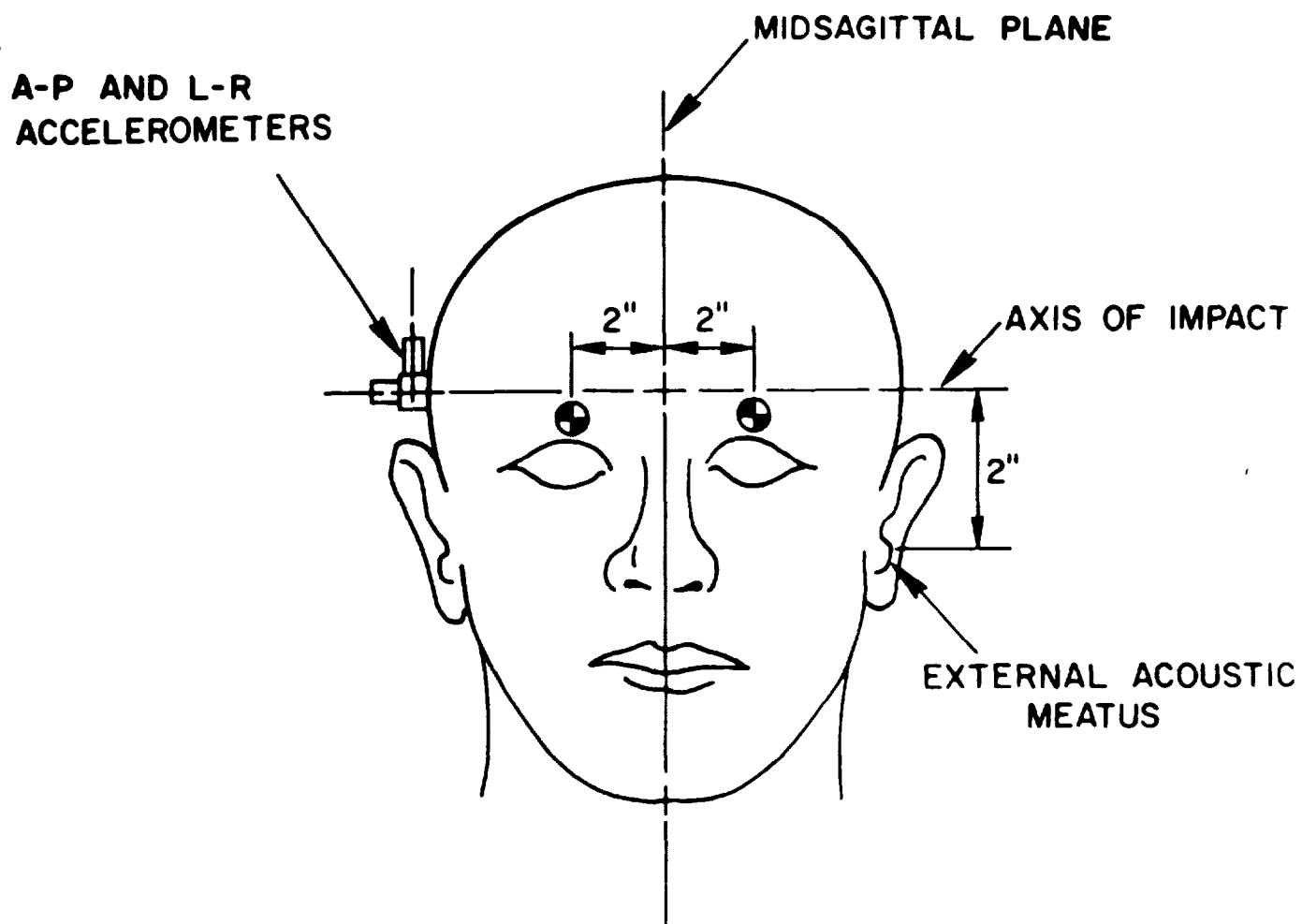


**FIGURE 6. TARGETING AND INSTRUMENTATION FOR SIDE HEAD IMPACTS.**

surgical thread. This thread supported only the weight of the head and broke easily on impact (Figure 7). The impacts were carried out in the HSRI Impact Facility described in the animal test set-up section of this report.

The same polystyrene plastic materials used in the animal study were used in the cadaver study to obtain a wide range of pulse durations. The impact velocity as well as the polystyrene materials were varied to give a wide range and combination of accelerations and pulse duration impacts. Pulse durations of up to 20 msec were needed to make these human head impacts comparable to those of the monkeys.

### 2.2.2 Torso Impacts

The thorax and abdominal body areas were divided into three major impact regions. Region I consisted of the thorax as located between the jugular notch of the sternum and the diaphragm. Region II was defined as including the area between the diaphragm (9th rib) and a horizontal plane transisting the abdomen along the inferior margin of the liver and stomach, and located approximately 1-3 cm superior to the umbilicus on the surface. Region III included the entire thorax and abdominal area, from the jugular notch to the iliac crest. All body impacts to Region I were carried out midway between the superior mediastinum and the diaphragm. All impacts were carried out with the axis of the impactor in the transverse plane. Impacts to Region III included all of Region III. All of these points were located as accurately as possible on sub-human primates before each test. The body regions are illustrated for the left and right side views in Figures 8 and 9.

All impacts made to Regions I and II used a 22-pound impactor with a scaled arm rest for contacting surface. This contacting surface was made from a 9 lb/ft<sup>3</sup> high density polyethylene foam to distribute the contact load. The

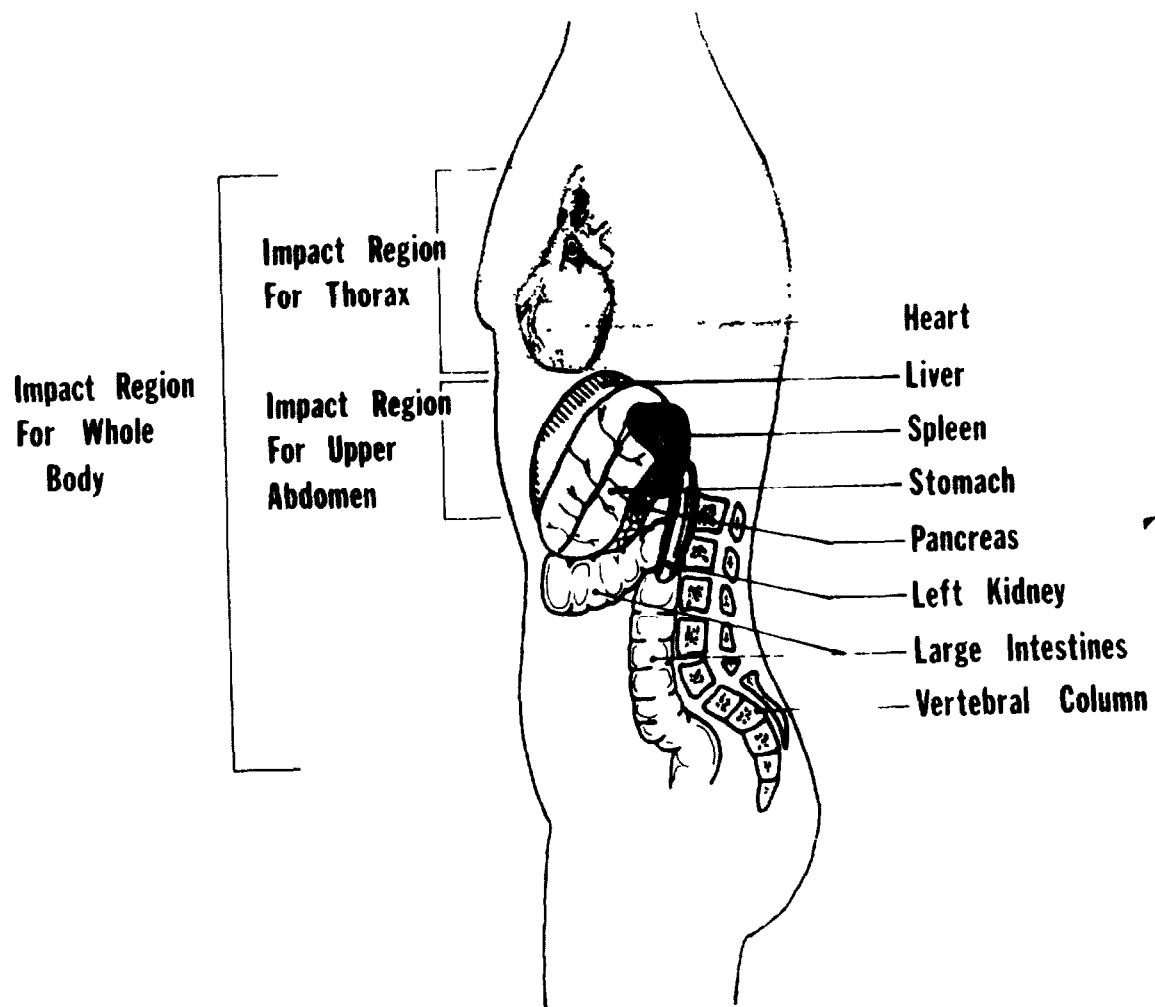


**FIGURE 8. BODY IMPACT REGIONS FOR LEFT SIDE**

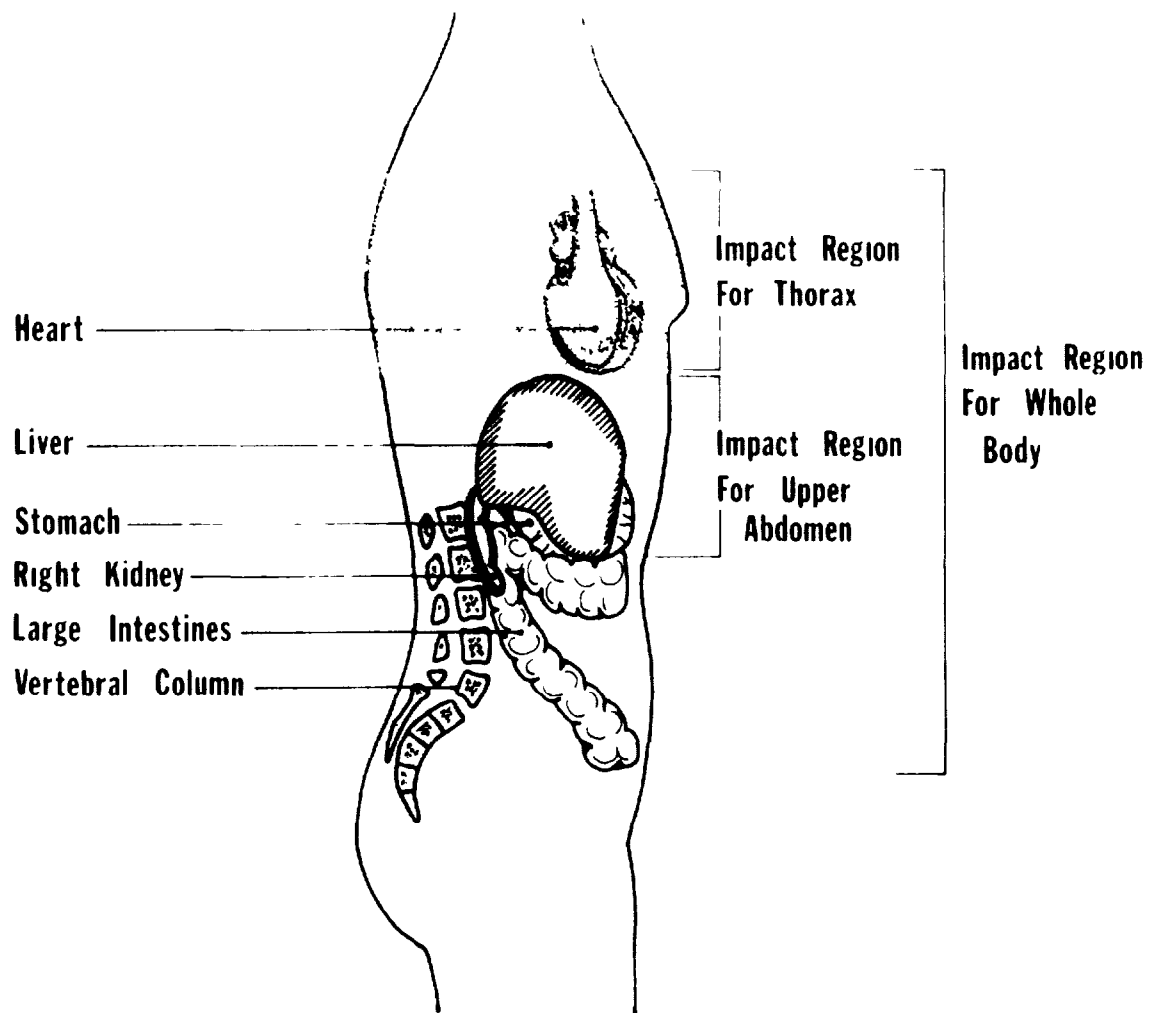


FIGURE 9. BODY IMPACT REGIONS FOR RIGHT SIDE

scaled arm rest was replaced by a scaled flat rigid plate for all impacts to Region III.

#### 2.2.2.1 Sub-Human Primate Impacts

The animals were positioned to limit the depth of penetration between 35% and 60% of body width, and a one-foot thick soft foam pad was arranged to prevent injury after impact.

The same testing procedure was used for each test sequence. The animal was impacted on the right side, and the injury evaluated. If the injury was not serious, then the next animal was impacted at a higher velocity. This procedure was continued until a serious injury was obtained. The next sequence of impacts was on the left side of the region completed (Figure 10).

The engineering parameters recorded for each test were force-time histories from an oscilloscope trace, depth of penetration from the photographic record, and velocity from an electronic chromometer.

#### 2.2.2.2 Human Cadaver Impacts

The cadavers were positioned in a heavily padded chair with no side supports. The test subject was held in an upright position by a harness under the arms, which was in turn fastened to a sliding mechanism over the chair. This support system was found to allow the cadaver to behave as a free body on impact, and still produce repeatable results (Figure 11). A 2" x 2" target for determining depth of penetration was fixed to the cadaver's side at a point directly opposite the point of impact. All cadaver thoracic impacts were made with the impactor centered over the 6th rib.

Two types of impactor heads were used in this study. One was a six-inch diameter rigid flat plate with 0.5 inch radius edges. The other head was a simulated arm rest made from the polyethylene material used in the animal study.



The weight of the impactor used in all tests was 22 pounds. This impactor weight was found to give a constant velocity impact up to three inches of penetration. Six side thoracic impacts were made with each head at two velocities. The depth of penetration was preset for any desired value between 1.8 inches and 3.8 inches.

### 2.2.3 Direct Organ Impacts

The purpose of this experiment was to quantitatively describe the relationship between impact parameters (energy, organ penetration, pressure, and impact velocity) and injury to exposed organs. The two organs studied were the liver and kidney because clinical experience indicates that these organs are most frequently injured in side impacts.

The organ to be tested was surgically mobilized in an anesthetized Rhesus monkey. The organ was laid onto a small load cell while still being perfused by the living animal (Figure 12). Load deflection curves were obtained for each impact. Impact velocity and depth of penetration were varied in turn to yield injuries of various severity levels.

The testing machine used in this study to provide both static and dynamic test data was the Plastechon High-Speed testing machine. This machine is an electrohydraulic servo-controlled unit with static load capacities of 3,000 and 12,000 lbs and a stroke of 11 inches. The ram velocity can be varied from a static rate of about 10 inches per minute, to a maximum servo-controlled rate of 12,000 inches per minute at the low load and 3000 inches per minute at the higher load rating. The maximum open loop rates are 30,000 and 12,000 inches per minute respectively.

The load cell used in the tests was a Kistler 933A Piezoelectric force link. This cell has a resonant frequency of 40KHz and compression load capacity of 6000 pounds. The ram displacement was measured by a Physitech Gage-It Optical Extensometer. The resulting data was recorded on storage

oscilloscopes in two forms: organ load and ram displacement versus time and organ load versus ram displacement. Photographs of the oscilloscope traces were taken as a permanent record.

#### 2.2.4 Thoracic Mechanical Impedance

The design of protective devices for humans subjected to an impact or a vibrational environment requires a knowledge of their mechanical behavior in such environments. Consequently, much effort has been devoted to the concept of treating the human body as a mechanical system and cataloging the system response to mechanical energy transfer from the surrounding environment and its distribution throughout the system.

The overall mechanical response of man, or of a sub-system of man, is perhaps best characterized by its driving point mechanical impedance, defined as the ratio of driving force to velocity, which can be used to determine the energy transfer between environment and man for a known excitation. Impedance techniques thus have a two-fold purpose in biomechanical response: to model the body or sub-system of the body as a mechanical system and to minimize energy transfer in the design of isolation systems.

Each monkey used in this study was anesthetized with 25 mg/kgm I.V. of Sodium Pentobarbital. A six-millimeter circular hole for squirrel monkeys, a ten-millimeter circular hole for Rhesus, and a 15-millimeter circular hole for the baboon was cut in the test subject's thorax between the 4th and 5th rib on the side to be tested. An adapter was then attached to the rib cage as shown in Figure 13. The space between the rib cage and the adapter was then sealed to prevent any more air from entering the interpleural space. A hypodermic needle was then inserted into the interpleural space and the trapped air withdrawn by a syringe. The living monkey's thorax was then attached to the platen of a 300-pound electromagnetic shaker, and the rest of the body

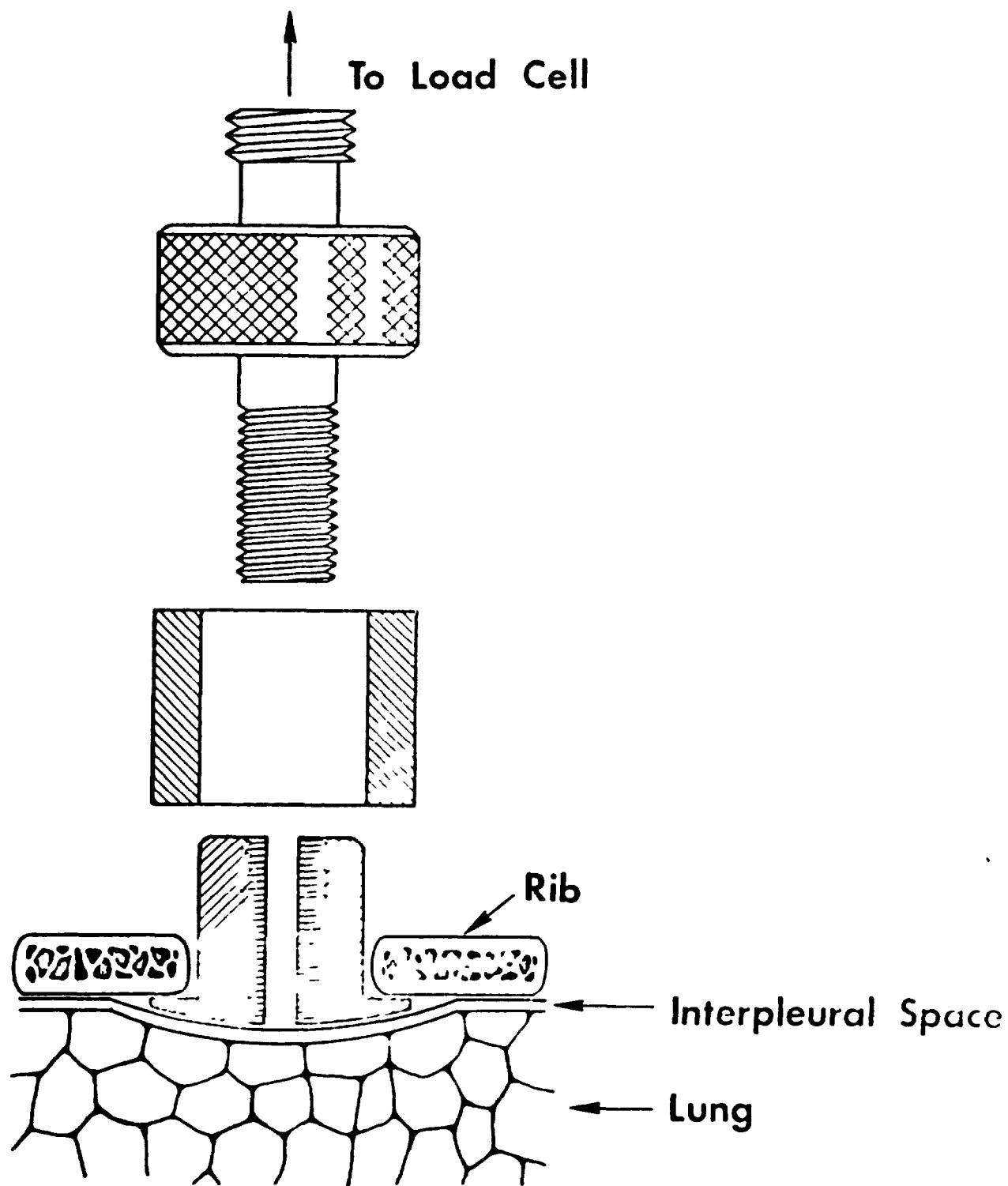


**FIGURE 13. LOADING FIXTURE**

was supported in a sling (Figure 14). The shaker servo-controller was set to apply a sinusoidal force to the thorax over the frequency range 5 to 100 Hz. A sweep oscillator was used to drive the shaker system while a mass cancelling automatic on-line impedance computer converted the force-time and acceleration-time information into plots of phase and impedance versus frequency. A one gram piezoelectric accelerometer with a low frequency response of one Hertz and a high frequency response to 1800 Hertz was attached to the fourth rib on the opposite side of the thorax from the shaker attachment. The acceleration was then recorded for the same frequency range used for the driving-point test. Runs were made at force levels of 50 and 100 pounds for the baboon, at 25 and 50 pounds for the Rhesus, and 5 to 10 pounds for the squirrel monkey. Driving-point and transfer point accelerations were recorded for each run. All monkeys survived the test and showed no injuries other than those caused by the surgery for attachment to the shaker.

The cadaver mechanical impedance tests were conducted in a manner similar to those of the monkey study. The load adapter used in the human cadaver study was 22 millimeters and the applied loads of 50 and 100 pounds. The accelerations on the opposite side of the chest were also recorded.

### 2.3 BIOMEDICAL DATA COLLECTION

Gross autopsy was conducted in the Autopsy Laboratory, specially equipped for dissection. Autopsies were conducted as a blind, according to accepted research procedure, with the investigator conducting the gross autopsy having no knowledge of physical data on the intensity, location of impact, or circumstances of each test. Careful anatomical dissection of the head, face and neck tissues, where head impacts occurred allowed discrete identification of many sites of vascular failure. When gross trauma was found

it was photographically recorded using a specially modified Pentax camera with close-up lens, either in situ or as an isolated entity, to provide a permanent record of the injury.

Tissues were saved from all major organs for further histopathologic examination. Weights of major organs including the heart, brain, lungs, liver, spleen, pancreas, adrenals, and kidneys, were obtained. Each autopsy report includes gross and microscopic pathology, anthropometry, color photographic documentation of dissections, injuries, and the animal test preparation. Isoenzyme determinations in the case of larger primates were also made. Included are all background information relative to the history, case, and any medication of the particular subject.

It should be noted that no animal carcass was destroyed after autopsy without making an effort to fully utilize the remains within the Medical School community. In this connection, some 12 departments received carcass materials which were of direct benefit to other medical research studies in progress. Some examples included the testis which were used by the Department of Gynecology and Obstetrics for hormone studies, thighs by the Department of Surgery for fascia graft experiments, and other 'discarded' materials were received by the Human Growth Center, Department of Anatomy, Department of Ophthalmology, Department of Otorhinolaryngology, Department of Pathology, Kresge Hearing Research Institute, Department of Anthropology, University of Michigan Museum, and hands and feet were used for a study of dermatoglyphics by School of Public Health investigators. Thus, the animal subjects were optimally utilized in accordance with all animal utilization codes of ethics.

Tissue specimens were prepared in the HSRI Histology Laboratory for microscopic examination. Fixed in a solution of formalin, the specimens

were dehydrated with alcohol, cleaned, infiltrated and finally imbedded in paraffin. The paraffin blocks were placed in the microtome and tissues were sectioned at a thickness of 5 microns, using an AO Sencer 820 microtome and mounted on a glass slide. Various stains were used, but in the case of brain tissue some slides for each subject were prepared with Gallocyamin stain for Nissl substance, since early dissolution of Nissl substance has been found to occur subsequent to nerve cell injury.

Microscopic examination and study of the tissue preparations was accomplished with an AO Spencer Series 10 microscope using 4X, 10X and 45X objectives with trinocular body, which permits the use of a Pentax H/a camera for microphotography. Histopathology was evaluated by specialists from the university school of medicine. As a further check on interpretation, selected brain tissues were submitted for evaluation by two additional pathologists experienced in infra-human brain pathology. Dr. Trollope of the section of general surgery of The University of Michigan Medical Center aided in evaluation of all thoracic and abdominal injuries. A difference in histopathology observations of the brain and other organs as well as interpretation is not unusual among pathologists, and the submission of critical tissue specimens to more than one pathologist without the knowledge of the others was intended as a check to decrease the chances of missing any pertinent pathology, as well as to alert us to any specific cases where there might be a difference of opinion as to interpretation of pathology. A similar procedure was also followed in the final interpretation of injury severity related to both gross and microscopic findings, with separate ratings made by two researchers experienced in infra-human primate injury investigations. Interpretations and scoring were consistently within 1/2 scaling point out of 5, giving considerable confidence to our final scaling

design. The following Estimated Severity of Injury (ESI) was used to rate the injury of all test animals.

0. No Injury - No treatment required
1. Minor Injury - Requires no hospitalization
2. Mild Injury - May require hospitalization
3. Serious Injury - Reversible trauma only
4. Severe Injury - Non-reversible trauma, life threatening
5. Fatal

The post impact injury evaluation of the human cadavers was conducted in a quite different manner. After the impact, the cadaver was sent to the Anatomy Department where it was embalmed by a special technique whereby brain damage could be assessed. This technique consists of injecting a solution containing red lead into the circulatory system, which then stains the tissue where blood vessels have hemorrhaged. The circulatory system was held under fluid pressure for several days to insure that all injuries were made visible. The calvarium was then removed and the brain examined within two weeks of embalming.

A study duplicating this test procedure with monkeys was initiated in an effort to enable us to better distinguish the various grades of injuries to the cadavers. The monkeys were terminated and kept in cold-storage for three days before impact to simulate the preimpact period for the cadavers. They were then impacted, taken to the Anatomy Department to be injected with the same red-lead embalming solution, and held under fluid pressure for several days. Finally, a necropsy was performed, and the effects of trauma noted.

Five Rhesus monkeys were used in this test; four were impacted and one served as a control. All four were impacted at a velocity designed to yield

an ESI of 3. The results were that two of the four monkeys had ESI ratings of 2 and one monkey had an ESI of 1. The fourth and control monkeys showed little or no evidence of trauma, and therefore were assigned ESI's of 0.

Based on the Rhesus monkey study it was believed that some indication of injury level could be learned from the red lead technique; although the injury seemed to be less in cadaver monkeys than in live monkeys for similar impacts. This may be because the vascular system is not pressurized in cadaver monkeys and hence not as easily ruptured or injured.



### 3.0 TEST RESULTS

#### 3.1 RESULTS OF PADDED HEAD IMPACTS

The head injuries evident from the primate autopsies were of several distinct types. The following injuries were the most significant or most common types of injuries found in the long duration head impact study.

The contre-coup hemorrhage resulting from the short duration head impacts reported in the 1971 "Door Crashworthiness Criteria," final report was seen only once in this study. This injury occurred in a padded impact to a Rhesus monkey of 3.5 msec. duration using only two inches of soft padding material. The monkey's head bottomed-out the padding against the impactor resulting in very high G's for a very short pulse duration.

A second type of injury which was observed in this study is illustrated in Figure 15. This injury consists of damage to the "Arteries of Internal Cerebral Hemorrhage" (Arteries of Charcot) which supply blood to the corpus striatum, internal capsule, and thalamus. The location of the most diffuse hemorrhaging was the Putamen area of the brain (Figure 16).

This type of closed brain trauma has been reported clinically by Zulc, 1969; Strich, 1969; and Sano, 1968; and experimentally by Gennarelli in 1972. It is most commonly found in long duration and rotational impacts. The mechanism for this type of injury is not well understood.

The most common type of injury seen in this study was failure of the superior sagittal sinus along a region beginning at the junction of the occiput with the parietal bones and extending to the crown region (Figure 17). The sagittal sinus is securely attached to the skull through the sagittal suture, and to the brain by the Falx Cerebri. Because of this tethering arrangement, any relative motion between the brain and the skull results in a stretching and possible tearing of the walls of the superior sagittal sinus.

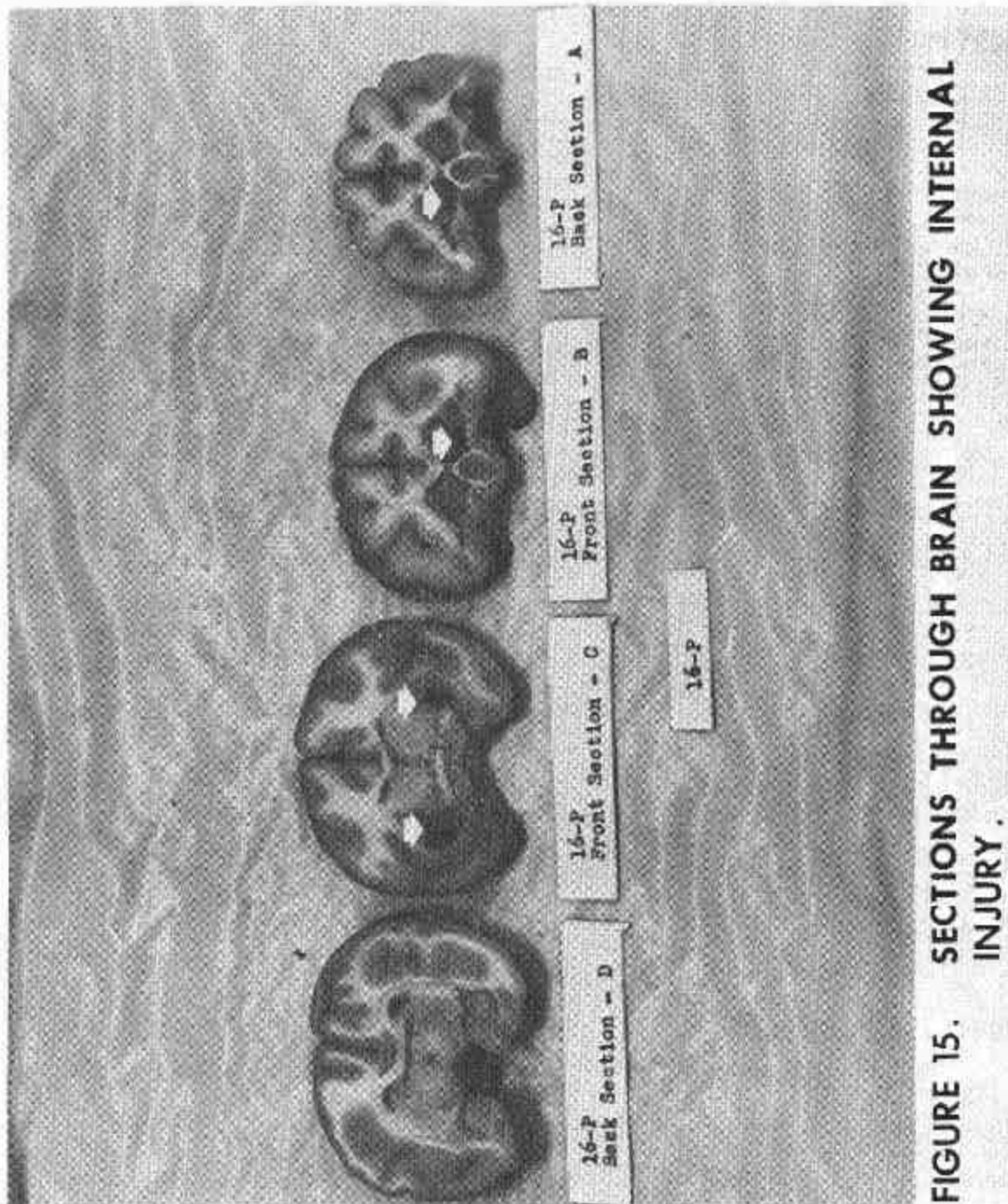
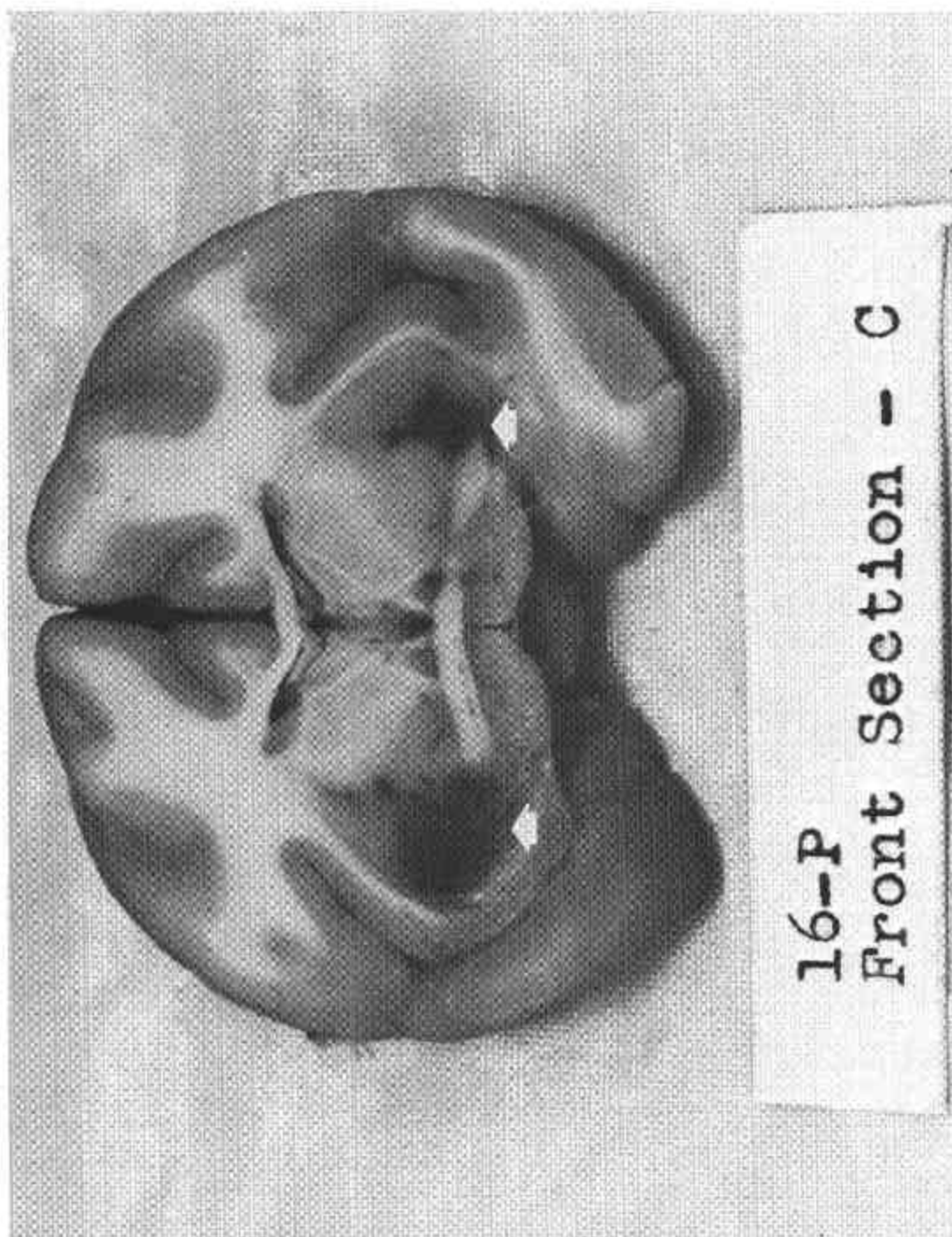


**FIGURE 15. SECTIONS THROUGH BRAIN SHOWING INTERNAL INJURY.**



16-P  
Front Section - C

FIGURE 16. SECTION OF CEREBRUM, SHOWING HEMORRAGING IN THE  
PUTAMEN

J - 16



FIGURE 17. HEMORRHAGING OF SUPERIOR SAGITTAL SINUS.

Other common injuries observed were: hemorrhaging in the medullary region and about the brain stem; slight subdural and subarachnoid hemorrhaging throughout the calvarium. The mechanism of these vascular failures appears to be related to displacement of the brain relative to the skull.

In some cases, particularly the very high velocity and high acceleration impacts of the squirrel monkey series, the accelerometer came loose from the head. In these tests the acceleration values were then obtained from the high speed motion pictures.

The mechanical parameters for the head impacts to the infra-human primates are given in Table 1. Also included are the anatomical measurements.

The results of the cadaver padded impactor head impacts study indicate that the staining technique described in the experimental method section was not sensitive enough to evaluate anything other than the most severe impacts. This was believed to be due to the lack of blood pressure in the vascular system. All head impacts, except for two, showed no injury. One showed definite signs of vascular damage on the surface of the brain opposite the side of impact. A broken neck and possible vascular damage to the brain was found in another impact. The data from all of the cadaver head impacts are given in Table 2. The force-time curve for each impact is given in Figure 18. The head resultant accelerations, as determined either from the head accelerometers or photometric analysis, are given in Figures 19 and 20.

### 3.2 RESULTS OF THORACIC IMPACTS

Typical injuries observed in this series of impacts are listed below in the order of most frequent occurrence. Petechial hemorrhage of the lung, massive hemorrhage to the tip of the lung as well as occasional tears to lung tissues were seen most frequently. Examples of injuries of these types

TABLE 1 SUMMARY OF LONG DURATION SUB-HUMAN PRIMATE HEAD IMPACTS

ANIMAL SPECIES	TOTAL BODY WEIGHT lbs	HEAD WEIGHT lbs	(a) AVERAGE SKULL RADIUS in	(h) AVERAGE SKULL THICKNESS in	IMPACT VELOCITY ft/sec	IMPACT DURATION msec	PEAK CONTACT FORCE lbs	MAX. HEAD VELOCITY ft/sec	MAX. HEAD ACCEL. G's	MAX. HEAD ANG. VEL. rad/sec	MAX. HEAD ANG. ACCEL. rad/sec <sup>2</sup>	IMPULSE lb-sec	TERMINATION (DAYS AFTER IMPACT)	LOSS OF CONSCIOUSNESS min	ESI	COMMENTS
SM	1.32	0.173	0.76	.040	63	3.8	234	67	1350	186	65	0.7	2	NONE	2	Epidural hemorrhage with some congestion.
SM	1.48	0.195	0.81	.043	77	2.8	550	83	2440	271	89	1.3	SD	NRC	5	Fracture of Occipital Bone around the Foramen Magnum, Brainstem Hemorrhages
SM	1.76	0.173	0.83	.042	82	5.5	310	87	1780	481	100	1.5	SD	NRC	5	Partial fracture of occipital bone around the Foramen Magnum, Brainstem Hemorrhage
SM	1.71	0.165	0.78	.038	78	5.8	280	83	1690	352	75	1.4	SD	4-5	4	Small Crack in Occipital bone around Foramen Magnum, moderate hemorrhaging around the Brainstem
SM	1.38	0.168	0.83	.031	70	6.0	250	75	1490	390	90	1.3	2	2-3	3	Subdural Brainstem Hemorrhage
RH	12.50	1.080	1.23	.080	79	6.0	2000	86	1000	254	100	9.5	1	20	4	Coup and contrecoup with focused Petechial Hemorrhage
RH	11.10	1.000	1.17	.078	58	L00	L00	65	L00	241	51	L00	2	2	2	Epidural and Subdural Hemorrhage, Congestion
RH	10.70	0.960	1.16	.079	83	4.8	1100	96	1100	278	60	4.2	2	NONE	1-2	Epidural and Subdural Hemorrhage, Congestion
RH	10.20	1.030	1.20	.079	85	8.2	2000	88	800	267	65	8.8	2	1-2	2	Epidural and Subdural Hemorrhage, Congestion
RH	9.40	0.990	1.15	.075	64	5.6	800	71	805	241	57	2.7	2	NONE	1	Epidural Hemorrhage with some Congestion
RH	11.00	1.000	1.18	.076	70	5.8	800	76	870	235	68	3.1	3	NONE	1	Epidural Hemorrhage with some Congestion
RH	12.00	1.110	1.27	.083	60	8.2	800	65	955	228	43	4.9	3	NONE	1	Epidural Hemorrhage with some Congestion
RH	10.20	1.070	1.21	.084	75	5.4	1050	81	960	251	55	5.6	5	3	2	Subdural & Epidural Hemorrhage, Congestion

TABLE 1 SUMMARY OF LONG DURATION SUB-HUMAN PRIMATE HEAD IMPACTS (Continued)

ANIMAL SPECIES	TOTAL BODY WEIGHT lbs	HEAD WEIGHT lbs	(a) AVERAGE SKULL RADIUS in	(h) AVERAGE SKULL THICKNESS in	IMPACT VELOCITY ft/sec	IMPACT DURATION msec	PEAK CONTACT FORCE lbs	MAX HEAD VELOCITY ft/sec	MAX. HEAD ACCEL. g's	MAX. HEAD ANG. VEL. rad/sec	MAX. HEAD ANG. ACCEL. rad/sec <sup>2</sup>	IMPULSE lb-sec	TERMINATION (DAYS AFTER IMPACT)	LOSS OF CONSCIOUSNESS min	ESI	COMMENTS
RH	12.0	1.13	1.23	.080	100	3.5	1800	112	1727	272	73	7.3	SD	1-2	5	Occipital Fracture, Subdural and Brainstem Hemorrhaging, contre-coup
RH	9.7	0.96	1.20	.079	75	4.8	1200	80	920	250	50	3.9	5	NONE	1	Epidural Hemorrhage, Congestion
RH	10.8	0.95	1.19	.076	97	6.5	1530	107	1545	265	90	10.0	SD	18	5	Occipital Fracture, Subdural and Brainstem Hemorrhaging
RH	9.5	0.97	1.18	.077	83	7.7	1190	88	1230	250	83	7.6	3	5	3	Brainstem and Subarachnoid Hemorrhage with some Brainstem involvement
RH	10.7	0.99	1.20	.085	87	7.7	1360	83	1375	245	95	8.8	3	12	4	Crack in occipital bone with Brainstem and Subdural Hemorrhage
RH	11.7	1.11	1.25	.086	91	8.1	1640	101	1485	264	75	11.5	SD	15	5	Very Heavy Brainstem Hemorrhage, Subarachnoid Hemorrhage
RH	12.9	1.13	1.24	.081	80	7.6	1330	86	1185	255	81	8.7	3	5	3	Brainstem and Subarachnoid Hemorrhage with some Brainstem involvement
CH	59.0	5.28	2.10	.185	80	11.0	2600	85	567	193	58	6.2	SD	7	1-2	Subdural & Subarachnoid Hemorrhage, Petechial Hemorrhage
CH	57.0	5.12	2.06	.178	72	10.0	1300	75	286	170	40	3.1	2	6	0-1	Epidural Hemorrhage with Congestion

SD - Same Day  
MRC - never regained consciousness  
LOD - Loss of Data

TABLE 2

## SUMMARY OF LONG DURATION HUMAN HEAD IMPACTS

TEST NO.	SEX	AGE	CAUSE OF DEATH	NO. OF DAYS DEAD	HEIGHT ft	WHOLE BODY WEIGHT lb	BRAIN WEIGHT lb	IMPACT VELOCITY ft/sec	IMPACT DURATION msec	PEAK CONTACT FORCE lb	MAX. HEAD VELOCITY ft/sec	MAX. HEAD ACCEL. g's	MAX. HEAD ANGULAR ACCEL. K-rad/sec <sup>2</sup>	MAX HEAD ANGULAR VEL. rad/sec	IMPULSE lb-sec	COMMENTS
1	M	64	Metastatic Nemanoma	7	5' 7"	112	2.93	19	6.0	2250	18	206	13.0	45	15.2	Small hemorrhage on right side of brain.
2	M	72	Asphyxiation	5	5' 7"	112	2.83	22	13.0	900	20	86	14.0	56	13.8	No Gross Trauma
3	M	99	Cerebral Vascular Accident	1	5' 9"	148	2.97	26	17.0	1500	24	140	21.0	71	29.0	Possible hemorrhage on right side of brain, broken neck
4	M	70	Coronary Occlusion	5	5' 3"	92	3.07	23	9.0	1425	23	125	11.0	56	12.0	No Gross Trauma
5	M	70	Acute Coronary	2	5' 6"	124	3.09	23	13.0	1000	26	95	11.0	63	14.1	No Gross Trauma
6	M	61	Pneumonia	4	5' 7"	135	2.98	36	17.0	810	34	85	9.0	70	14.3	No Gross Trauma
7	M	67	Respiratory Paralysis	4	5' 7"	143	3.01	39	22.0	680	38	65	7.0	65	19.0	No Gross Trauma
8	M	69	Acute Circulatory Failure	3	5' 5"	127	2.85	31	15.0	960	30	99	10.0	64	15.3	No Gross Trauma
9	M	58	Carcinoma Tonsilfossa	2	5' 7"	110	2.91	44	14.0	670	42	69	8.0	68	12.0	No Gross Trauma
10	M	50	Influenza	7	4' 9"	72	2.79	40	21.0	710	37	68	8.5	71	18.0	No Gross Trauma
11	M	77	Myocardial Infarction	5	5' 10"	163	3.05	26	20.0	320	24	54	9.4	58	7.1	No Gross Trauma
12	M	16	Aspirational Pneumonitis	1	5' 1"	96	2.75	27	21.0	460	25	48	4.1	43	8.6	No Gross Trauma

M - Male



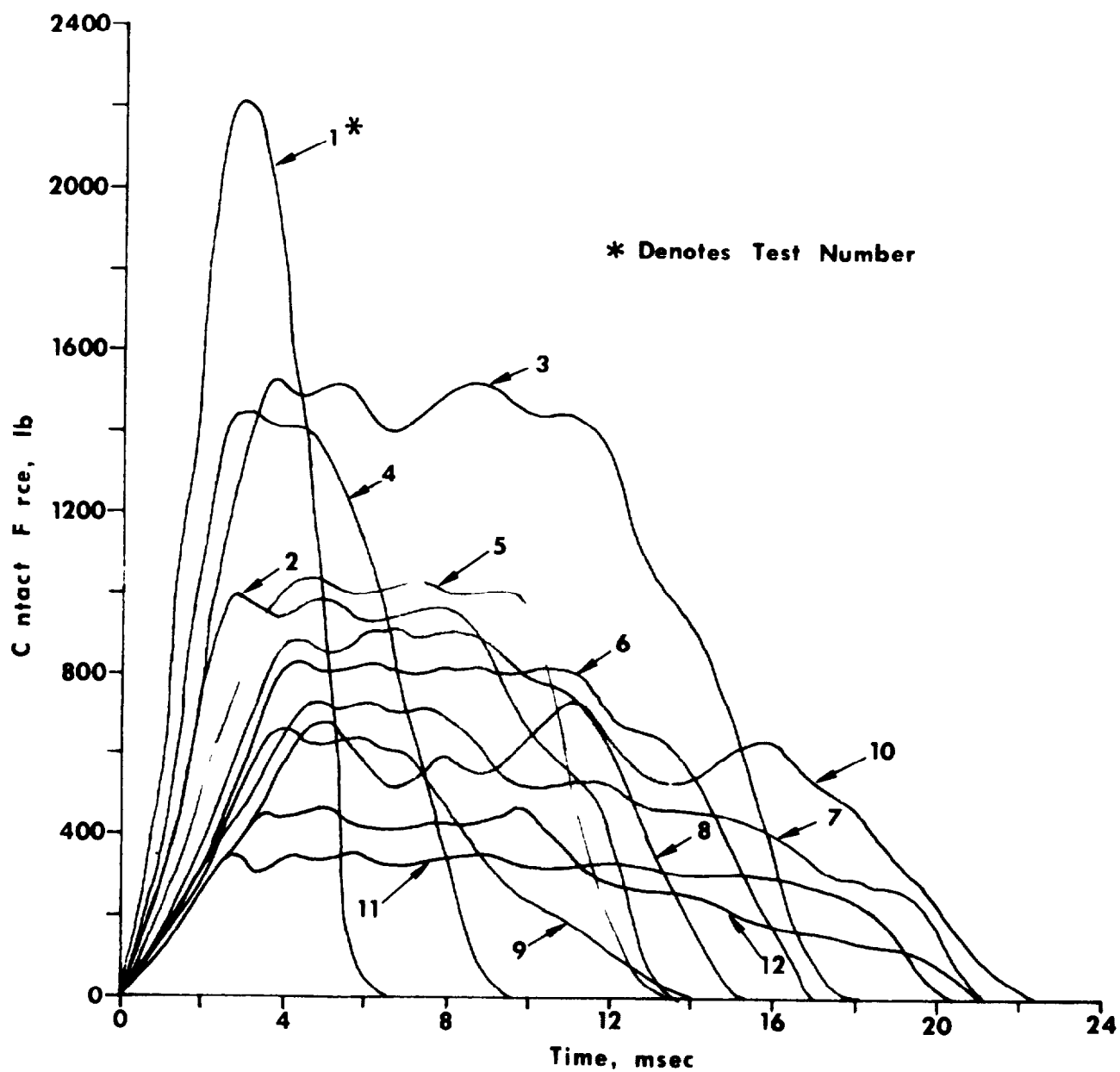
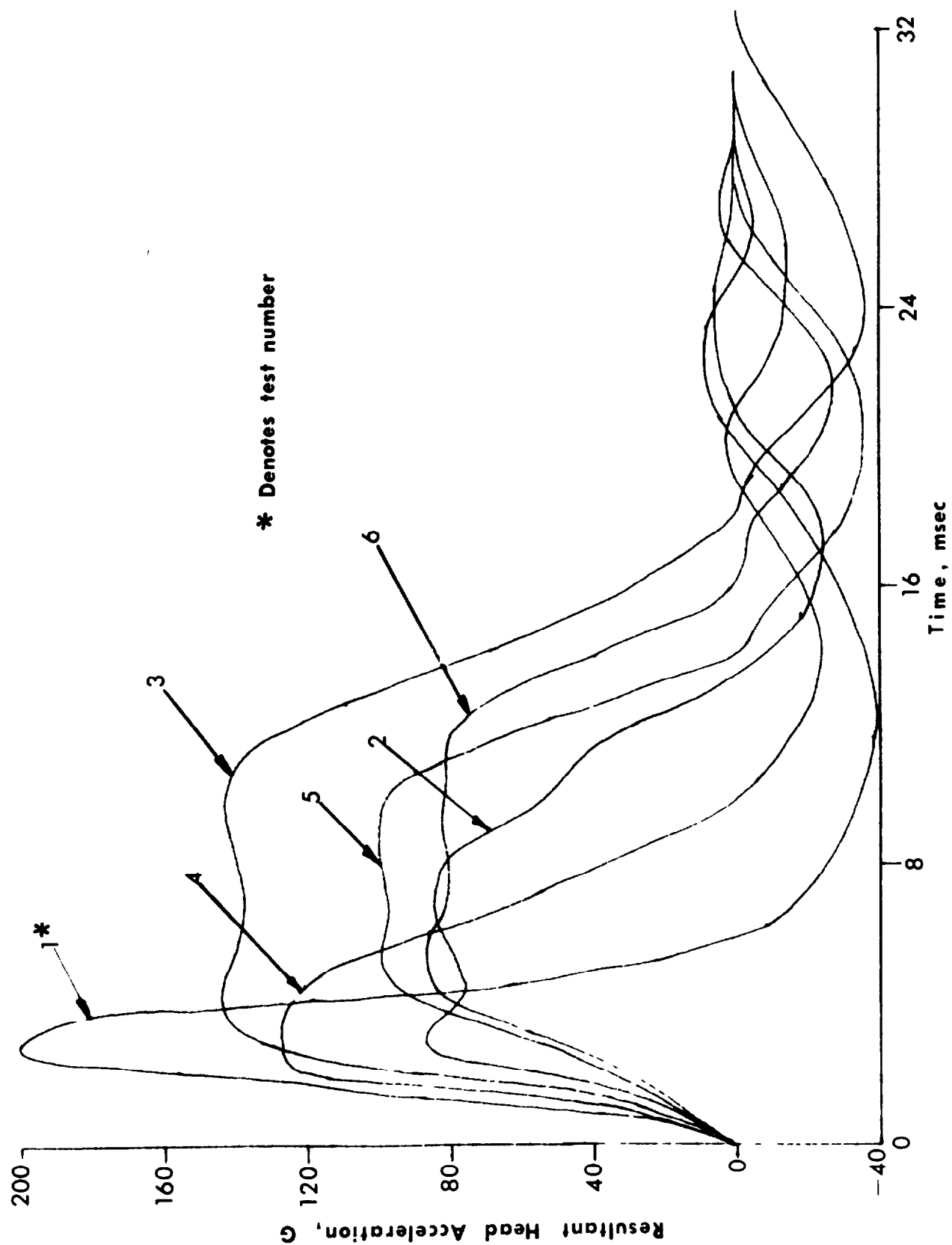


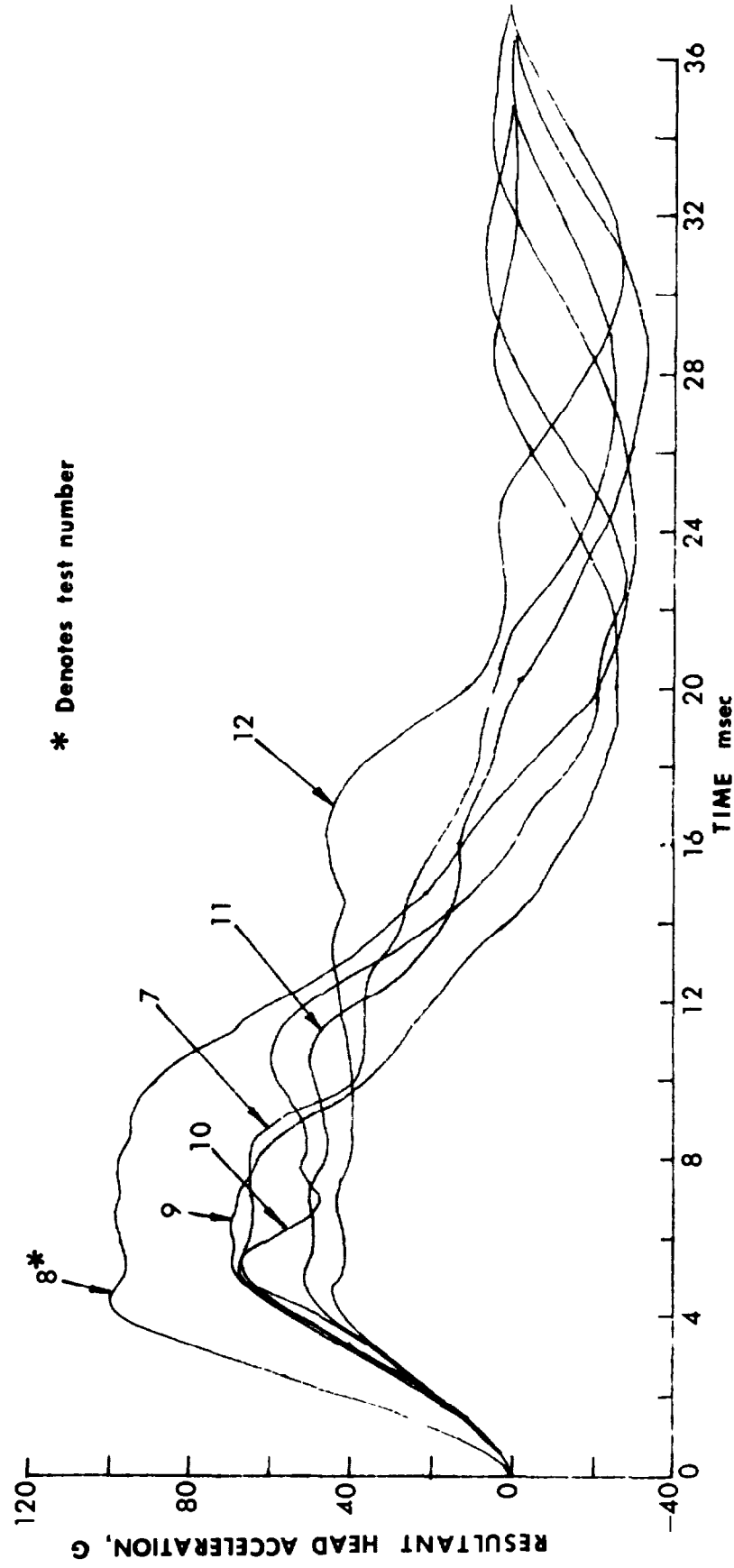
**FIG. 18. HUMAN CADAVER SIDE HEAD IMPACTS (PADDED)  
FORCE - TIME CURVES**



\* Denotes test number

HUMAN CADAVER SIDE HEAD IMPACT (PADDED) ACCELERATION - TIME CURVES

FIGURE 19



\* Denotes test number

HUMAN CADAVER SIDE HEAD IMPACT (PADDED) ACCELERATION - TIME CURVES

FIGURE 20

are shown in Figure 21. Ruptures of the heart were found in two cases. These ruptures occurred at the bifurcation of the heart and blood vessels. An example of one such injury is shown in Figure 22. This rupture occurred where the superior vena cava attaches to the right atrium and probably occurred when the impact coincided with the filling cycle of the atrium.

Liver injuries were frequently found in the area of the falciform ligament. In each case the liver itself was not impacted directly but pulled in such a way to cause tears around the ligament attachments. The results for the primate study are given in Table 3.

The cadaver chest impacts indicated that rib fractures would occur for penetrations greater than 2.40 inches for the age group of cadavers tested. In one case, a 16 year old youth was impacted to a penetration depth of approximately four inches without rib fracture. The results for the human cadaver impacts are given in Table 4 with the load-deflection curves for the flat impactor given in Figure 23. The results of the simulated arm rest impacts are given in Figure 24. The load-deflection curves for three consecutive impacts to the 16 year old cadaver are given in Figure 25.

Impacts with the flat impactor show an inertial spike followed by a falling off of load as the deflection increases. By contrast, the simulated arm rest impacts build up load as the displacement increases. This build up of load for the simulated arm rest is produced as the (roughly triangular shaped) arm rest penetrates the body, its area of contact increases thus increasing the load.

### 3.3 RESULTS OF ABDOMINAL IMPACTS

Impacts to the abdomens of infra-human primates resulted in injuries to the liver (primarily fractures, sub-capsular hemorrhaging and tears (Figure 26).



LUNG TISSUE, SHOWING THE THREE MOST COMMON KINDS OF INJURY.

FIGURE 21

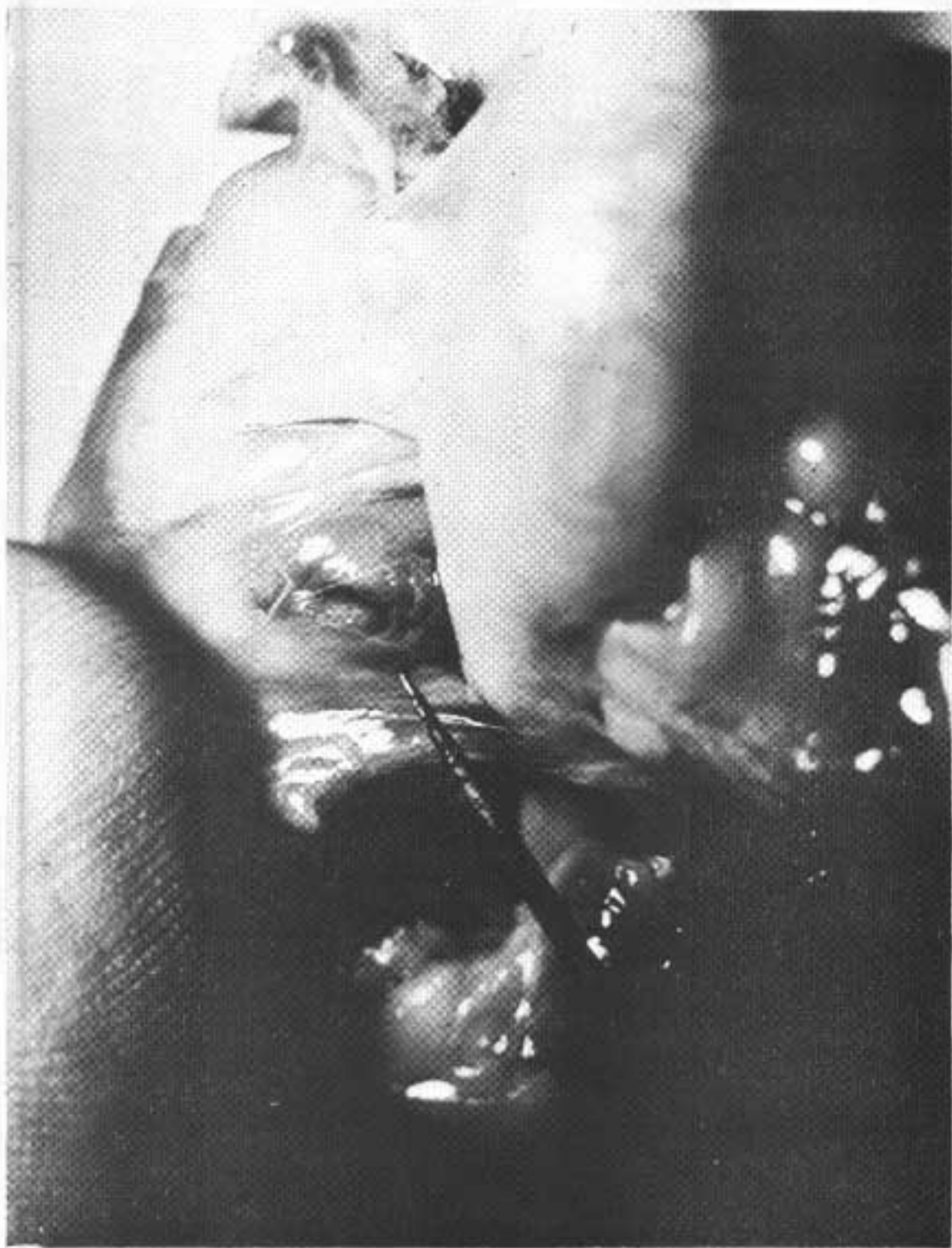


**FIGURE 22. BLOWOUT FAILURE AT THE JUNCTION OF THE  
SUPERIOR VENA CAVA AND THE RIGHT ATRIUM.**

TABLE 3 SUMMARY OF PRIMATE SIDE THORACIC IMPACTS

ANIMAL SPECIES AND SEX	BODY REGION AND TYPE OF IMPACT	BODY WEIGHT lbs	CHEST DIMENSIONS			ASPECT RATIO Breadth/Depth	IMPACT VELOCITY ft/sec	IMPACT DURATION msec	PEAK CONTACT FORCE lb	PERCENT PENETRATION	EFFECTIVE % PENETRATION	ESI	INJURY
			Circum. in	Breadth in	Depth in								
SM-F	Rt-I/AR	1.5	5.4	1.6	2.1	0.76	37	10.0	200	59	44.8	3	Petechial hemorrhage in right lung with focal hemorrhage surfaced. Large bruise on right atrium.
SM-F	Lt-I/AR	1.6	5.5	1.5	1.9	0.79	40	8.0	170	62	49.0	4	Petechial hemorrhage in left lung. Focal hemorrhage on right lung surfaced. Small amount of blood between heart and pericardium. Small subcapsular hemorrhage in liver.
SM-M*	Rt-I/AR	1.3	5.2	1.4	1.8	0.77	32	8.0	80	51	36.2	1	Moderate hematoma right kidney and right adrenal.
SM-M*	Lt-I/AR	1.3	5.2	1.3	1.7	0.76	33	5.2	60	50	38.0	1	Several petechiae on lungs.
SM-M*	Rt-I/AR	1.1	5.0	1.3	1.8	0.72	36	5.8	140	55	39.6	2	Several small petechiae on lungs, focal epicardial hemorrhage.
RH-F	Lt-I/AR	21.0	15.0	4.6	3.6	1.30	41	9.0	300	34	44.0	2	Minor subcapsular hematoma in liver; slight edema in right lung, hematoma of muscles on right side.
RH-F	Rt-I/AR	10.1	12.5	4.2	3.5	1.20	52	9.5	450	35	42.0	3	Edema in right lung, small subcapsular hemorrhage in liver.
RH-M	Rt-I/AR	9.5	12.0	4.1	3.5	1.17	58	9.4	440	38	42.5	3	Edema in right lung, 1-2 cc free blood in right side of thoracic cavity, small capsular tear on liver.
RH-M	Rt-I/AR	11.2	12.7	4.4	3.6	1.22	60	10.1	575	40	48.5	4	Large amount of edema on right lung, 10cc blood in right thorax; focal hemorrhage on right and left lungs.
RH-M*	Lt-I/AR	9.0	12.3	4.3	3.4	1.40	45	8.0	280	29	40.6	1	Minor hemorrhage on left lung.

TABLE 3 SUMMARY OF PRIMATE SIDE THORACIC IMPACTS (Continued)

ANIMAL SPECIES AND SEX	BODY REGION AND TYPE OF IMPACT	BODY WEIGHT lbs	CHEST DIMENSIONS			ASPECT RATIO Breadth/Depth	IMPACT VELOCITY ft/sec	IMPACT DURATION msec	PEAK CONTACT FORCE lb	PERCENT PENETRATION	EFFECTIVE % PENETRATION	ESI	INJURY
			Circum. in	Breadth in	Depth in								
RH-M*	Lt-I/AR	8.8	12.0	4.2	3.4	1.23	42	9.8	360	40	49.3	2	Focal hemorrhages on lower lobes of both lungs (non-prominent on left side).
BA-F	Lt-I/AR	22.0	16.0	4.5	5.5	0.82	55	10.0	1300	57	46.7	3	Edema in left lung; Diffuse hemorrhage at base of left lung; 10 cc blood in right side of abdomen, Larger subcapsular hemorrhage in liver.
BA-F	Rt-I/AR	18.0	17.0	4.7	5.6	0.84	68	9.3	1500	60	50.5	5	Large amount of edema on right and left lungs; 5-10 cc blood in right thorax; focal hemorrhage of right and left lungs; blow out of right heart; liver torn in half around the porta hepatis.
BA-F	Rt-I/AR	24.0	17.2	4.8	5.7	0.84	50	10.0	1100	47	39.5	2	Edema in right lung with some focal hemorrhages.
BA-M*	Rt-I/AR	31.0	18.2	4.9	5.9	0.83	53	8.6	1020	52	43.2	2	Edema in right and left lungs; diffuse hemorrhage at base of both lungs; 5 cc blood in right side of abdomen; small subcapsular hemorrhage in liver.
BA-M*	Lt-I/AR	31.0	18.5	4.9	6.1	0.80	56	8.4	1020	58	46.3	3	10 cc blood in left thorax, focal hemorrhage of left lung; heart hemorrhage; liver lacerated.

\*From 1971 Final Report "Door Crashworthiness Criteria"

Rt - Right  
 Lt - Left  
 AR - Arm Rest  
 I - Thoracic Region  
 M - Male  
 F - Female



TABLE 4 CADAVER SIDE THORACIC IMPACT DATA

TEST NO.	SEX	AGE (YRS)	CAUSE OF DEATH	NO. DAYS DEAD	HEIGHT	BODY WEIGHT LBS	CHEST DIMENSIONS			TYPE IMPACT	PISTON VELOCITY ft/sec	PEAK CONTACT FORCE (LBS)	PULSE DURATION MSEC	MAXIMUM PENETRATION (INS)	COMMENTS
							CIRCUM. IN	BREADTH IN	DEPTH IN						
C-25A	M	67	Pneumonia	4	5'7 1/2"	135	31.5	11.2	8.0	LR(FL)	20	970	17	1.9	No external signs of fractures. Cadaver showed signs of being in full rigor
C-26	M	67	Respiratory Paralysis	4	5'7"	143	36.5	12.0	10.0	LR(FL)	29	1100	19	3.2	Multiple Rib fractures
C-27	M	69	Acute Circulatory failure	3	5'5"	127	35.0	13.0	8.3	RL(FL)	20	480	19	2.9	No external signs of fracture
C-28A	M	58	Carcinoma Tonsilfossa	2	5'7"	110	35.0	12.0	8.5	RL(FL)	29	1100	13	2.4	Multiple rib fractures
C-28B	M	58	Carcinoma Tonsilfossa	2	5'7"	110	35.0	12.0	8.5	LR(FL)	21	800	16	2.3	No external signs of fracture
C-29A	M	68	Cardio Pulmonary Arrest	6	5'5"	111	31.0	12.2	8.2	RL(FL)	21	600	18	2.3	No external signs of fracture
C-29B	M	68	Cardio Pulmonary Arrest	6	5'5"	111	31.0	12.2	8.2	LR(AR)	26	950	10	2.3	Multiple Rib Fractures
C-30A	M	50	Influenza	7	4'8 1/2"	71	29.0	9.3	7.2	LR(AR)	19	625	20	2.2	No external evidence of injury
C-30B	M	50	Influenza	7	4'8 1/2"	71	29.0	9.3	7.2	RL(AR)	20	1000	20	3.2	Multiple Rib Fractures

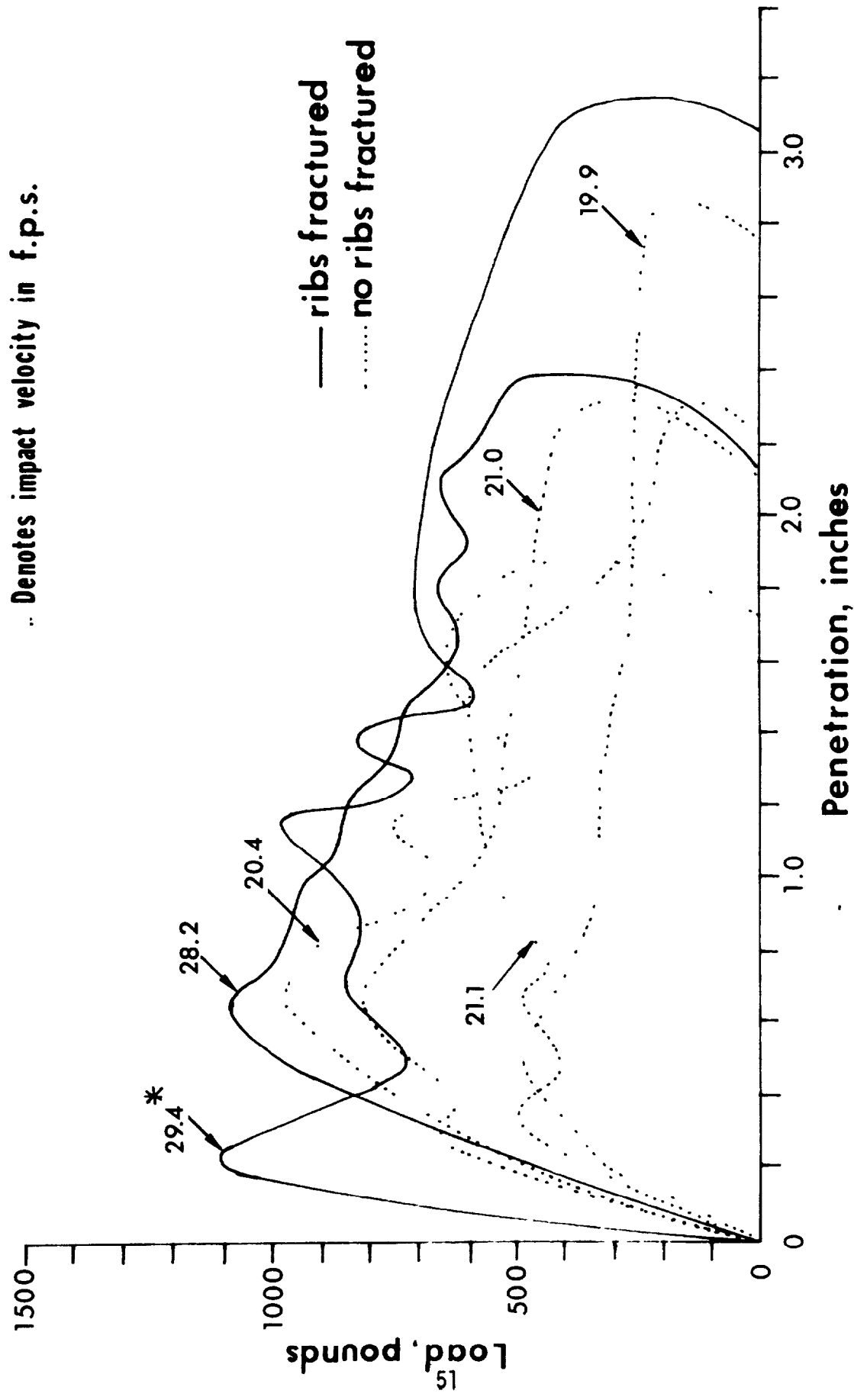
TABLE 4 CADAVER SIDE THORACIC IMPACT DATA (Continued)

TEST NO.	SEX	AGE (YRS)	CAUSE OF DEATH	NO. DAYS DEAD	HEIGHT	BODY WEIGHT LBS	CHEST DIMENSIONS			TYPE IMPACT	PISTON VELOCITY ft/sec	PEAK CONTACT FORCE (LBS)	PULSE DURATION MSEC	MAXIMUM PENETRATION (INS)	COMMENTS
							CIRCUM. IN	BREADTH IN	DEPTH IN						
C-31B	M	77	Myocardial Infarction	5	5'10"	163	38.0	13.8	8.7	LR(AR)	20	560	40	3.2	Rib Fractures
C-31C	M	77	Myocardial Infarction	5	5'10"	163	38.0	13.8	8.7	RL(AR)	26	870	30	3.3	Rib Fractures
C-32A	M	16	Aspirational Pneumonitis	1	5' 1"	96	30.0	10.8	6.1	RL(AR)	20	575	25	2.1	No External Evidence of Injury
C-32B	M	16	Aspirational Pneumonitis	1	5' 1"	96	30.0	10.8	6.1	RL(AR)	34	700	38	3.0	No External Evidence of Injury
C-32C	M	16	Aspirational Pneumonitis	1	5' 1"	96	30.0	10.8	6.1	RL(AR)	45	800	47	3.8	No External Evidence of Injury

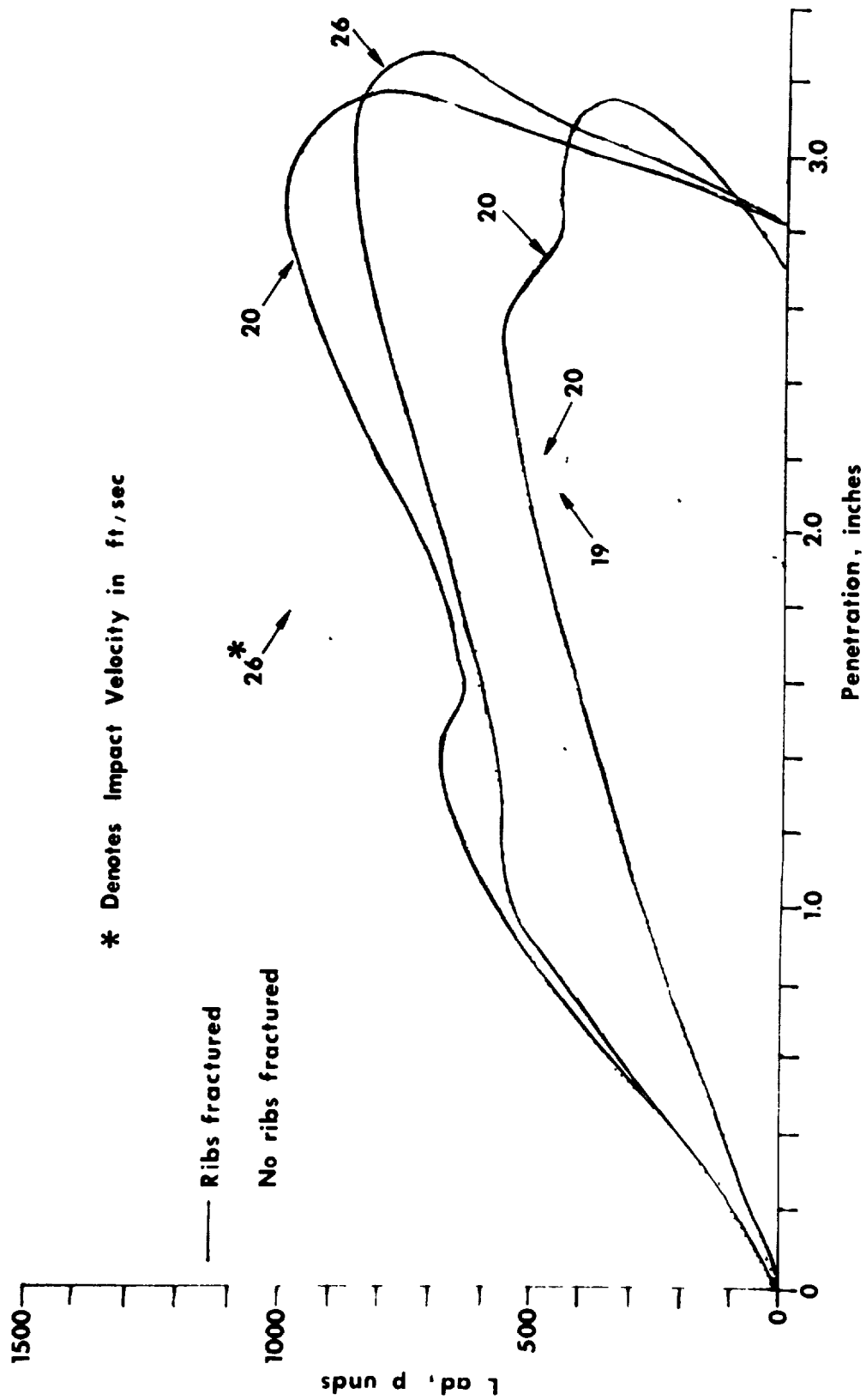
FL - Flat Impactor      LR- Left Side  
AR - Arm Rest      RL- Right Side

M - Male

F - Female

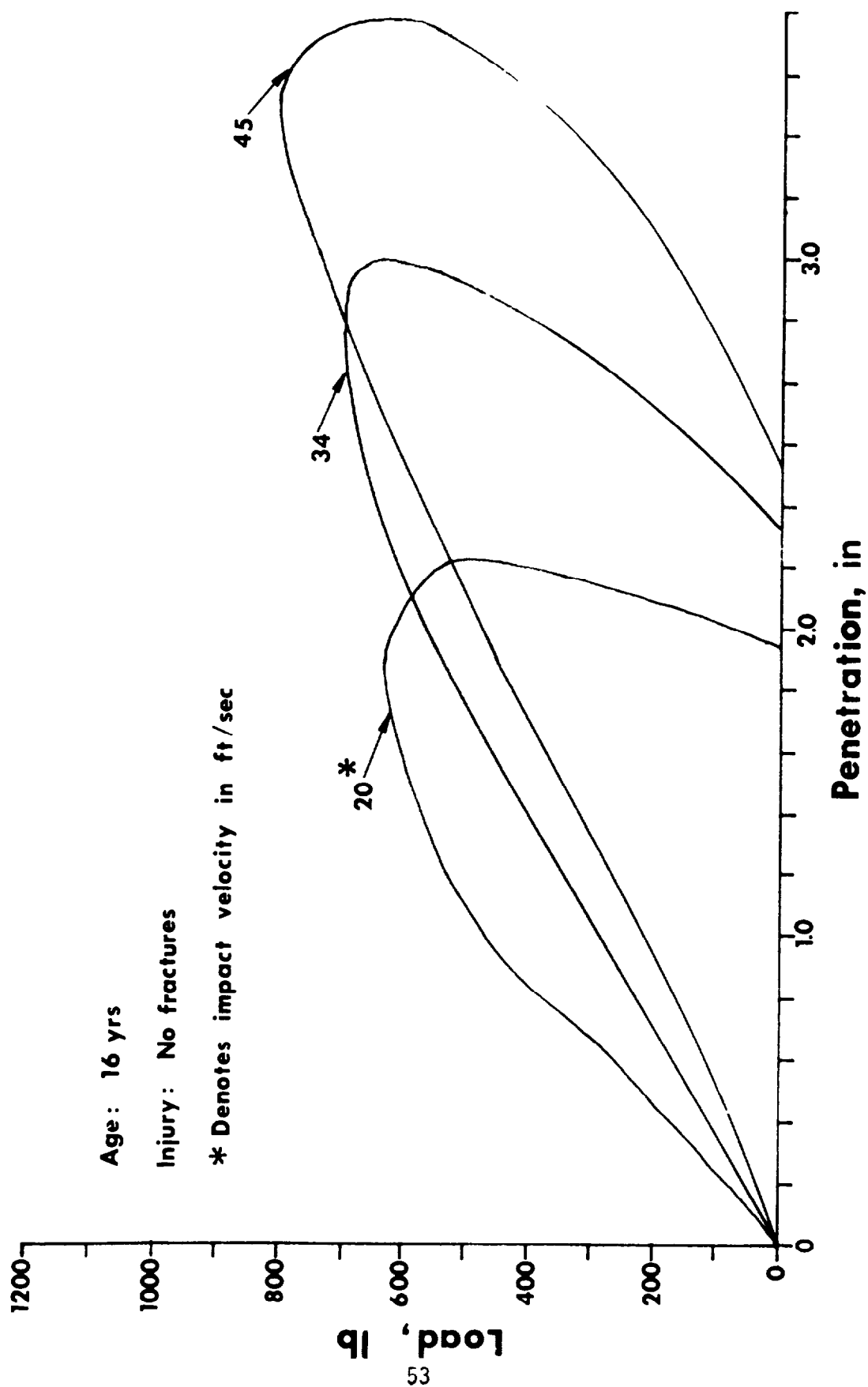


**DYNAMIC LOAD-PENETRATION CURVES FOR SIDE CHEST IMPACTS  
WITH 6" DIA. FLAT IMPACTOR.  
FIGURE 23.**



**DYNAMIC LOAD-PENETRATION CURVES FOR SIDE CHEST IMPACTS  
WITH SIMULATED ARM REST IMPACTOR**

**FIGURE 24**



**DYNAMIC LOAD - PENETRATION CURVES FOR HUMAN CADAVER  
SIDE CHEST IMPACTS**  
**FIGURE 25**



TYPICAL LIVER INJURIES  
FIGURE 26

The kidneys were commonly involved in these impacts with hemorrhaging throughout the organ. The pancreas was injured in most severe abdominal impacts with contusions to the surface as well as rupturing of the pancreatic duct. The stomach, colon, and jejunum were bruised slightly in most impacts. Injuries to the spleen were considerably less common and less severe than would be expected from clinical experience. This is thought to be due to the greater mobility of the spleen in the monkeys relative to that of the humans.

In most cases the injuries were the result of direct impact over the organ location. A difference in tolerance for right and left side impacts was noted and is thought to be due to the asymmetry of the abdominal cavity. The results of all abdominal impacts are shown in Table 5.

#### 3.4 RESULTS OF WHOLE BODY IMPACTS

The whole body impacts resulted in a combination of injuries obtained in the chest and abdominal impacts. The most significant injuries were found to be to the liver, kidney and lungs. The pancreas was involved in most of the severe impacts.

The contact force was found to be on the average higher than that necessary to cause a comparable ESI injury in an abdominal impact. The percent penetration for equivalent injuries was found to be much less in the whole body impacts than in the abdominal impacts. The results of the whole body impacts are given in Table 6.

#### 3.5 RESULTS OF DIRECT ORGAN IMPACTS

The 6000 ipm (8.3 fps) and the 12000 ipm (16.6 fps) impacts tended to cause subcapsular hemorrhaging, tears, and fractures. Static loading tended to crush the parenchyma while the capsule remained intact.

A typical force-deflection curve for a liver impact is shown in Figure 27.

TABLE 5 SUMMARY OF PRIMATE SIDE ABDOMINAL IMPACTS

ANIMAL SPECIES AND SEX	BODY REGION AND TYPE OF IMPACT	BODY WEIGHT lb	IMPACT VELOCITY ft/sec	IMPACT DURATION msec	PEAK CONTACT FORCE lb	CONTACT AREA in <sup>2</sup>	AVERAGE CONTACT PRESSURE psi	PERCENT PENETRATION	ABDOMINAL SCALING FACTOR	ESI	INJURY
SM-M	Rt-II/AR	1.1	35	3.8	120	3.5	34.2	52	.316	2	Small subcapsular hemorrhage in spleen and right kidney.
SM-M	Lt-II/AR	1.2	36	3.7	130	3.7	35.1	55	.298	2	Small tear on tip of left lobe of liver 3-4 mm. bruise on left side of stomach and colon.
SM-M	Rt-II/AR	1.4	45	4.4	155	4.0	39.0	60	.416	3	Several lacerations and liver contusions and hemorrhages in right kidney and pancreas
SM-M	Lt-II/AR	1.3	46	5.3	189	5.0	38.0	75	.693	5	Several large lacerations in liver 4-5 cc free blood in peritoneal cavity, kidney and pancreas hemorrhage noted.
RH-M	Rt-II/AR	11.5	28	8.0	200	4.1	49.0	46	.212	1	Small subcapsular hemorrhage in liver.
RH-M	Rt-II/AR	10.7	32	10.7	260	4.9	53.0	55	.482	3-4	Several small tears on liver hemorrhage on right kidney, right lower lung lobe hemorrhaged.
RH-M	Lt-II/AR	10.5	33	9.6	256	5.3	50.0	59	.384	1	Subcapsular hemorrhage in spleen and stomach.
RH-M	Lt-II/AR	9.4	38	10.7	305	5.7	53.5	63	.598	4	Multiple petechiae in left lobe of lung, large laceration of liver hemorrhage in left adrenal and pancreas. 5-6 cc free blood in peritoneal cavity.
RH-M *	Lt-II/AR	8.4	55	9.8	180	5.4	33.4	60	.341	3	Subpleural hemorrhage in left lung, marked dilatation of right side of heart; single laceration of liver superior to coronary ligament.



TABLE 5 SUMMARY OF PRIMATE SIDE ABDOMINAL IMPACTS (Continued)

ANIMAL SPECIES AND SEX	BODY REGION AND TYPE OF IMPACT	BODY WEIGHT lb	IMPACT VELOCITY ft/sec	IMPACT DURATION msec	PEAK CONTACT FORCE lb	CONTACT AREA in <sup>2</sup>	AVERAGE CONTACT PRESSURE psi	PERCENT PENETRATION	ABDOMINAL SCALING FACTOR	ISSI	INJURY
RH-M*	Rt-II/AR	13.4	37	13.1	280	6.4	43.8	71	.548	5	Cause of death exsanguination of 150 cc's blood into peritoneal cavity, also noted multiple liver lacerations.
RH-M*	Lt-II/AR	8.9	44	13.0	260	6.3	41.5	74	765	5	Lacerations and fractures of left lateral lobe of liver, small lacerations and fracture of right lateral lobe of liver, 20 cc hemoperitoneum. Cause of death (possible) - blood loss associated with liver damage.
RH-M*	Rt-II/AR	11.3	35	10.6	260	5.0	52.0	56	443	4	Ruptured left lower lobe of liver. Hemorrhage in right lung. right adrenal hemorrhage.
RH-M*	Rt-II/AR	9.3	28	8.0	80	4.4	18.2	49	101	1	Hemorrhage on diaphragmatic surface of both lungs. left lower lung lobe atelectatic; petechiae on lesser curvature of stomach.
BA-M*	Lt-II/AR	32.6	56	12.6	1220	27.6	24.4	69	440	5	Multiple petechiae in all lobe of lung. 50 cc hemoperitoneum, large laceration of liver, hemorrhage in right kidney, right adrenal, and pancreas
BA-M*	Rt-II/AR	31.0	38	8.7	505	17.2	29.4	43	115	2	Contusion of left lower lobe, petechiae in right lung, small subcapsular hemorrhage
BA-M*	Lt-II/AR	26.0	46	10.0	755	20.8	36.2	52	245	3	Small hemorrhage in right and left lower lobes, contusion of left lung at 8th rib, extensive hemorrhage in several areas. Adrenals, spleen evidence of hemorrhage.
BA-M*	Lt-II/AR	42.0	52	11.0	890	24.4	36.5	61	201	4	Hemorrhage in 7th-11th intercostal spaces, large contusion left lung, massive hemoperitoneum, contusions and hemorrhages in both kidneys, pancreas, and liver, several lacerations in liver.

TABLE 5 SUMMARY OF PRIMATE SIDE ABDOMINAL IMPACTS (Continued)

ANIMAL SPECIES AND SEX	BODY REGION AND TYPE OF IMPACT	BODY WEIGHT lb	IMPACT VELOCITY ft/sec	IMPACT DURATION msec	PEAK CONTACT FORCE lb	CONTACT AREA in <sup>2</sup>	AVERAGE CONTACT PRESSURE PSI	PERCENT PENETRATION	ABDOMINAL SCALING FACTOR	ESI	INJURY
BA-M*	Rt-II/AR	43	47	13.0	1140	25.6	44.5	64	337	5	Hemorrhage in left lung, massive hemoperitoneum, fracture inferior right lobe of liver, hemorrhage noted in liver, pancreas, left adrenal, and both kidneys
BA-M*	Rt-II/AR	32	45	11.0	816	23.2	35.0	58	.246	4	Hemorrhage in left lung, hemoperitoneum, rupture and contusions of right side of liver, right adrenal.
BA-F*	Rt-II/AR	35	41	12.0	756	19.4	39.0	48	266	3	Several petechiae in right lung; severe contusion of right kidney and adrenal.
BA-F*	Lt-II/AR	34	48	11.0	750	21.6	34.8	54	221	3	Several petechiae in left lung, contusions of left adrenal, spleen and descending colon, rupture of splenic artery, contusion left lobe liver

Rt - Right  
 Lt - Left  
 AR - Arm Rest  
 II - Upper abdominal Region  
 M - Male

\*From 1971 Final Report  
 "Door Crashworthiness Criteria"

TABLE 6 SUMMARY OF TORSO SIDE IMPACTS FOR PRIMATES

ANIMAL SPECIES & SEX	BODY REGION & TYPE OF IMPACT	BODY WEIGHT lbs	IMPACT VELOCITY ft/sec	IMPACT DURATION msec	PEAK CONTACT FORCE lbs	PERCENT PENETRATION	ESI	INJURY
SM-M	Lt-III/FL	1.5	44	4.0	900	54	5	Hematoma tip of right lung, small hole in right atrium, tears on on liver, deep bruise in kidney, jejunum & colon, left femur broken at lesser trochanter.
SM-F	Rt-III/FL	1.6	54	5.5	750	37	4	Petechial hemorrhage all over right lung, tip of right ventricle bruised, liver fractures on right lobe, right kidney bruised, bruises on colon and jejunum.
SM-M	Rt-III/FL	1.5	45	5.3	525	36	3	Petechial hemorrhage all over right lung, liver fractures on right lobe, bruises on colon.
SM-M	Rt-III/FL	1.4	44	5.7	500	35	3	Petechial hemorrhage right lung, liver fractures, bruises on right kidney, colon and jejunum.
SM-M*	Lt-III/FL	1.2	32	6.6	397	31	2	Multiple petechiae on both lungs; retroperitoneal hematoma, small omental hematoma.
SM-M*	Lt-III/FL	1.8	43	9.0	456	33	1	Petechial hemorrhage in left lung.
RH-M	Rt-III/FL	9.3	44	10.5	1975	49	3	Large liver fracture, petechial hemorrhage, right lung, bursting to right kidney.
RH-M*	Lt-III/FL	11.3	46	8.8	2350	51	4	Marked congestion of left lung; scattered petechiae in right lung; severe autolysis noted in pancreas.
RH-M*	Rt-III/FL	12.9	40	13.8	1820	50	2	Focal hemorrhage in right lower lobe of lung.
RH-M*	Lt-III/FL	7.5	36	8.4	1700	48	1	Acute passive congestion of left lung; pancreas: hemorrhage into interstitium.

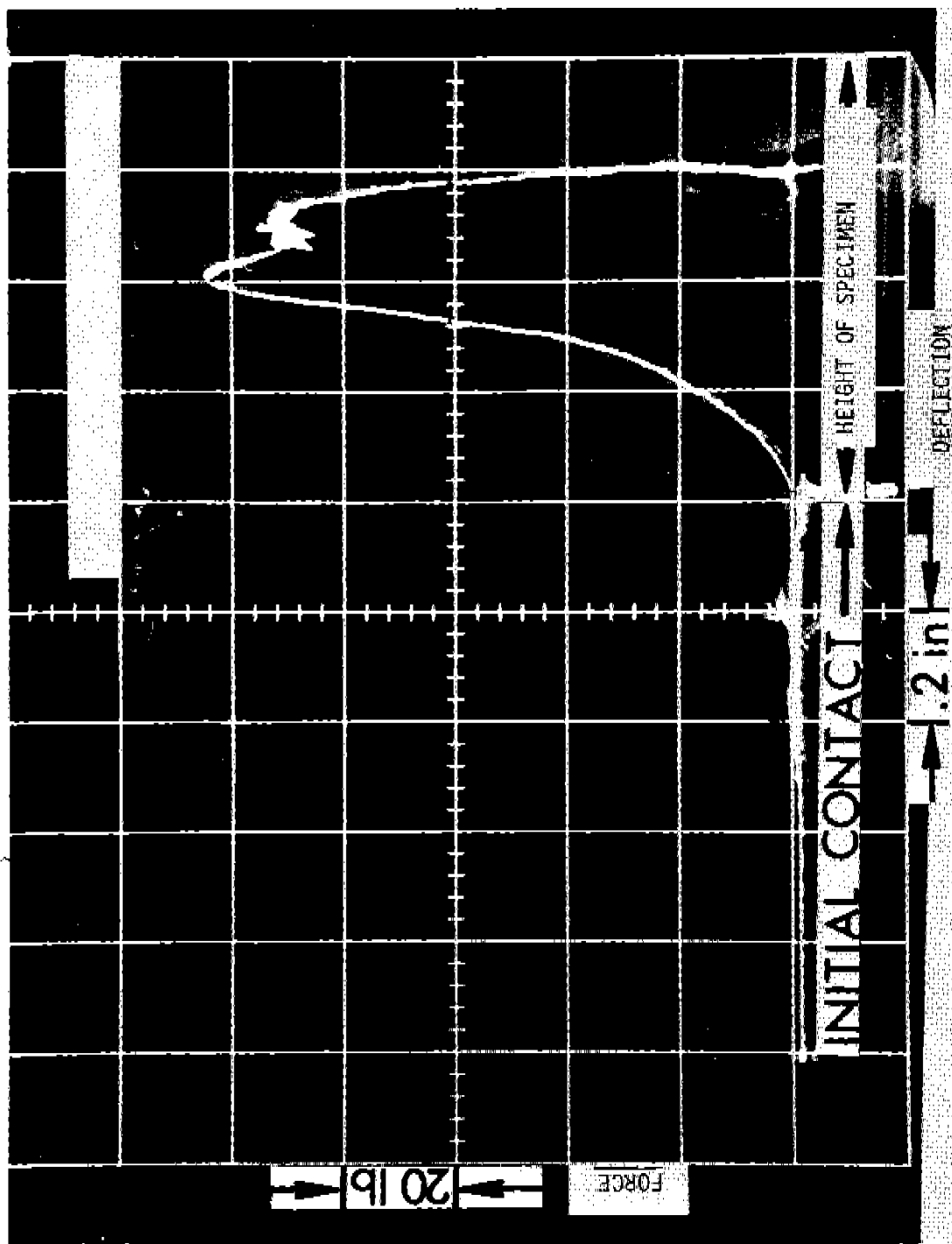
TABLE 6 SUMMARY OF TORSO SIDE IMPACTS FOR PRIMATES (Continued)

ANIMAL SPECIES & SEX	BODY REGION & TYPE OF IMPACT	BODY WEIGHT lbs	IMPACT VELOCITY ft/sec	IMPACT DURATION msec	PEAK CONTACT FORCE lbs	PERCENT PENETRATION	ESI	INJURY
RH-M*	Lt-III/FL	10.9	39	11.2	2360	48	2	Liver: laceration of capsula and parenchyma, hematoma noted in liver substance; Pancreas focal hemorrhage; lungs, kidney, spleen: Acute passive congestion.
RH-M*	Rt-III/FL	9.3	45	10.0	2380	52	4	Focal hemorrhage in both lungs, liver, and pancreas; severe autolysis noted in pancreas; acute passive congestion of adrenals.
BA-F	Rt-III/FL	20.0	70	8.0	1650	42	4	Multiple rib fractures on right side. Lower right lung macerated, mild contusion right ventricle, bursting injury of liver, crush fracture of right kidney.
BA-F	Lt-III/FL	21.0	70	8.0	2000	37	3	Petechial hemorrhage - left lung, large hematoma tip of left lung, small petechial hemorrhage right lung, large liver fracture, subcapsular hematoma or liver bruise in stomach.

Rt - Right  
Lt - Left  
FL - Flat Impactor  
III - Whole Body Region

M - Male  
F - Female

\* From 1971 Final Report "Door Crashworthiness Criteria"



LOAD-DEFLECTION TRACE FOR DIRECT LIVER IMPACT  
FIGURE 27

The specimen height, force and deflection are read directly from this oscilloscope trace. The force was normalized by the impactor cross-sectional area which was  $1.77 \text{ in}^2$  for the liver and  $1.18 \text{ in}^2$  for the kidney. The deflection was then normalized by the specimen height. Typical normalized force (stress) and deflection (strain) curves for static, 6000 ipm and 12000 ipm loading rates are shown for liver tissue in Figure 28. The maximum average stress and strain as well as the strain energy density (that is, the area under the stress-strain curve) was computed for the region loading up to failure.

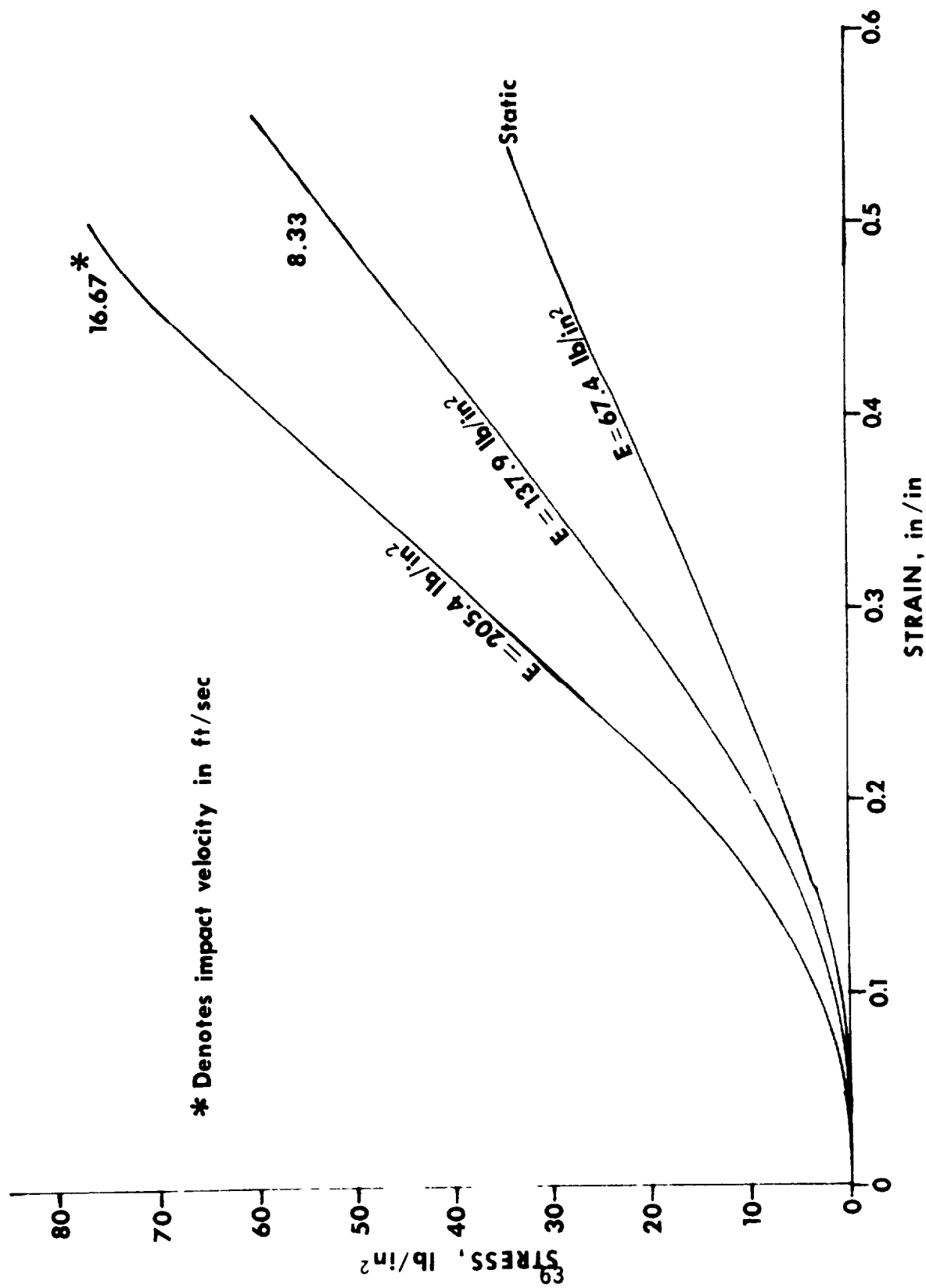
In the kidney impacts, outright fracture of the renal capsule was observed only once. Most of the injuries were internal to the renal cortex. The kidney was found to have a higher tolerance to impact than the liver. The results for the liver and kidney impacts are given in Table 7.

### 3.6 RESULTS OF CHEST MECHANICAL IMPEDANCE TESTS

The results of the driving point impedance response for the chest of three monkeys and one human are given in Figure 29. In each test the driving point impedance response was found to be quite similar to the response of a pure damper. The impedance was independent of frequency and the force was very nearly in phase with the velocity.

The acceleration as a function of frequency for the side opposite the driving point is shown in Figure 30. The input acceleration at the driving point was 10 G's.

Over the acceleration range studied, (10 G's to 20 G's), no dependency was found between the impedance and the input acceleration.



**STRESS-STRAIN CURVES FOR DIRECT IMPACTS ON PERFUSED LIVERS (RHEBUS)**

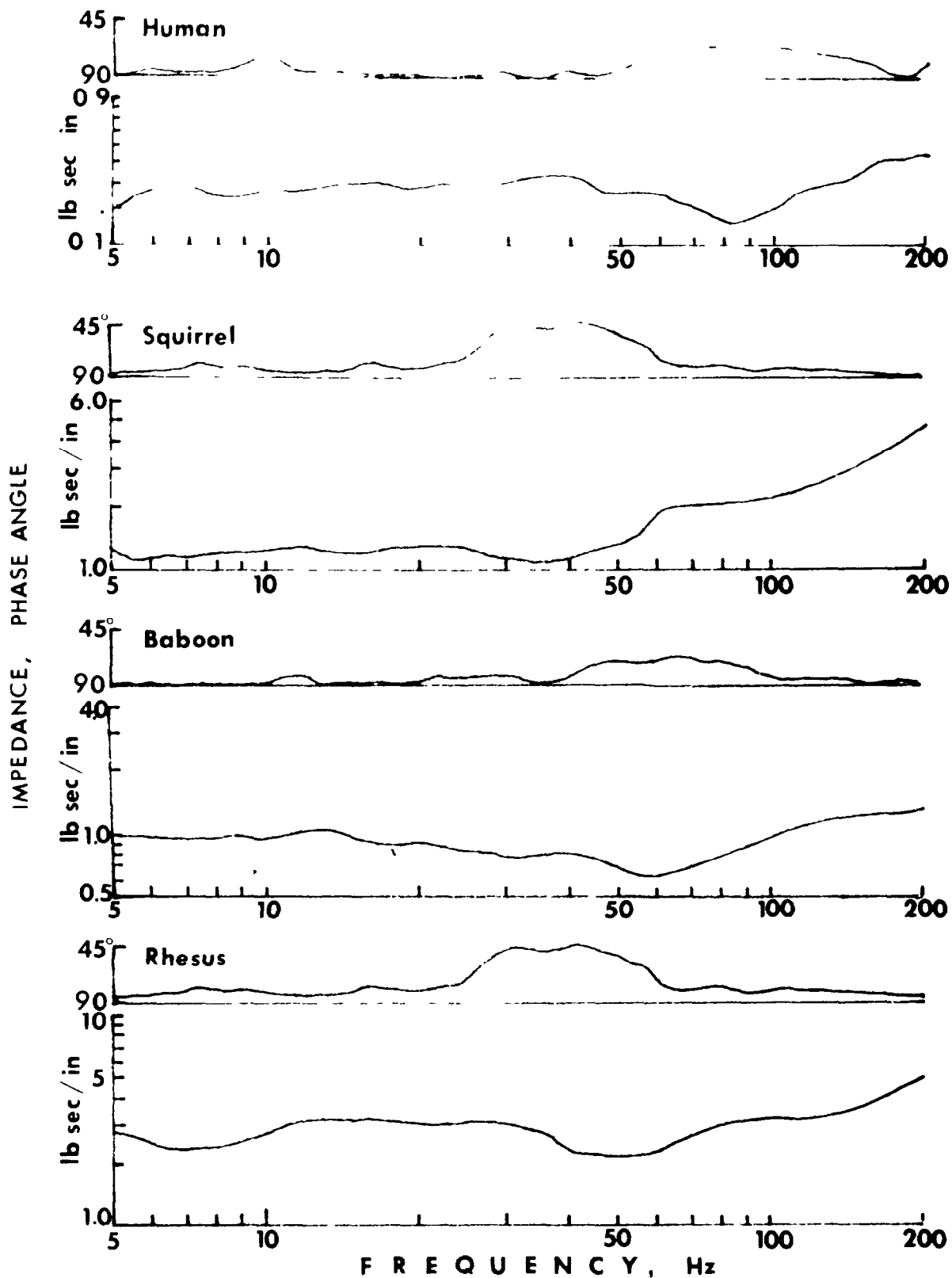
**FIGURE 28**

TABLE 7 SUMMARY OF DIRECT ORGAN IMPACTS

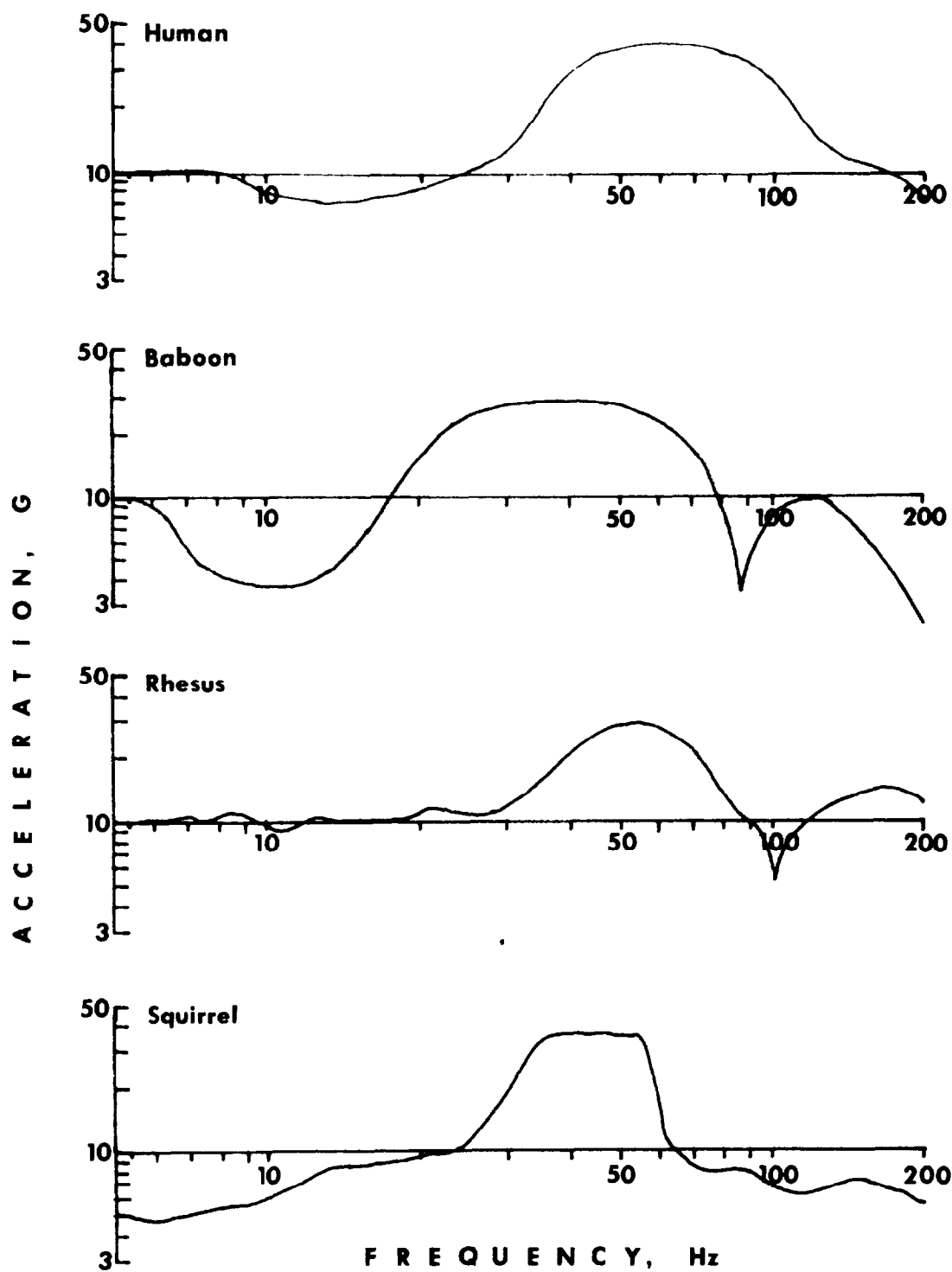
Organ Type	Impact Velocity in/min	Max. Average* Stress psi	Max. Average * Strain in/in	Strain Energy Density in-lb/in <sup>3</sup>	Modulus of Elasticity psi	Estimated Severity Index
Liver	Static	21.47	.541	4.28	55.6	3-4
Liver	Static	33.90	.533	8.53	67.4	5
Liver	Static	50.85	.569	11.66	115.8	5+
Liver	Static	50.70	.443	8.80	148.2	5
Liver	6000	44.07	.354	5.42	196.7	2
Liver	6000	44.00	.383	6.78	115.1	2
Liver	6000	45.20	.570	12.30	150.0	3
Liver	6000	44.00	.550	10.83	102.6	3
Liver	6000	46.32	.414	9.85	152.4	3
Liver	6000	53.67	.523	15.13	102.6	4
Liver	6000	59.32	.510	26.38	137.9	5+
Liver	12000	36.72	.416	6.00	126.6	0-1
Liver	12000	33.90	.378	6.41	89.7	1-2
Liver	12000	45.20	.438	8.78	150.7	3
Liver	12000	76.84	.500	13.28	205.4	4
Liver	12000	67.80	.480	13.50	222.2	4-5
Liver	12000	98.87	.470	17.81	299.6	5
Kidney	Static	46.61	.280	5.29	443.9	0-1
Kidney	6000	152.54	.410	31.52	994.1	4
Kidney	6000	145.76	.380	16.35	694.4	2-3
Kidney	12000	152.54	.444	27.39	950.0	4-5
Kidney	12000	139.83	.333	18.28	842.4	1-2

\* These are the peak values that the average stress and strain reached in each test.





**DRIVING POINT MECHANICAL IMPEDANCE  
CURVES FOR SIDE THORAX  
FIGURE 29**



**TRANSFER POINT ACCELERATION CURVES  
FOR SIDE THORAX**

**FIGURE 30**

## 4.0 PRIMATE SCALING

### 4.1 HEAD INJURY SCALING

The head contact force, duration of impact, head angular acceleration, linear acceleration and velocity were obtained for each side impact. The values of these parameters to be used in the scaling relationships were taken from tests where the animal received an injury considered to be just below life-threatening or approximately 3 on the ESI scale. If no ESI of 3 was obtained from the tests, the engineering parameters were obtained by extrapolating between ESI's of 2 and 4.

The head mass, brain mass, average skull radius and average skull thickness for each test animal in a particular species group were reported as average values for that species.

Previous work by McElhaney (1970) on the mechanical properties of bone, scalp and brain indicated that there is very little difference, if any, in the material properties of these tissues for primates. On the basis of this work, it was assumed that the material properties of scalp, brain, and bone were the same for all animals tested and that the results could be extrapolated to man.

For each of the species studied, the average values of the physical properties, force time profiles, and the resulting mechanical responses needed to produce a desired injury level were obtained. The extrapolation to man was then made by scaling relationships developed by dimensional analysis techniques.

The extrapolated tolerable acceleration and pulse duration for human padded impacts was compared to the Maximum Strain Criterion developed for side head impacts in the 1971 "Door Crashworthiness Criteria."

Considering the variables  $A$ ,  $\tau$ ,  $V$ ,  $a$ ,  $h$ , where

$A$  = linear head acceleration (ft/sec<sup>2</sup>)

$\tau$  = acceleration pulse duration (msec)

$V$  = velocity of Impact (ft/sec)

$a$  = average skull radius (in)

$h$  = average skull thickness (in)

Assuming that  $\pi$ , a dimensionless quantity, is a function of these variables.

$$\pi = f(V, A, \tau, a, h) \quad (1)$$

Then, from Buckingham's Theorem of Dimensional Analysis, Equation 1 (Langhear, 1951) can be written as follows:

$$\pi = f(\pi_1, \pi_2, \pi_3) \quad (2)$$

where  $\pi_1$ ,  $\pi_2$ ,  $\pi_3$  are dimensionless quantities of the form

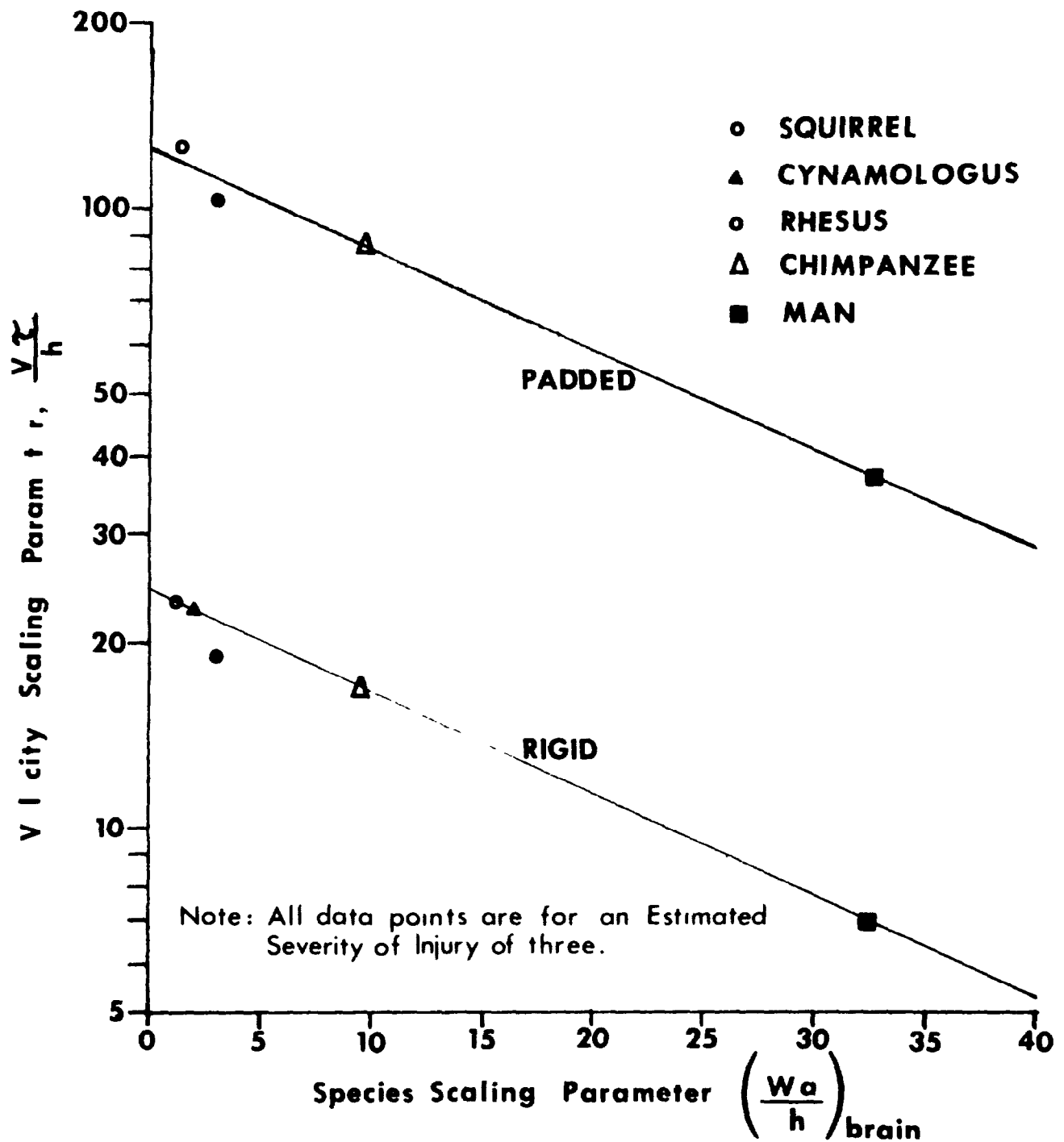
$$\pi_1 = \frac{h}{a} \quad (3)$$

$$\pi_2 = \frac{V\tau}{h} \quad (4)$$

$$\pi_3 = \frac{A}{V^2/h} \quad (5)$$

The dimensionless variable  $a/h$  was weighted by multiplying it by the brain weight of each species tested. This species dependent term  $\pi_1^*$  was then plotted against each of the remaining dimensionless variables.

The scaling parameter  $\pi_1^*$  was plotted against the dimensionless variable  $\pi_2$  for each species represented (Figure 31). From this plot the value of  $\pi_2$  was found for humans by extrapolation. The pulse duration of 20 msec was used in the evaluation of  $\pi_2$  as predicted by the MSC curve for humans. This yields a tolerable rigid impact velocity of 15 mph and a tolerable padded impact velocity of 29.5 mph for the human head when impacted to the



## VELOCITY SCALING PARAMETER FOR SIDE HEAD IMPACTS

FIGURE 31

side of the head.

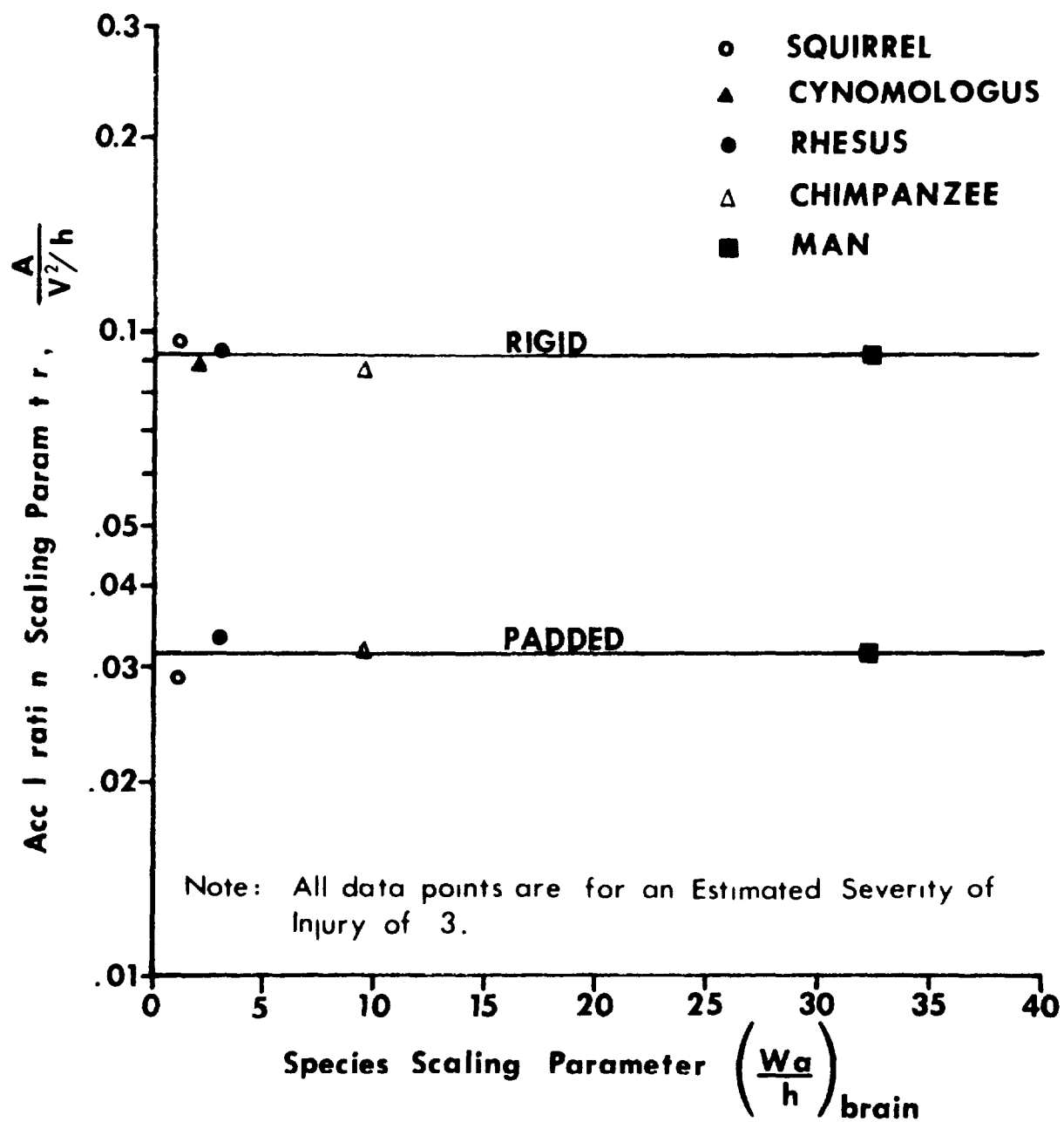
The scaling parameter  $\pi_1^*$  was plotted against the dimensionless variable  $\pi_3$  for each species (Figure 32). From this plot the value of  $\pi_3$  was found for humans. Knowing  $h$  and  $V$  from Figure 31 the tolerable acceleration for padded side head impacts was found to be 76 G's. This compared with 56 G's for rigid head impacts as reported in the 1971 "Door Crashworthiness Criteria" Report.

The ninth and tenth cadaver padded head impacts yielded accelerations and impact velocities very close to the predicted tolerance levels from the extrapolated monkey data. The head autopsy indicated no gross trauma to the skull, neck or brain. The head contact forces for these two impacts were approximately 200 pounds, with angular accelerations and velocities of approximately 8,200 rad/sec<sup>2</sup> and 70 rad/sec respectively.

The scaling parameters used in the extrapolation to man and the resulting human parameters derived from the scaling are given in Table 8.

The Maximum Strain Criteria as developed for the 1971 "Door Crashworthiness Criteria" report has been modified to take force as well as acceleration as an input parameter. This modification enables force to be inputted at the contact point for direct impacts and accelerations for the no impact case. The model response in both cases is based on the resultant acceleration of the center of gravity.

The MSC head injury criterion of 0.0061 in/in derived in the 1971 "Door Crashworthiness Criteria" report was used to predict human head tolerance for long pulse duration. The results of the experimental extrapolation and the MSC model are shown in Figure 33. This prediction was based on the extrapolation to man of the engineering parameter found to have high correlation with head injuries in monkeys.



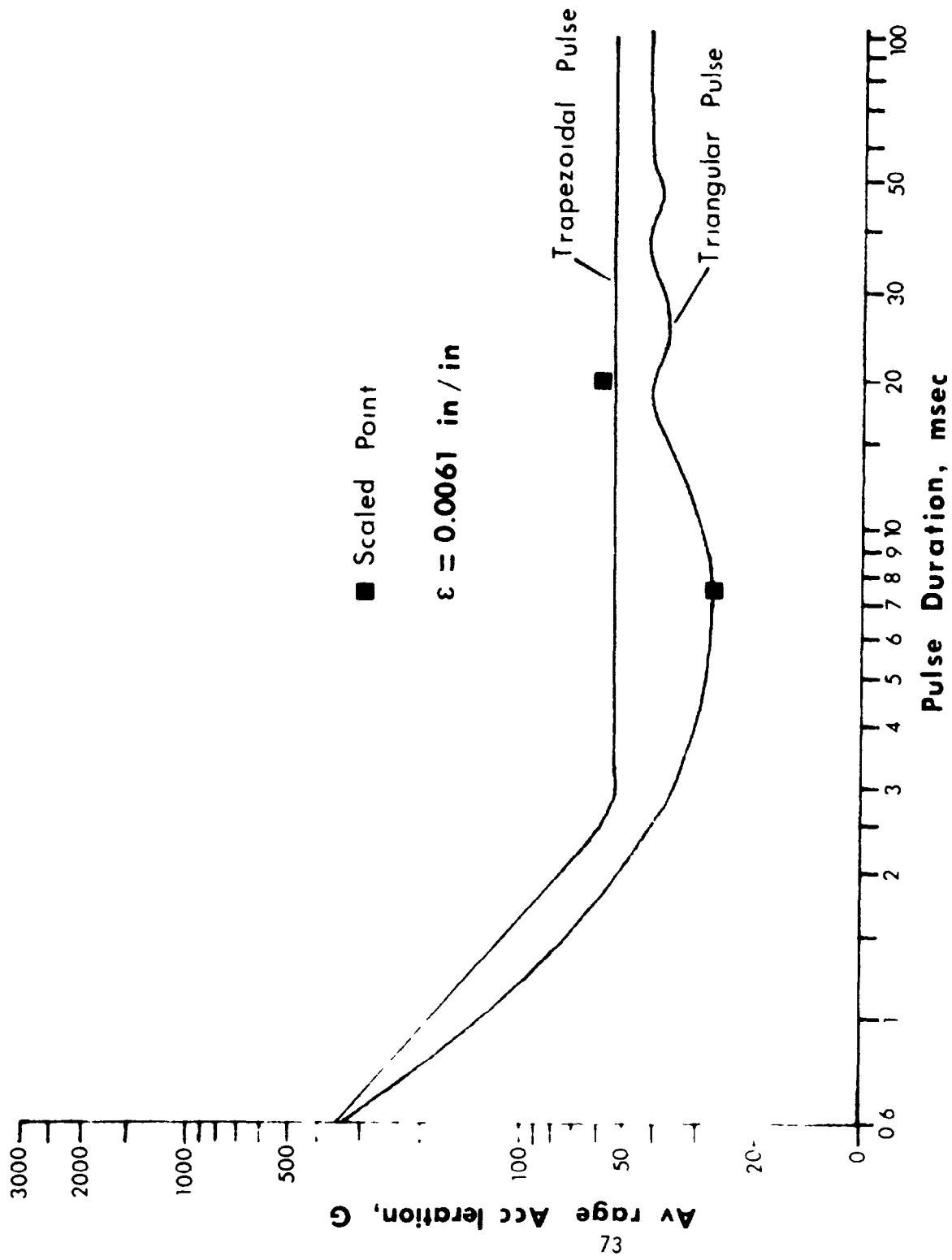
## ACCELERATION SCALING PARAMETER FOR SIDE HEAD IMPACTS

FIGURE 32

TABLE 8  
SUMMARY OF SCALING PARAMETERS FOR LONG DURATION HEAD IMPACTS

	SPECIES	AVERAGE $a/h$	AVERAGE BRAIN WEIGHT $W_B$	AVERAGE HEAD WEIGHT $W_H$	AVERAGE SKULL THICKNESS $h$	ACCELERATION PULSE DURATION <sup>1</sup>	PEAK HEAD ACCELERATION $A$	PEAK HEAD VELOCITY $V$	SCALING FACTORS		
									$\pi_1^*$ $\frac{a}{W_B h}$	$\pi_2$ $\frac{V_T}{h}$	$\pi_3$ $\frac{Ah}{V^2}$
			lb	lb	in	msec	G's	fps	1b	—	—
	Squirrel	18.8	0.064	0.19	.043	6.0	1490	75	1.21	125	.029
	Rhesus (10 lb)	15.2	0.165	1.03	.079	7.8	1200	88	2.50	103	.033
	Chimpanzee	11.4	0.835	5.26	.184	11.0	1000	124	9.54	89	.032
	Human	10.8	3.000	10.00	.283	20.0	76	43	32.50	36	.032





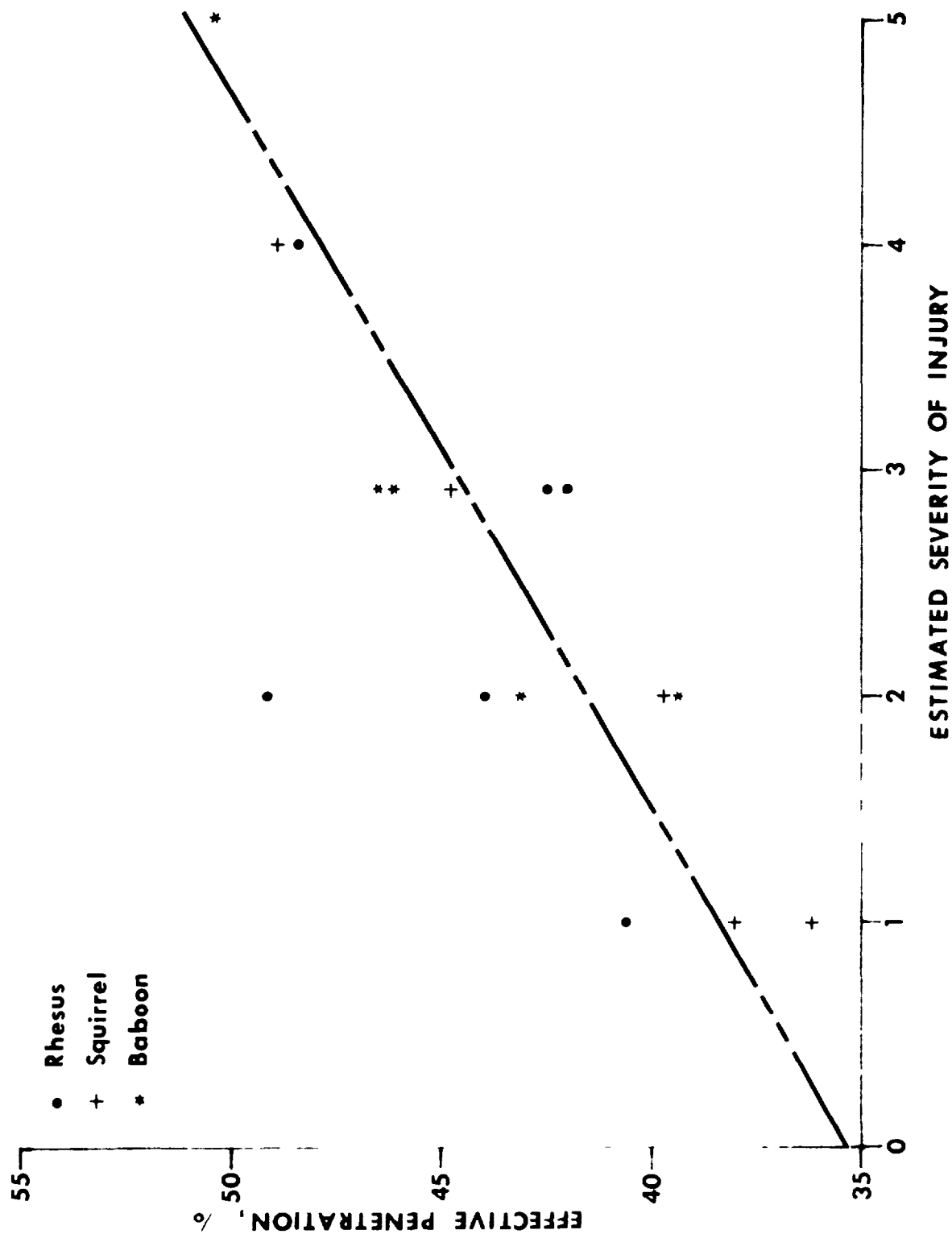
**MAXIMUM STRAIN CRITERION FOR HUMAN**

**FIGURE 33**

## 4.2 THORACIC INJURY SCALING

There have been several possible indicators suggested for predicting chest injuries, acceleration, force and displacement, to name a few. Use of acceleration as an indicator becomes very awkward because of the different accelerations encountered throughout the chest during impact. The use of force as an indicator can also become cumbersome because of its dependence on the weight of the upper torso. Since most chest injuries were found to be related to the deflections of the rib cage, chest displacement was chosen for this study as the indicator for thoracic injury. The chest displacement was normalized by dividing it by the chest breadth. Therefore, the ESI could be plotted against the percent chest penetration. When this was done for each species studied, no apparent correlation was found. An aspect ratio defined, as breadth divided by the depth of the chest, was calculated for each animal species. It was then noted that this quantity was inversely related to ordering of ESI versus penetration relationships. Therefore, each percent penetration value was multiplied by the aspect ratio to yield an Effective Percent Penetration versus ESI relationship (Figure 34). This relationship now groups all the various species tested into a narrow band independent of the species type. Extrapolation to man was then made by using the Effective Percent Penetration for an ESI of three. This yields an actual percent penetration of 31% and an actual penetration of 2.65 inches based on the average chest depth of 8.5 inches and aspect ratio of 1.45 for twelve cadaver impacts.

Based on the cadaver impacts, rib fracture did not occur on the average for impact velocities of 14 mph and penetrations of 2.1 inches. When the velocity of impact was raised to 20 mph and the penetration increased to 3.0 inches, rib fracture did occur. This was for a group of cadavers whose average age at the time of death was 58 years. It should be noted that for the 16 year old youth, rib fracture did not occur for penetrations of up to approximately four inches. Any internal injuries will be reported at a future date after a detailed autopsy is performed.



SCALING FACTOR FOR THORACIC IMPACT INJURY SENSITIVITY

FIGURE 34

Therefore, based on the animal scaling and the cadaver chest impacts, an impact of 21 mph velocity with 2.65 inches of deflection could result in a force of 900 pounds, a pulse duration of 25 msec, and an injury level of three to the human chest from either the right or left side. See Figure 23.

#### 4.3 ABDOMINAL INJURY SCALING

The results of the simulated arm rest impact to region II are summarized in Figure 35, which shows the average peak contact pressure (computed by dividing the peak impactor force by the maximum projected impactor contact area) versus the ESI. For an ESI of 3, this contact pressure was approximately 31 psi for all species of primates, including humans. If a contact area of 22.5 in<sup>2</sup> is used as the area of impact to humans then a contact force of 700 lb should result in an ESI of 3 to Region II.

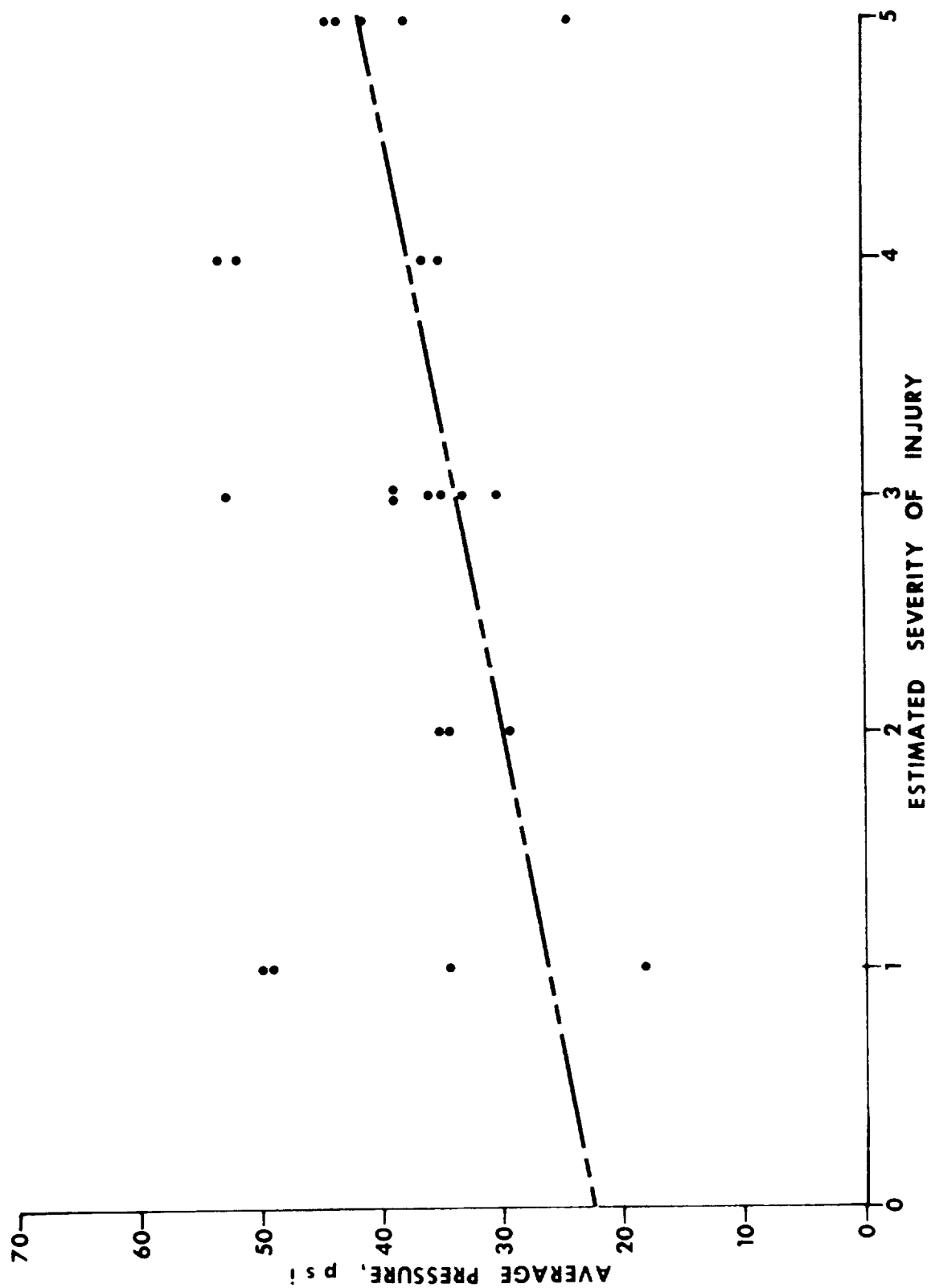
All of the animal impact data to Region II was submitted to a computer-assisted statistical analysis for both positive and negative correlations between the various parameters and ESI. It was found that the peak force and pulse duration had a high level of correlation with the ESI. Using this correlated data, a dimensional analysis study was made to develop a scaling factor to predict abdominal injury in man.

The scaling factor which was determined is given below:

$$ESI \propto \text{Log} \frac{F\tau^2}{M\sqrt{A}}$$

where    F = Peak contact force  
           $\tau$  = Pulse duration  
          M = Mass of animal  
          A = Impactor Contact Area

This scaling factor was originally developed for front abdominal impacts, which was reported by Stalnaker, et. al. (1972) at the Symposium held at



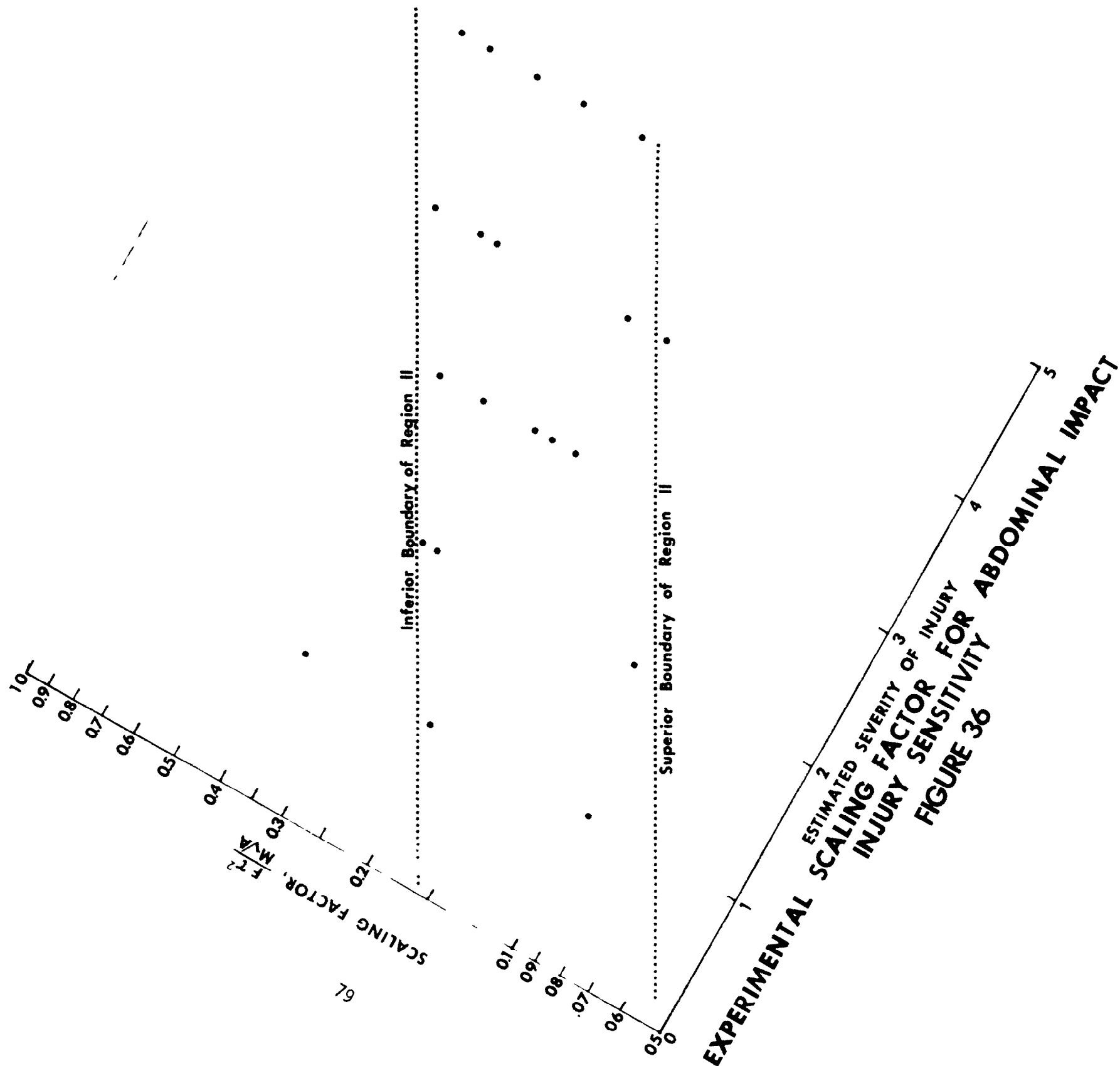
**AVERAGE PRESSURE vs INJURY INDEX FOR PRIMATE SIDE ABDOMINAL IMPACTS WITH SCALED ARMREST**

**FIGURE 35**

General Motors Research Laboratories in Warren, Michigan.

The results of the side abdominal impacts are shown in Figure 36. The boundaries in this figure represent the upper and lower boundaries of region II. The higher the scaling factor, the greater the region's tolerance to impact.

The velocity of impact can be calculated from this scaling factor. Using the body weight for an average man (165 pounds), a contact area of  $22.5 \text{ in}^2$ , percent penetration of 54%, for right side impacts, the velocity of impact for right side impact was found to be approximately 20 fps. Using Figure 40 of the 1971 "Door Crashworthiness Criteria" report, the left side impact velocity required to yield the same percent penetration will be 20% higher than that for the right, making it approximately 24 fps. The average pulse duration for this impact would be found to be 28 msec.



## 5.0 DISCUSSION AND CONCLUSIONS

The conclusions of this study are based on the accumulated data from the 1971 "Door Crashworthiness Criteria" report and the data contained in this report.

1. A padded side head impact of 29.5 mph and an impact pulse duration of 20 msec to humans will result in a head contact force of 200 pounds, a resultant linear acceleration of 76 G's, and an ESI of three.

The types of injuries found for the long duration impacts involve brain stem and internal brain hemorrhaging not directly associated with the impact location. All injuries observed in this study are found clinically.

2. Impacts to the chest resulted in a deflection criteria for evaluating chest side impacts. A deflection to the right or left side of the chest of 2.65 inches was found to yield an ESI of three. Rib fractures were found in the older cadavers studied for impact velocities of approximately 19 mph and deflections of 2.9 inches. In the one case where a 16 year old cadaver subject was impacted, a penetration of 3.8 inches was obtained with no rib fractures.

3. In the abdominal study a scaling factor was derived for rating abdominal injuries. The injury produced by a given force was found to be a function of the projected contact area, duration of impact, and mass of the animal. The location of the impact greatly influenced the injury produced. When the location of impact and mass of the subject are chosen, the composite function  $ESI \propto \log F \tau^2 / M \sqrt{A}$ , relates well to the degree of injury produced in a side abdominal impact. Relatively small forces were required to produce severe injuries of the solid viscera when the impact was made in the upper abdomen. However, much greater forces were required to produce comparatively severe injuries when force was applied to the lower



abdomen. The contact pressure to the abdominal area was found to be independent of species. It was also found that the tolerance values for the right side of the abdomen was not necessarily the same for the left. Table 9 summarizes the abdominal tolerance values for an ESI of three.

TABLE 9 SUMMARY OF ABDOMINAL TOLERANCE VALUES

	Right Side	Left Side
Velocity of Impact	20 fps	24 fps
Percent Penetration	54%	60%
Impact Duration	28 msec	28 msec
Force of Impact	700 lbs	700 lbs

## 6. REFERENCES

Aldman, B., "A Protective Seat for Children - Experiments with a Safety Seat for Children Between One and Six," 8th Stapp Car Crash Conference, Oct., pp. 320-328, 1964.

Appoldt, F.A., "Dynamic Tests of Restraints for Children," 8th Stapp Car Crash Conference, Oct., pp. 329-345, 1964.

Beeding, E.L., Daisy Tract Tests 1956-270, June 13 - December 17, 1957. USAF Missile Development Center, Holloman Air Force Base, New Mexico, Project No. 7850, Test Report No. 7, March, 1958.

Brink, H., "Automotive Side-Window Glass Impact Study," Proceedings, 7th Stapp Car Crash Conference, Charles C. Thomas, Springfield, Ill., pp. 250-268, 1955.

Brown, W.K., J.D. Rothstein and P. Foster, "Human Response to Predicted Apollo Landing Impacts in Selected Body Orientations," Aerospace Medicine, 37(4): 394-398, April 1966.

Chandler, R.F., Lateral Impact Data. Daisy Decelerator Tests, 6751st Aeronautical Field Lab, Holloman Air Force Base, New Mexico, Unpublished manuscript, January 1966.

Clarke, N.P., E.B. Weis, J.W. Brinkley, and W.E. Temple, "Lateral Impact Tolerance Studies in Support of Apollo," Report I. AMRL Memo, M-29, Wright Patterson Air Force Base, Ohio, February 1963.

Eiband, M., "Abrupt Transverse Decelerations," Bioastronautics Data Book, p. 70, 1965.

Friedberg, M., J.W. Garrett and J.K. Kehlberg, "Automobile Side Impacts and Related Injuries," Cornell Aeronautical Laboratory, Inc., Buffalo, CAL No. VJ-2721-R8, December 1969.

Gadd, C.W., "Criteria for Injury Potential," Proceedings, Impact Acceleration Stress Symposium, National Academy of Sciences/National Research Council, Publication No. 977, 1962.

Gadd, C.W., "Use of Weighted Impulse Criterion for Estimating Injury Hazard," 10th Stapp Car Crash Conference, Society of Automotive Engineers, Inc., New York, Paper No. 660793, 1966.

Galford, J.E. and J.H. McElhaney, "A Viscoelastic Study of Scalp, Brain, and Dura," Journal of Biomechanics, Vol. 3, No. 2, pp. 211-221, March 1970.

Gennarelli, T.A., L.E. Thibault, and A.K. Ommaya, "Pathophysiological Responses to Rotational and Translational Accelerations of the Head," 16th Stapp Car Crash Conference, pp. 296-308.

Greene, J.E., "Basic Research In Crashworthiness II-Side Impact Tests of Unmodified Vehicles," Interim Technical Report, Calspan Corp. Buffalo, N.Y., February 1973 242 p. Report No. CAL YB-2987-V-9 Contract No. FH-11-7622.

Gurdjian, E.S., H.R. Lissner and L.M. Patric, "Concussion-Mechanism and Pathology," Proceedings, Seventh Stapp Car Crash Conference, Society of Automotive Engineers, Inc., New York, pp. 470-482, 1965.

Hirsch, A.C., A.K. Ommaya and R.H. Mahone, "Tolerance of Subhuman Primate Brain to Cerebral Concussion," Impact Injury and Crash Protection, Chap. 16, pp. 352-369, 1970.

Huelke, E.F. and H.W. Sherman, "Automobile Occupant Ejection Through the Side Door Glass," Society of Automotive Engineers, Inc., New York, Paper No. 710076, 1971.

Langhear, H.L., "Dimensional Analysis and Theory of Model," Wiley, New York, 1951.

Lister, R.D. and I.D. Neilson, "Protection of Car Occupant Against Side Impacts," Proceedings, 13th Stapp Car Crash Conference, pp. 38-60, 1969.

Lombard, C.F., S.D. Bronson, F.C. Thiede and F.M. Larmie, "Pathology and Physiology of Guinea Pigs Under Selection Conditions of Impact and Support Restraint," Aerospace Medicine, 35:860-865, 1964.

Mayor, R.P. and K.W. Naab, "Basic Research in Automobile Crashworthiness - Testing and Evaluation of Modifications for Side Impacts," CAL Report No. 113-2684-U-3, Nov. 1969.

McElhaney, J.H., L.L. Fogle, J.W. Melvin, R.R. Haynes, V.L. Roberts and N.M. Alem, "Mechanical Properties of Cranial Bone," Journal of Biomechanics, Vol. 3, No. 5, pp. 495-511, Oct. 1970.

McElhaney, J.H., R.L. Stalnaker, V.L. Roberts, R.G. Snyder, "Door Crashworthiness Criteria", Fifteenth Stapp Car Crash Conference, pp. 489-517.

McHenry, P.R. and K.N. Naab, "Computer Simulations of the Crash Victim - A Validation Study," Proceedings, 10th Stapp Car Crash Conference, Nov. 1966.

Ommaya, A.K., A.E. Hirsch, E.S. Flam and R.M. Mahone, "Cerebral Concussion in the Monkey: An Experimental Model," Science, Vol. 153, pp. 211-212, July 1966.

Ommaya, A.K., F. Fass and D. Yarnell, "Whiplash Injury and Brain Damage: An Experimental Study," JAMA, Vol. 204, pp. 285-289, April 1968.

Patrick, L.M., H.R. Lissner and E.S. Gurdjian, "Survival by Design - Head Protection," 7th Stapp Car Crash Conference, pp. 483-499.

Patrick, L.M., J.H. Mertz, Jr. and C.K. Kroell, "Cadaver Knee, Chest and Head Impact Loads," Proceedings, Eleventh Stapp Car Crash Conference, Society of Automotive Engineers, Inc., Anaheim, California, October 1967.

Payne, P.R., "The Dynamics of Human Restraint Systems" Acceleration Stress Symposium, November, pp. 195-285, 1961.

Ranson, S.W. and S.L. Clark, "Anatomy of the Nervous System Its Development and Function" Tonda Edition, W.B. Saunders Co. Philadelphia and London.

Reader, D.C., "The Restraint Afforded by the USAF and Proposed RAF 1AM Seat Harness for the F-111 Under High Forward and Lateral Decelerations," Royal Air Force Institute of Aviation Medicine, "Furnsborough, 1967.

Robbins, D.H., R.O. Bennett and J.M. Becker, "Two-Dimensional Crash Victim Simulator Users' Manual," Highway Safety Research Institute, The University of Michigan, Ann Arbor, Michigan, 1968.

Robbins, D.H., R.O. Bennett and V.L. Roberts, "HSRI Three Dimensional Crash Victim Simulator: Analysis, Verification and Users Manual," Final Report, U.S. Dept. of Transportation, Contract No. FH-11-6962, June 1970.

Robbins, D.H., R.O. Bennett, N.M. Alem and A.W. Henke, "Predictions of Mathematical Models Compared with Impact Sled Test Results Using Anthropometric Dummies," 14th Stapp Car Crash Conference, Ann Arbor, Mich., pp. 299-328, Nov. 1970.

Roberts, V.L. and Robbins, D.H., "Multidimensional Mathematical Modeling of Occupant Dynamics Under Crash Conditions," Society of Automotive Engineers, Inc., New York, Paper No. 690248, January 1969.

Robinson, F.R., R.L. Hamlin, W.M. Wolff and R.R. Coermann, "Response of the Rhesus Monkey to Lateral Impact," *Aerospace Medicine*, 34(1):56-62, Jan. 1963.

Sano, Keiji, et al., "Correlative Studies of Dynamics and Pathology in Whip-Lash and Head Injuries," *Scand J. Rehab Med* 4:47-54, 1972.

Severy, D.M., J.H. Mathewson and A.W. Siegle, "Auto Crash Studies," Dept. of Engineering, Univ. of California, Los Angeles, Jan. 1959.

Siegel, A.W., W.T. Wagoner and A.M. Nahum, "Case Comparisons of Restrained and Nonrestrained Occupants and Related Injury Patterns," Society of Automotive Engineers, Inc. Paper No. 690245, 1969.

Snyder, R.G., "Human Survivability of Extreme Impacts in Free-Falls," Civil Aeromedical Research Institute, Report 63-15, 1963.

Snyder, R.G., "Human Tolerances to Extreme Impacts in Free-Falls," 34th Annual Meeting, Aerospace Medical Assoc., Los Angeles, (Abstract: *Aerospace Medicine* 34(4); 34(8):795-811), April 1963.

Snyder, R.G., "Human Survival of High Velocity Free-Falls in Water," CARI Rept. 64-12, Office of Aviation Medicine, Federal Aviation Agency, Washington, D.C., 1964.

Snyder, R.G., "Human Tolerance Limits in Water Impact," (Abstract: *Aerospace Medicine*, 36(2):163), presented at 36th Annual Meeting of Aerospace Medical Assoc., New York, April 26; *Aerospace Medicine* 36(10):940-947, 1965.

Snyder, R.G. "Human Tolerance Data Relative to All-Out Safety Car Program 1B," Ford Motor Co., Memo, Nov. 23, 1966.

Snyder, R.G., "Center-Facing (Lateral) Seating in Station Wagons," Ford Motor Co., Memo, Nov. 23, 1966.

Snyder, R.G., "Physiological Effects of Impact. Man and Other Mammals," Environmental Biology, Federation of American Studies for Experimental Biology. pp. 231-242, 1966.

Snyder, R.G., C.C. Snow, J.W. Young, G.T. Price and P. Hanson, "Experimental Comparison of Trauma in Lateral (+Gy) and Forward-Facing (-Gx) Body Orientation; When Restrained by Lap Belt Only," Aerospace Medicine, 38(a):889-894, 1967.

Snyder, R.G., C.C. Snow, J.W. Young, G.T. Price, P. Hanson and R. Chandler, "Injury in Lateral Impact (-Gy) When Restrained by Lap Belt Only," Presented, 38th Annual Meeting, Aerospace Medical Assoc., Washington, D.C., April 1967.

Snyder, R.G., C.C. Snow, J.W. Young, W.H. Crosby and G.T. Price, "Pathology of Trauma Attributed to Restraint Systems in Crash Impacts," Presented, Joint Committee on Aviation Pathology, Toronto, Canada, 12 Sept.; Aerospace Medicine 39(8):812-829, Aug. 1968.

Snyder, R.G., C.C. Snow and J.W. Young, "Experimental Impact Protection with Advanced Automotive Restraint Systems: Preliminary Primate tests with Air Bag and Inertia Reel/Inverted-Y Yoke Torso Harness," Proceedings, 11th Stapp Car Crash Conference, Anaheim, Calif. Society of Automotive Engineers, Inc., Paper No. 670972, 1968.

Snyder, R.G., Impact, Chapter in NASA Bioastronautics Data Book, Sponsored by National Academy of Sciences/National Research Council and National Aeronautics and Space Administration (in preparation) 1969.

Sontag, R., Personal Communication (Unpublished Holloman Test Data), 1966.

Stalnaker, R.L., "Mechanical Properties of the Head,: Ph.D. Dissertation, West Virginia University, 1969.

Stalnaker, R.L., J.C. Fogle and J.H. McElhaney, "Driving Point Impedence Characteristics of the Head," American Society of Mechanical Engineers, New York, ASME Paper No. 70-BHF-14, 1970.

Stalnaker R.L. and J.H. McElhaney, "Head Injury Tolerance for Linear Impacts by Mechanical Impedence Methods," American Society of Mechanical Engineers, New York, ASME Paper No. 70-WA/BHF-4, 1970.

Stalnaker, R.L., J.H. McElhaney, R.G. Snyder, and V.L. Roberts, "Door Crashworthiness Criteria" June 1971, U.S. Dept. of Transportation Report No. HS-800-S34.

Stalnaker, R.L., J.L. Fogle and J.H. McElhaney, "Driving Point Impedence Characteristics of the Head," Vol. 4, No. 2, pp. 127-139, March 1970.

Stapp, J.P., "Tolerance to Abrupt Deceleration," Collected Papers on Aviation Medicine, Advisory Group for Aeronautical Research and Development, Butterworths Scientific Publications, London, 1955.

Stapp, J.P., "Voluntary Human Tolerance Levels," Presented, Wayne State Univ. Centennial, Biomechanics Symposium, Detroit, Mich., 1968.

Stapp, J.P., "Human Criteria for Protection from Vehicle Crash Impact," Society of Automotive Engineers, Inc., Paper No. 690104, 1964.

State, J.D. and D.J. States, "The Pathology and Pathogenesis of Injuries Caused by Lateral Impact Accidents," Proceedings, 12th Stapp Car Crash Conference, Society of Automotive Engineers, Inc., New York, Paper No. 680773, pp. 72-93, 1968.

Stritch, S.J., "The Pathology of Brain Damage Due to Blunt Head Injuries," pp. 501-526. The Late Effects of Head Injury Walker, Caveness, Critchley Chas. C. Thomas, publisher, Springfield, Ill. 1969.

Thompson, J., "Control of Structural Collapse in Automotive Side Impact Collisions," Doctoral Thesis Univ. of Detroit, 1972.

Thompson, J.E., "Occupant Response Versus Vehicle Crash: A Total System Approach," 12th Stapp Car Crash Conference, 1968.

Weiss, C.B., N.P. Clarke and J.W. Brinkley, "Human Response to Several Impact Acceleration Orientations and Patterns," Aerospace Medicine, 34(12):1122-1129, December 1963.

Whitehouse, A.C., W.K. Brown, P. Foster and H.F. Scherer, "Quantitative Effects of Abrupt Deceleration on Pulmonary Diffusion in Man," ARL Report TR-66-12, May 1966.

Yost, C.D., Accident Reviews: Ford, Automotive Safety Research Office, Ford Motor Co., Rept. No. S-67-22, 1967.

Zaborowski, A.V., J.D. Rothstein and W.K. Brown, "Investigations in Human Tolerance to Lateral Impact," (Presented, 36th Annual Meeting, Aerospace Medical Association, April 26-29, New York City, Abstract: Aerospace Medicine 36:168-169), Unpublished, 1963.

Zaborowski, A.V., "Lateral Impact Studies - Lap Belt Shoulder Harness Configurations," Proceedings, 9th Stapp Car Crash Conference, Society of Automotive Engineers, Inc., New York, 1965.

Zaborowski, A.V., "Human Tolerance to Lateral Impact with Lap Belt Only," Proceedings, 8th Stapp Car Crash Conference, Wayne State Univ., Detroit, pp. 34-68, 1966.

Zulch, Klaus-Joachim, "Medical Causation" pp. 453-472, The Late Effects of Head Injury. Walker, Caveness, Critchley. Chas. C. Thomas, publisher, Springfield, Ill. 1969.